

**Virginia Polytechnic Institute  
and State University**

**The Charles E. Via, Jr.  
Department of  
Civil and Environmental Engineering**

**CENTER FOR  
GEOTECHNICAL PRACTICE AND RESEARCH**

**Performance and Use of the Standard Penetration Test in  
Geotechnical Engineering Practice**

by

**Jeffrey A. McGregor  
and  
J. Michael Duncan**

**Report of a study performed by the Virginia Tech Center for  
Geotechnical Practice and Research**

**October, 1998**



## Table of Contents

List of Figures.....	iii
List of Tables.....	vii
List of Symbols.....	ix
Introduction .....	1
SPT Equipment and Procedures.....	2
ASTM Specifications for the Standard Penetration Test (SPT).....	8
Standard Penetration Test Procedures Recommended by Various Authorities	10
Factors and Variables That Affect SPT Results.....	17
Corrections to Measured Blow Counts.....	26
Becker Penetration Test (BPT) Correlations with the SPT.....	35
Correlations Between SPT and Soil Properties.....	54
Relative Density of Sands.....	55
Friction Angles ( $\phi$ ) of Sands and Silts.....	67
Undrained Shear Strength ( $S_u$ ) of Clays.....	76
Undrained Residual Steady State Strengths ( $S_r$ ) of Sands.....	83
Soil Modulus Values.....	86
Correlations Between SPT and Foundation Performance.....	92
Settlement of Shallow Foundations on Sand.....	93
Settlement of Pile Groups in Sand.....	97
Bearing Capacity of Footings on Sand.....	100
Bearing Capacity of Piles in Sand.....	102
Bearing Capacity of Drilled Shafts.....	113
Correlations Between SPT and Liquefaction Potential of Sands.....	116
Appendix - ASTM Specification D 1586.....	120

Appendix B - Unit Conversions and Drill Rod Sizes.....	126
References.....	129

## List of Figures

Figure 1.	Donut hammer .....	3
Figure 2.	Safety hammer .....	4
Figure 3.	Automatic hammer.....	5
Figure 4.	SPT drilling and sampling configuration.....	6
Figure 5.	Split-barrel sampler for use with the SPT .....	7
Figure 6.	Definitions of the number of turns of rope and the angle $\alpha$ for CCW and CW rotation of the cathead.....	13
Figure 7.	Effect of energy ratio (on impact) on the number of turns of rope around the cathead .....	14
Figure 8.	Overburden correction factors .....	28
Figure 9.	Chart for values of $C_N$ .....	29
Figure 10.	Sample liner configuration.....	33
Figure 11.	Schematic diagram of Becker sampling operation.....	36
Figure 12.	Operating principle of double-acting atomized fuel injection diesel pile hammer .....	38
Figure 13.	Computed BPT vs. SPT correlation for different BPT casing shaft resistance .....	40
Figure 14.	Correction curves adopted to correct Becker blow counts to constant combustion curve adopted for correlation.....	41
Figure 15.	Examples illustrating the use of the correction curves in Fig. 14 .....	42
Figure 16.	Correlation between corrected Becker and SPT blow counts .....	44
Figure 17.	Correlation between Becker and SPT blow counts developed from Canadian data obtained from Becker Drills, Inc.....	47
Figure 18.	Correlation between Becker and SPT blow counts developed by Sergent, Hauskins, and Beckwith.....	48
Figure 19.	Correlations between Becker and SPT blow counts developed by Geotechnical Consultants, Inc.....	49

Figure 20.	Correlation between Becker and SPT blow counts developed by Jones and Christensen.....	50
Figure 21.	Summary of correlations between Becker and SPT blow counts.....	51
Figure 22.	Conventional BPT mud-injection FBPT casing configurations .....	52
Figure 23.	FBPT-SPT correlations for 170mm and 220mm diameter shoes.....	53
Figure 24.	Variations of relative density with penetration resistance at different overburden pressures (Gibbs and Holtz) .....	57
Figure 25.	Variations of relative density with penetration resistance at different overburden pressures (Meyerhof) .....	58
Figure 26.	Variations of relative density with penetration resistance at different overburden pressures (Peck and Bazaraa) .....	59
Figure 27.	Variations of relative density with penetration resistance at different overburden pressures for fine sands (Yoshida and Ikemi) .....	60
Figure 28.	Variations of relative density with penetration resistance at different overburden pressures for soils with a gravel fraction equal to 25% (Yoshida and Ikemi).....	61
Figure 29.	Variations of relative density with penetration resistance at different overburden pressures for soils with a gravel fraction equal to 50% (Yoshida and Ikemi).....	62
Figure 30.	Variations of relative density with penetration resistance at different overburden pressures (average for all cohesionless soils) (Yoshida and Ikemi).....	63
Figure 31.	Correlations between relative density and standard penetration resistance (Mitchell et al.).....	65
Figure 32.	Correlations between relative density and standard penetration resistance (NAVFAC).....	66
Figure 33.	Correlations between internal friction angle and penetration resistance.....	69
Figure 34.	Empirical correlation between friction angle of sands and normalized standard penetration blow count.....	71
Figure 35.	Estimation of the angle of shearing resistance of granular soils from standard penetration test results.....	72

Figure 36.	Angle of internal friction as a function of relative density for different types of sand and gravel.....	73
Figure 37.	Method for estimating effective friction angle from SPT blow count.....	74
Figure 38.	Variations of friction angle with $N_{1,60}$ for silts and clays .....	75
Figure 39.	The variation of $S_u/N$ with plasticity index, PI.....	79
Figure 40.	Relationship between standard penetration blow count, $N$ and undrained shear strength, $S_u$ .....	80
Figure 41.	Relationship between standard penetration resistance and unconfined compressive strength, $q_u$ .....	81
Figure 42.	Estimated decrease in standard blow count with increasing clay sensitivity at constant undrained strength .....	82
Figure 43.	Some correlations between SPT blow count and unconfined compressive strength, $q_u$ in clays .....	82
Figure 44.	Relationship between corrected “clean sand” blow count, $N_{1,60-cs}$ and undrained residual strength, $S_r$ from case studies .....	84
Figure 45.	Relationship for compressibility modulus as a function of standard penetration resistance .....	88
Figure 46.	Correlations of stress-strain modulus and penetration resistance .....	89
Figure 47.	Correlation between constrained modulus and average value of SPT blow count.....	90
Figure 48.	Shear modulus vs. $N$ values at very small strains .....	91
Figure 49.	Location of equivalent footing .....	98
Figure 50.	Empirical relation between ultimate point resistance of piles and standard penetration resistance in cohesionless soil.....	104
Figure 51.	Empirical relationships between ultimate skin friction of piles and penetration resistance in cohesionless soil .....	105
Figure 52.	Relation between ultimate point resistance of pile and depth in thin sand layer overlying weak soil .....	106
Figure 53.	Photograph of exhumed Franki piles showing expanded bases.....	108
Figure 54.	Empirical relation between ultimate point resistance and standard penetration resistance for long expanded-base piles.....	110

Figure 55.	Empirical relation between ultimate point resistance and standard penetration resistance for short expanded-base piles.....	110
Figure 56.	Simplified base curve recommended for estimating CRR from SPT data along with empirical liquefaction data .....	117

## List of Tables

Table 1.	Summary of the ASTM specification for the standard penetration test (D 1586) .....	9
Table 2.	Energy correction factors proposed by Seed et al.....	11
Table 3.	Factors which may affect measured penetration resistance.....	18
Table 4.	Estimates of the change in N-values due to some common factors.....	22
Table 5.	Estimates of the change in N-values due to various factors.....	23
Table 6.	Changes in N-values due to faulty equipment and non-standard procedures .....	24
Table 7.	Changes in N-values due to various factors.....	25
Table 8.	Overburden correction factors ( $C_N$ ).....	27
Table 9.	Energy correction factors ( $C_E$ ).....	30
Table 10.	Ranges of energy correction factors ( $C_E$ ).....	30
Table 11.	Rod length correction factors ( $C_R$ ) (Tokimatsu) .....	31
Table 12.	Rod length correction factors ( $C_R$ ) (Youd and Idriss).....	31
Table 13.	Borehole diameter correction factors ( $C_B$ ).....	31
Table 14.	Liner correction factors ( $C_S$ ).....	32
Table 15.	Anvil correction factors ( $C_A$ ).....	32
Table 16.	Blow count frequency correction factors ( $C_{BF}$ ) .....	34
Table 17.	Hammer cushion correction factors ( $C_C$ ).....	34
Table 18.	Elevation corrections for bounce chamber pressures.....	43
Table 19.	Correlations between Becker and SPT blow counts.....	46
Table 20.	Correlations of relative density and SPT N-values .....	56
Table 21.	Relationship among relative density, penetration resistance, dry unit weight, and angle of internal friction of cohesionless soils .....	64
Table 22.	Correlations of internal friction angle and SPT N-values .....	68
Table 23.	Empirical values for $\phi$ , $D_r$ , and unit weight of granular soils based on the standard penetration number with corrections for depth and	



	for fine saturated sands .....	70
Table 24.	Approximate values of undrained shear strength for cohesive soils based on SPT blow counts .....	77
Table 25.	Approximate undrained shear strength for cohesive soils based on SPT blow counts.....	77
Table 26.	Empirical values for $q_u$ and consistency of cohesive soils based on the standard penetration number.....	78
Table 27.	Recommended fines correction for estimation of residual undrained strength by Seed-Harder and Stark-Mesri procedures.....	85
Table 28.	Equations for stress-strain modulus by the SPT method.....	87
Table 29.	Correlations of settlements of footings on sand and SPT N-values .....	94
Table 30.	Width correction factor, $C_B$ .....	96
Table 31.	Load inclination factors, $R_l$ .....	101
Table 32.	Correlations of pile capacities and penetration resistance for piles in cohesionless soil.....	111
Table 33.	Correlations of pile capacities and penetration resistance for piles in cohesive soil.....	112
Table 34.	Summary of procedures for estimating shaft resistance of drilled shafts in sand .....	113
Table 35.	Summary of procedures for estimating base resistance of drilled shafts in sand .....	114
Table 36.	Fines content corrections .....	119

## List of Symbols

Symbol	Represents
<u>ENGLISH</u>	
$a_{max}$	Peak horizontal acceleration at the ground surface
$A_p$	Area of pile tip or area of base of drilled shaft
$B$	Footing width
$BP_{SL}$	Bounce chamber pressure at sea level
$BPT$	Becker penetration test
$C_A$	Anvil correction factor
$C_B$	Borehole diameter correction factor
$C_B$	Width correction factor
$C_{BF}$	Blow count frequency factor
$C_C$	Hammer cushion correction factor
$C_E$	Energy correction factor
$C_f$	Factor used to estimate relative density in normally consolidated sands
$C_N$	Overburden correction factor
$C_R$	Rod length correction factor
$CRR$	Cyclic resistance ratio
$C_S$	Liner correction factor
$CSR$	Cyclic stress ratio
$C_{w1}, C_{w2}$	Correction factors based on the position of the water table
$D$	Embedment depth
$d$	Pile diameter or width
$D'$	Effective depth
$D_b$	Diameter of expanded base pile
$D_f$	Embedment depth

Symbol	Represents
$D_p$	Diameter of shaft base
$D_r$	Relative density
$D_w$	Distance from the ground surface to the water table
$E, E_s$	Young's modulus of elasticity
$E_d$	Deformation modulus
ER, ENTHRU	Hammer energy ratio
$g$	Acceleration due to gravity
$I$	Influence factor of effective group embedment
I.D.	Inside diameter
$I_c$	Influence factor for use in immediate settlement equation
$K_0$	Ratio of effective horizontal stress to vertical stress
$K_{onc}$	For normally consolidated sand, approximately equal to $(1 - \sin \phi')$
$M$	Compression modulus
$\bar{N}$	Average SPT blow count
$N, N_m, N_{field}$	Measured penetration resistance
$N_{1,60}$	Blow count corrected to 1 tsf of overburden pressure and 60% of the theoretical free-fall hammer energy
$N_{1,60 - cs}$	Equivalent clean sand SPT blow count
$N_{60}$	Blow count corrected to 60% of the theoretical free-fall hammer energy
$N_b, N_B$	Measured Becker blow count
$N_{b,30}$	Becker or Foundex Becker penetration test blow count normalized to the 30% reference energy level
$N_{BC}$	Corrected Becker blow count

Symbol	Represents
$N_1$	The average corrected SPT blow count within the seat of settlement (corrected to 1 tsf of overburden pressure)
$N_p$	Average SPT N-value within a distance of 1d beneath the pile tip and 3.75d above it
$N_s$	Average SPT N-value along pile shaft
O.D.	Outside diameter
OCR	Overconsolidation ratio
$q_p$	Bearing pressure
$q_{limit}$	Limiting point resistance
$q_p, q_b$	Ultimate unit point resistance of piles or drilled shafts
$Q_{p,ult}$	Ultimate point resistance of a pile or drilled shaft
$q_{pr}$	Reduced base resistance for $D_p > 50$ inches
$q_s, f_s$	Ultimate unit side resistance of piles or drilled shafts
$q_u$	Unconfined compressive strength
$q_{ult}$	Ultimate bearing capacity
$r_d$	Stress reduction coefficient
$R_l$	Load inclination factor
$R_s$	Shaft resistance on Becker casing
$S_1, S_2$	Factors used to estimate modulus from N-values
SPT	Standard penetration test
$S_r$	Undrained residual steady state strength
$S_u$	Undrained shear strength
$z$	Depth

Symbol	Represents
<u>GREEK</u>	
$\sigma_v', \sigma', \sigma_{vo}'$	Effective overburden pressure
$\sigma_{vo}$	Total overburden pressure
$\phi$	Angle of internal friction
$\rho, \rho_i$	Immediate settlement of footing

## Introduction

The Standard Penetration Test (SPT) is one of the oldest and most frequently used tests for geotechnical exploration. It is useful in a wide variety of soils, from weak clays and loose sands to very hard clays and dense sands. It provides a measure of the resistance of the soil to penetration through the blow count "N," and a disturbed but representative soil sample that can be used for classification and index tests.

The SPT has been used widely for preliminary exploration, and many useful correlations have been established between the blow count, N, and soil properties, foundation performance, and susceptibility to liquefaction. In recent years some engineers have developed various "corrections" for measured N-values to account for the effects of using different types of hammers, the effects of overburden pressure, and various other factors of less importance. While these corrections are desirable, their use has led to confusion regarding which correlations use corrected N-values and which use uncorrected N-values. The main purpose of this report is to remove that confusion.

The report presents what are considered to be the most useful and reliable correlations between SPT N-values and soil strength, soil compressibility, foundation bearing capacity, foundation settlement, and liquefaction potential. In each case it is made clear what corrections should be applied to the measured N-values.

The report also contains correlations between the Standard Penetration Test and the Becker Penetration Test, which is useful for soils that contain large gravel particles, where the SPT is unreliable.

## SPT Equipment and Procedures

The Standard Penetration Test, as defined by the American Society for Testing and Materials (ASTM D 1586), involves driving a standard split-spoon sampling tube (2-inch O.D. and 1 3/8-inch I.D.) 18 inches into the ground at the bottom of a borehole with a 140 lb. hammer falling 30 inches. The borehole is advanced to the desired testing depth, the drilling tools are removed, the sampler is attached to a series of drill rods, and the entire assembly is lowered to the bottom of the borehole. The hammer is positioned over the top of the drill rods and blows are applied at the rate of 30 to 40 blows per minute.

Three types of hammers can be used in the SPT. The donut hammer, shown in Figure 1, provides approximately 45% of the maximum free-fall energy to the drill stem. The safety hammer, shown in Figure 2, is the most commonly used hammer for the SPT. It provides about 60% of the maximum free-fall energy. Figure 3 shows the automatic trip hammer. The automatic hammer mechanism raises and lowers the hammer at a preset blowcount frequency. Because the hammer falls in a nearly "free-fall" mode, the automatic trip hammer provides 95% to 100% of the maximum free-fall energy to the drill stem.

The most common method of raising and lowering the donut or safety hammer is the rope and cathead method (also called the rope and pulley method). A rope wrapped around a rotating pulley (a cathead) is used to lift the hammer. The drill rods are marked in three 6-inch increments. As the sampler is driven, the number of hammer blows required to drive the sampler each 6-inch increment is recorded. The blow counts for the last two 6-inch increments added together are the standard penetration resistance or N-value. Upon completion of driving, the sampler is withdrawn from the borehole. The split-spoon sampler is opened and the soil sample is removed and logged. The SPT drilling and sampling configuration is shown in Figure 4, and the dimensions of the standard split-spoon sampler are shown in Figure 5.

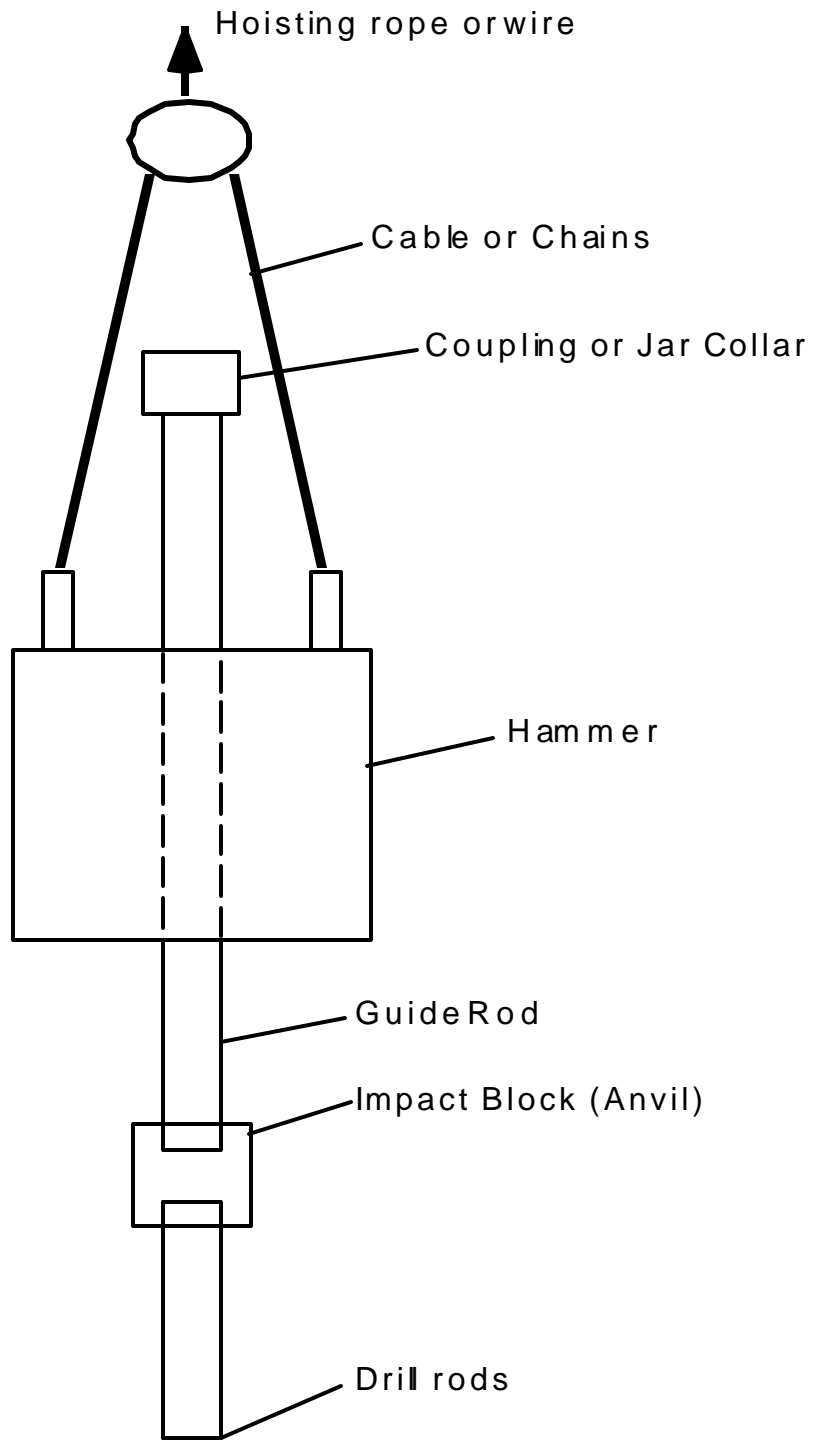


Figure 1. Donut hammer



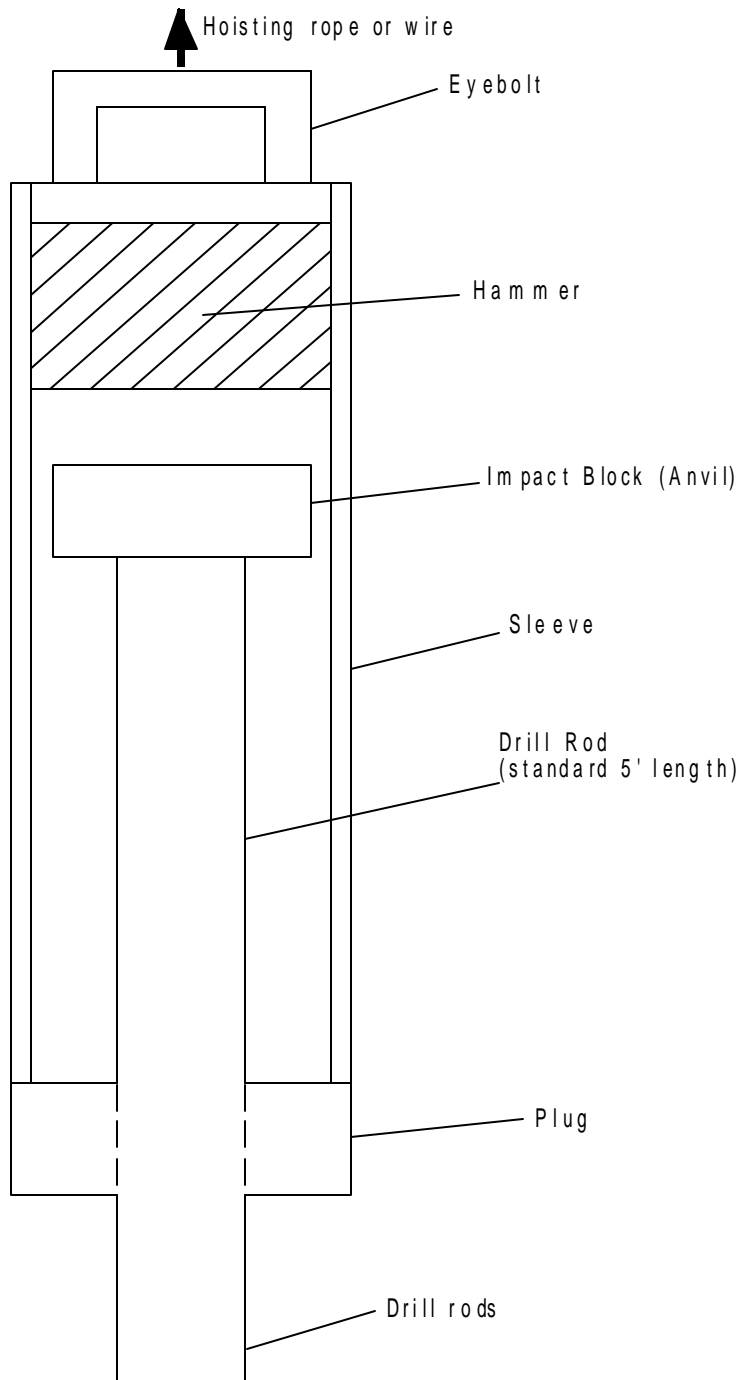


Figure 2. Safety hammer

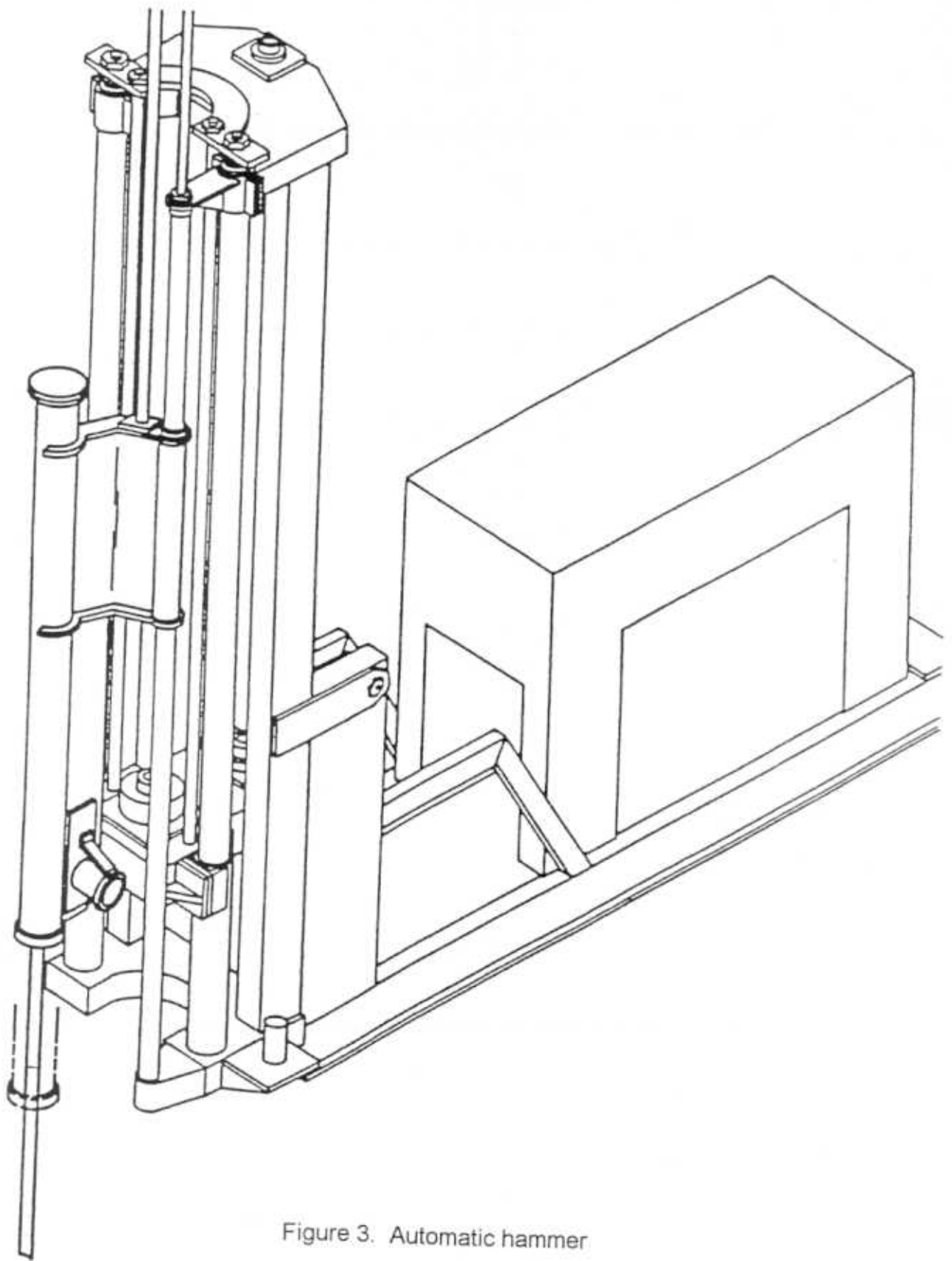


Figure 3. Automatic hammer

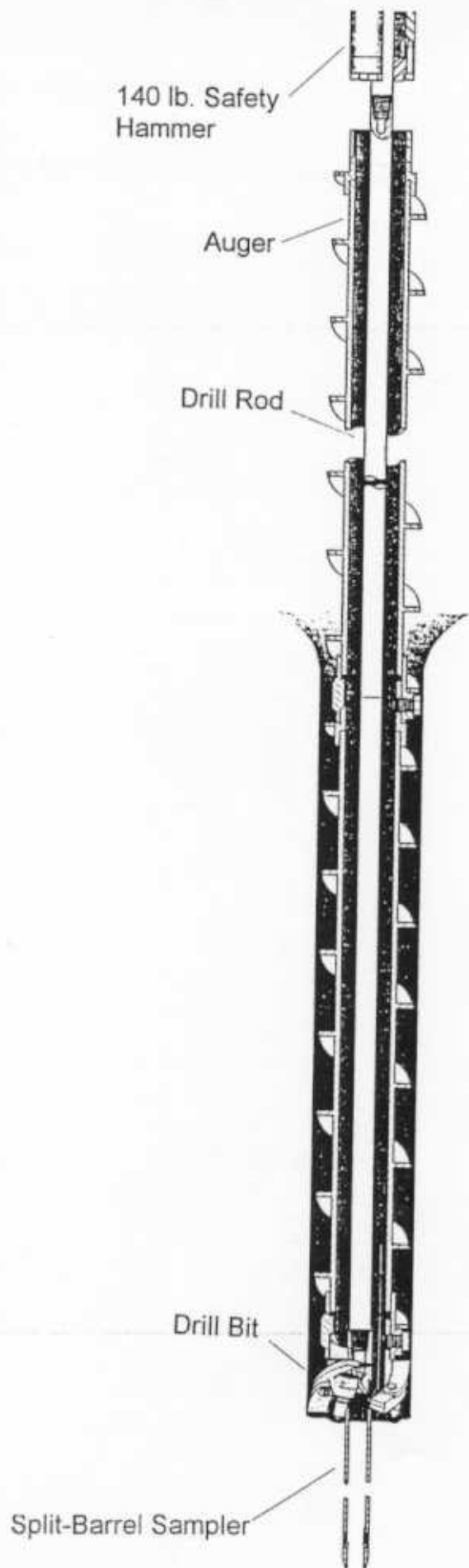
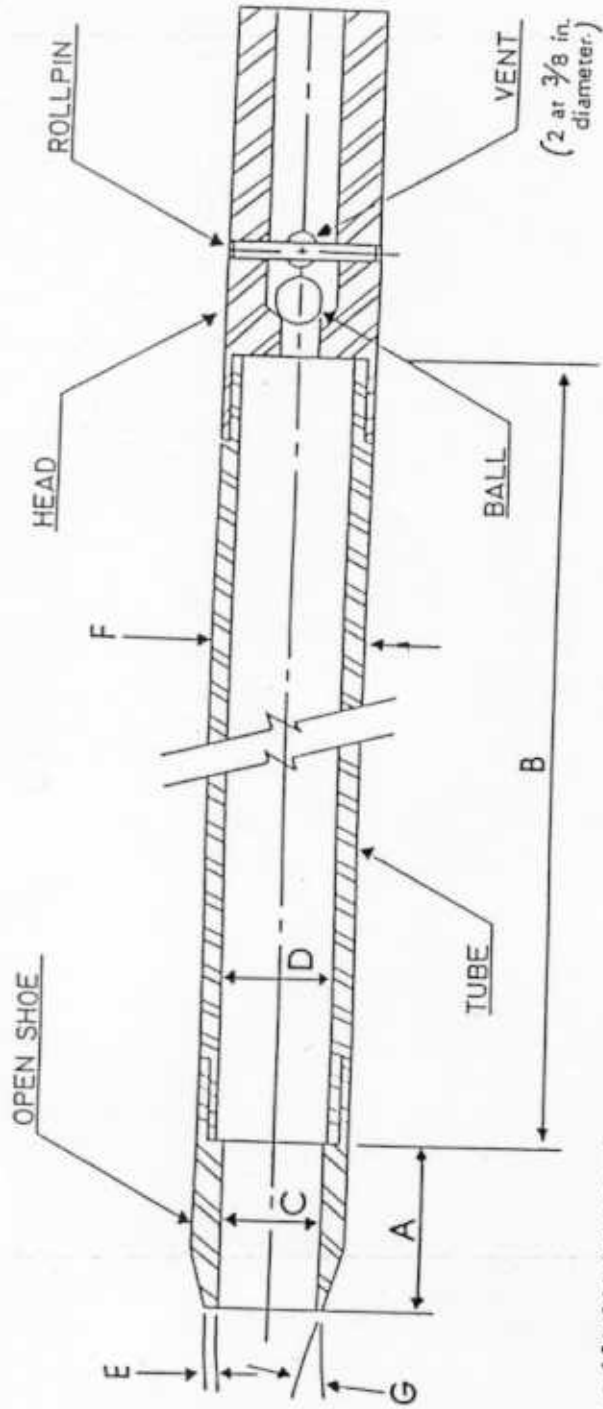


Figure 4. SPT drilling and sampling configuration (from Mobile Drilling Co., 1986)

D 1586



- A = 1.0 to 2.0 in. (25 to 50 mm)
- B = 18.0 to 30.0 in. (0.457 to 0.762 m)
- C = 1.375 ± 0.005 in. (34.93 ± 0.13 mm)
- D = 1.50 ± 0.05 - 0.00 in. (38.1 ± 1.3 - 0.0 mm)
- E = 0.10 ± 0.02 in. (2.54 ± 0.25 mm)
- F = 2.00 ± 0.05 - 0.00 in. (50.8 ± 1.3 - 0.0 mm)
- G = 15.0\* to 23.0\*

The 1/2 in. (38 mm) inside diameter split barrel may be used with a 16-gage wall thickness split liner. The penetrating end of the drive shoe may be slightly rounded. Metal or plastic retainers may be used to retain soil samples.

Figure 5. Split-barrel sampler for use with the SPT (from ASTM, 1997)

## **ASTM Specifications for the Standard Penetration Test**

The “standard” procedure for the Standard Penetration Test is set by ASTM D 1586. This specification, titled “Standard Test Method for Penetration Test and Split-Barrel Sampling of Soils” can be found in its entirety in Appendix A. As stated in Paragraph 1 of the specification, its scope is to “describe the procedure, generally known as the Standard Penetration Test (SPT), for driving a split-barrel sampler to obtain a representative soil sample and a measure of the resistance of the soil to penetration of the sampler.” ASTM D 1586 provides information on drilling procedures and equipment, the sampler, the hammer, the anvil, the drop system, borehole sizes, and sampling and test procedure. The ASTM requirements regarding these items are summarized in Table 1.

Table 1. Summary of the ASTM Specification for the Standard Penetration Test (D 1586)

Item	Standard
Drilling Procedure	Any drilling equipment that provides a suitably clean and stable hole before sampler insertion and ensures that the penetration test is performed in essentially undisturbed soil.
Drill Rods	Flush joint steel, stiffness $\geq$ stiffness of "A" rod. For a list of drill rod designations, see Appendix B.
Sampler	1.5 inch (inner diameter) split-barrel sampler. See Figure 5 for dimensions. Use driving shoe of hardened steel. Use of liners and/or retainer baskets is permitted, but must be noted.
Hammer	Solid rigid metallic mass of $140 \pm 2$ lb.
Hammer Drop System	Rope-cathead, trip, semi-automatic, or automatic hammer drop systems may be used. Use a hammer guide that permits free-fall. The hammer shall be dropped $30 \pm 1$ inches.
Borehole	2.2 to 6.5 inches in diameter.
Anvil	Shall make steel on steel contact with hammer.
Sampling and Test Procedure	<p>Remove excess cuttings from borehole. Lower drill rods and sampler into hole (do not drop). Apply a seating blow. Mark three successive 6-inch increments on the drill rods. Drive the sampler with blows from the hammer and count the number of blows applied in each 6-inch increment until one of the following occurs:</p> <ul style="list-style-type: none"> <li>• A total of 50 blows has been applied during any one of the three 6-inch increments.</li> <li>• A total of 100 blows has been applied.</li> <li>• No observed advance of the sampler has occurred during applications of 10 successive blows.</li> <li>• The sampler has advanced 18 inches.</li> </ul> <p>Record the number of blows for each 6 inch increment. The "N" value is the sum of the second and third 6 inches of penetration. Upon completion of sampling, remove sampler from borehole. Record percent recovery or length of the sample. Describe the recovered soil samples with respect to composition, color, stratification, and condition. Place representative portions of each sample in moisture-proof containers and label appropriately.</p>

## Standard Penetration Test Procedures Recommended by Various Authorities - All Are Allowable by ASTM

Because the ASTM specifications for the SPT are not fully comprehensive, and are subject to interpretation to some degree, various authorities have developed recommendations concerning SPT procedures and equipment. These recommendations range from a full set of instructions for the SPT to merely a few comments that address drilling methods, drill rods, borehole size and stabilization, the sampler, blow count rate, hammer configuration, energy corrections and test procedure. The following recommendations are allowable by ASTM D 1586, and may be used for conducting the SPT for geotechnical investigation. This section contains guidance from authorities in from the US and other countries in which the SPT is routinely used.

This section presents recommendations and guidance for performing the SPT. All of the recommendations are allowable within the ASTM standard specification. This section is organized by author.

**Seed et al. (1984)** developed a relatively complete procedure for the SPT for use in liquefaction correlations. The following is a summary of the equipment and procedures they recommend:

- Borehole: 4 to 5-inch diameter rotary borehole with bentonite drilling mud for borehole stability.
- Drill Bit: Upward deflection of drilling mud (tricone or baffled drag bit).
- Sampler:
  - O.D. = 2.00 inches
  - I.D. = 1.38 inches - constant (i.e. no room for liners in barrel).
- Drill rods:
  - A or AW for depths < 50 feet
  - N or NW for greater depths
- Blow count rate: of 30 to 40 blows per minute.

The energy delivered to sampler should be 2520 in-lbs (60% of theoretical maximum) per blow. This is the energy delivered by the safety hammer. If a hammer other than a safety hammer is used, the field blow count ( $N_{\text{field}}$ ) should be corrected to the appropriate energy which is 60% of the theoretical energy. Energy correction factors will be discussed further in Section 5. The following correction for the various hammer types are recommended:

$$N_{60} = N_{\text{field}} C_E$$

where

$N_{60}$  = N-value corrected to 60% of the maximum theoretical energy delivered by 140 lbs. falling 30 inches

$N_{\text{field}}$  = SPT N-value for measured in the field

$C_E$  = energy ratio correction factor (see Table 2)

Table 2. Energy Correction Factors proposed by Seed et al. (1984)

Hammer	Correction Factor, $C_E$
Automatic	1.3
Safety	1.0
Donut	0.75

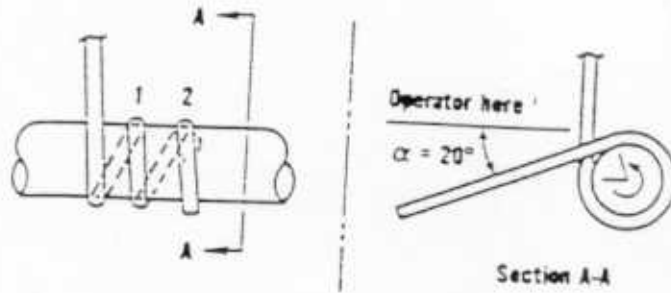
The SPT Working Party (**Thorburn et al., 1989**) also made recommendations for performing the SPT. The International Reference Test Procedure (IRTP) was developed by the Working Party with the intent to create one standard specification to be followed by all countries using the SPT. The following recommendations are from the IRTP report:

- Carefully clean out the borehole to the test elevation using equipment that will not disturb the soil to be tested.
- Do not use hollow stem augers for tests below groundwater.
- Withdraw drilling tools slowly to prevent suction effects that can loosen the soil.
- If casing is used, do not drive the casing below the elevation where the test is to be performed.
- The N-value is zero if the sampler and drill rods penetrate the soil more than 18 inches under their weight.
- The rate of application of hammer blows shall:
  - 1) Not be excessive such that there is the possibility of not achieving the standard drop.
  - 2) Not prevent equilibrium conditions from occurring between blows. Use a maximum blow count rate of 30 blows per minute.

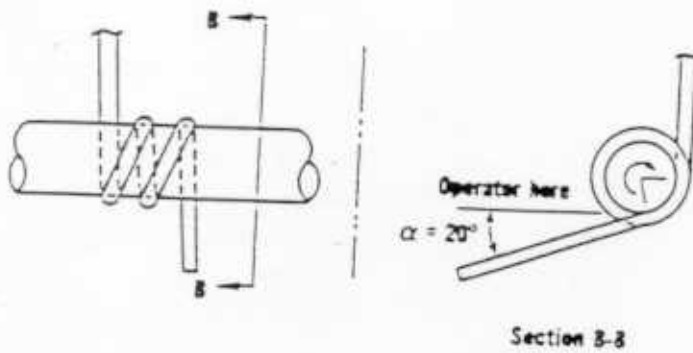
**Kovacs (1979, 1980, 1994), Kovacs and Salomone (1982), Kovacs et al. (1977), and Kovacs et al. (1981)** have done extensive research on the SPT, especially with energy ratios and energy transfer. The following recommendations come from this work:



- Use 2 turns of rope around the cathead (Kovacs and Salomone, 1982). Kovacs (1980) claims that one of the most significant variables that affects SPT results is the number of turns of rope around the cathead. When operators use more than 2 turns of rope, frictional resistance causes the N-values obtained to be erroneously high. The hammer no longer is able to fall freely. The velocity of the hammer decreases as more turns of rope are used. As the velocity decreases, so does the kinetic energy and overall efficiency of the hammer (Kovacs and Salomone, 1982). The reduction in hammer velocity is more pronounced as the number of turns increases from 2 to 3 than as it increases from 1 to 2. In order to obtain the best results in terms of the energy ratio and the ability of the operator to achieve a 30-inch drop height, Kovacs et al. (1981) recommend using 2 turns of rope around the cathead. The definition of a turn of rope as noted by Kovacs (1980) is seen in Figure 6. The actual number of turns is defined by the total angle of rope contact with the cathead divided by 360. As shown in Figure 6, the number of turns is different depending on the direction of cathead rotation and operator orientation. As the number of turns increases beyond two, the energy ratio for a 30-inch fall decreases sharply, as can be seen in Figure 7.
- It may become desirable to specify only one permissible direction of cathead rotation for future standard of SPT (Kovacs, 1980).
- Do not use hollow stem augers below the groundwater table (Kovacs, 1994).
- Use a hammer that delivers 60% of its maximum rated free-fall energy, i.e. a safety hammer (Kovacs, 1994).
- Adjust the fall height of automatic hammers to give 60% energy delivered to the drill stem (Kovacs, 1994).
- Perform SPT in each identifiable layer or every 3 feet (Kovacs et al., 1981).
- Record the penetration resistance as zero if the sampler and drill rods advance under their own weight (Kovacs et al., 1981).
- Do not subject the sampler spoon to more than 50 blows. The penetration resistance should be expressed as a ratio of the number of blows to the distance penetrated in inches if more than 50 blows are required (Kovacs et al., 1981).
- Using a trip monkey may be desirable in order to get consistent, reproducible results (Kovacs, 1979).
- Eliminate donut and pin-guided hammers because of the low energy they deliver to the drill stem (Kovacs, 1994).



(a) CCW rotation (1.81 turn shown)



(b) CW rotation (2.19 turns shown)

Figure 6. Definitions of the number of turns of rope and the angle  $\alpha$  for (a) CCW rotation and (b) CW rotation of the cathead (from Kovacs, 1980)

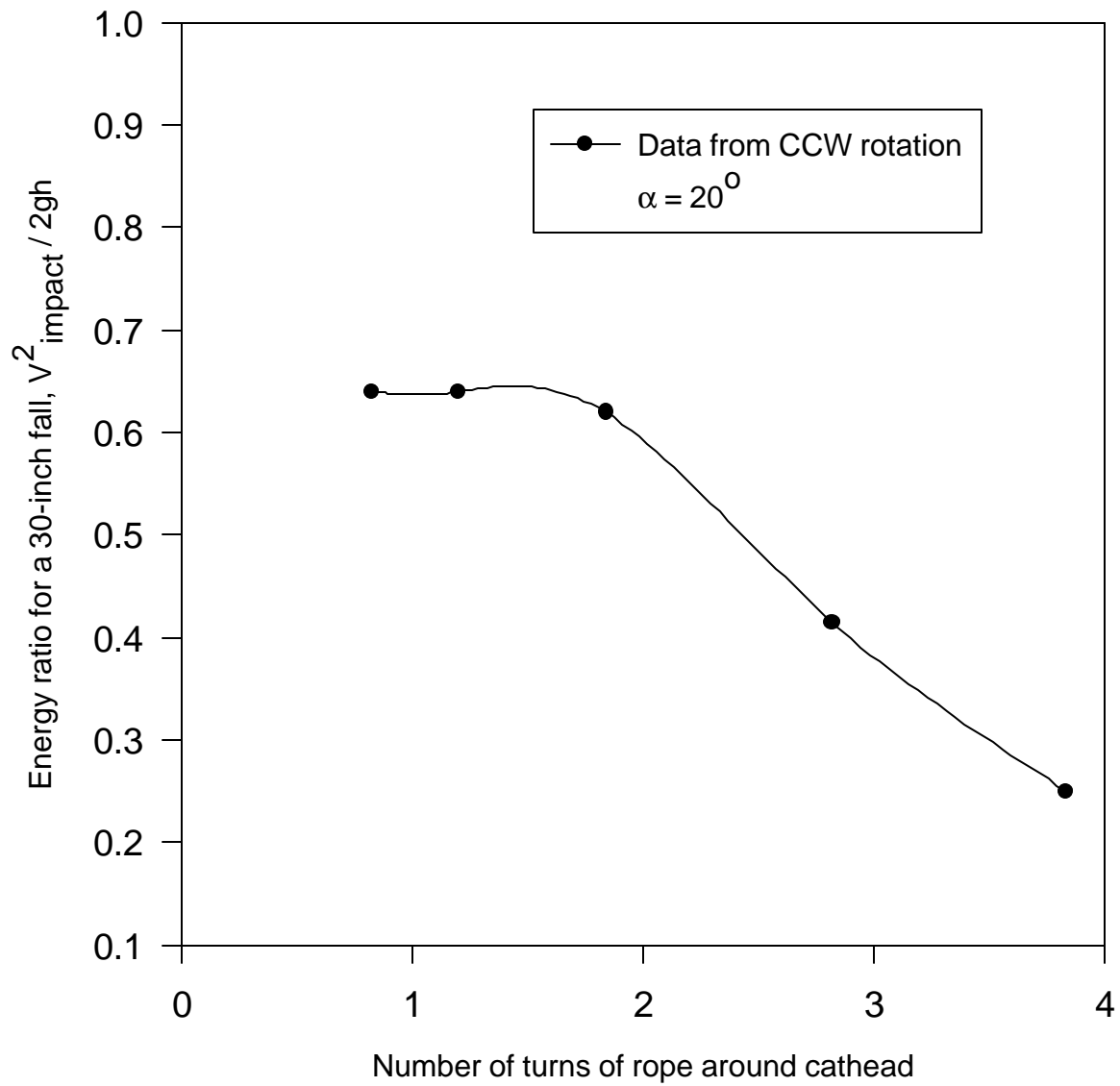


Figure 7. Effect of energy ratio (on impact) on the number of turns of rope around the cathead (after Kovacs, 1980)

- Do not use liners (Kovacs, 1994).

In order to aid in the interpretation of SPT results, **Kovacs et al. (1977)** recommend that the following information be made a standard part of a boring log:

1. Number of turns of rope around cathead
2. Rope age
3. Cathead speed
4. Number of sheaves
5. Mast dimensions
6. Type of guide
7. Type of drop weight (included on most boring logs)
8. Details of striker plate (with or without wood cushion, material)

**Decourt (1990)** makes the following recommendations for equipment and procedures:

- Use size A drill rods weighing 3.4 to 4.0 lb / ft.
- Use a borehole diameter of 2.5 to 4 inches.
- Use a hammer that does NOT have at its base a hard wood cushion block.
- Use casing (not drilling mud).

When the 18 inches of penetration of the sampler cannot be achieved, Decourt recommends that the following procedure be used to find the extrapolated penetration resistance ( $N_{ext}$ ):

$N_{ext}$  is either  $4N_1$  or  $2.4N_2$ , whichever is less

where

$N_1$  = blows required for the first 6 inches of penetration

$N_2$  = blows required for the second 6 inches of penetration

**Skempton (1986)** has developed these recommendations for the SPT:

- Use the wash boring technique or rotary drilling with a tricone drill bit and mud flush. Water or mud in the borehole should be maintained up to groundwater level.
- Use boreholes not less than 2.5 inches or greater than 6 inches in diameter (preferably not more than 4 inches), with the casing (if used) not advanced below the bottom of the borehole.

**Fletcher (1965)** makes the following procedural recommendations for the SPT:

- The drilling fluid or water level inside the borehole should be maintained at or above groundwater level to prevent soil from blowing or heaving into the borehole.
- Use heavy mud if an artesian condition is encountered.
- If the borehole diameter is more than 4 inches, a 2.5-inch casing should be inserted.

## Factors and Variables That Affect SPT Results

Many factors and variables affect the validity and usefulness of SPT results. As a result of these factors, measured penetration resistance may be too high or too low. A measured penetration resistance that is too high leads to unconservative estimates of soil properties and bearing capacity. A measured penetration resistance that is too low leads to overconservative results. Because the ASTM specification allows leeway concerning execution of the test, results obtained from a specific test might not be “wrong”, but may require adjustment to be useful for geotechnical design. Many authors have recognized factors that affect SPT results, as summarized in the following section. Some authors have provided numerical estimates of the change in N-values related to specific factors. Others have indicated an “increase” or “decrease” in the penetration resistance due to these factors. These factors and variables are summarized in this section.

Factors that can affect SPT results include improper drilling methods, improper borehole stabilization, improper testing procedure, use of non-standard or faulty equipment, and incorrect recording of results. This section provides both descriptive and numerical estimates of the effects that these factors have on the measured penetration resistance.

**NAVFAC (1982)** discusses a number of factors that can affect measured penetration resistance. The factors listed in Table 3 are results of faulty equipment and non-standard procedures.

Table 3. Factors which may affect measured penetration resistance (From NAVFAC, 1982)

Procedure	Comments
Inadequate cleaning of the borehole	SPT is only partially made in undisturbed soil. Sludge may be trapped in the sampler and compressed as the sampler is driven, increasing the blow count. This may also prevent sample recovery.
Not seating the sampler spoon on the undisturbed material	Incorrect N-values obtained.
Driving of the sample spoon above the bottom of the casing	N-values are increased in sands and reduced in cohesive soils.
Failure to maintain sufficient hydrostatic head in boring	The water level in the borehole must be at least equal to the piezometric level in the sand , otherwise the sand at the bottom of the borehole may be transformed into a loose state.
Attitude of operators	Blow counts for the same soil using the same rig can vary, depending on who is operating the rig, and perhaps the mood of the operator and time of drilling.
Overdrive sampler	Higher blow counts usually result from overdriven sampler.
Sampler plugged by gravel	Higher blow counts result when gravel plugs sampler, resistance of loose sand could be highly overestimated.
Plugged casing	High N-values may be recorded for loose sand when sampling below groundwater table. Hydrostatic pressure causes sand to rise and plug casing.
Overwashing ahead of casing	Low blow count may result for dense sand since sand is loosened by overwashing.
Drilling method	Drilling technique (e.g., cased holes vs. mud stabilized holes) may result in different N-values for the same soil.

Table 3 continued

Procedure	Comments
Free fall of the drive weight is not attained	Using more than 1.5 turns of rope around the drum and/or using wire cable will restrict the fall of the drive weight.
Not using correct weight	Driller frequently supplies drive hammers with weights varying from the standard by as much as 10 lbs.
Weight does not strike the drive cap concentrically	Impact energy is reduced, increasing N-values.
Not using a guide rod	Incorrect N-value obtained.
Not using a good tip on the sampling spoon	If the tip is damaged and reduces the opening or increases the end area the N-value can be increased.
Use of drill rods heavier than standard	With heavier rods more energy is absorbed by the rods causing an increase in the blow count.
Not recording blow counts and penetration accurately	Incorrect N-values obtained.
Incorrect drilling procedures	The SPT was originally developed from wash boring techniques. Drilling procedures which seriously disturb the soil will affect the N-value, e.g. drilling with cable tool equipment.
Using drill holes that are too large	Holes greater than 4 in. in diameter are not recommended. Use of larger diameters may result in decreases in the blow count.
Inadequate supervision	Frequently a sampler will be impeded by gravel or cobbles causing a sudden increase in blow count; this is not recognized by an inexperienced observer. Accurate recording of drilling, sampling, and depth is always required.
Improper logging of soils	Not describing the sample correctly.
Using too large a pump	Too high a pump capacity will loosen the soil at the base of the hole causing a decrease in blow count.



**Fletcher (1965)** has recognized that many variables and factors can affect SPT results. These include:

- Inadequate cleaning of the borehole.
- failure to maintain sufficient hydrostatic head in the boring.
- variations from an exact 30-inch drop of the drive weight.
- use of drill rods heavier than 1-inch extra heavy pipe or A rods.
- extreme length of drill rods (over 175 feet).
- interference with free fall of the drive weight from any cause.
- use of 140-lb weight without hardwood cushion, block, or guide rod.
- use of sliding weight that can strike the drive cap eccentrically.
- deformed tip on sample spoon.
- excessive driving of sample spoon before the blow count.
- failure to seat sample spoon on undisturbed material.
- driving of sample spoon above bottom of casing.
- carelessness in counting the blows and measuring penetration.

Fletcher comments that the SPT can be used to depths of about 140 feet. At depths greater than 200 feet, the SPT results are too high and unreliable. This is due mainly to energy loss through the drill rods. Farrar (1998) recommends a correction of 1 percent reduction in energy for every 10 ft of rod length in excess of 100 ft. With this correction it may be possible to perform SPT at depths greater than 140 ft.

The SPT may be misleading in very fine sands and inorganic silts above the water table. If water is used as a drilling fluid in these soils, the soil mass to be tested and sampled may be softened or loosened, and this can lead to erroneously low blow counts.

**Broms and Flodin (1988)** have recognized the following as variables that affect SPT results:

- The dimensions of the sampler can vary from country to country. In North America, the sampler has an inside diameter that is 0.118 inches (3 mm) larger than the diameter of the cutting shoe. In Asia and Europe, these diameters are the same. The difference in these diameters can affect SPT N-values by 10 to 30%.
- In the U.K. and Australia, a solid cone can be used in gravel or stony soils, instead of an open split barrel sampler. Penetration resistances obtained with a solid cone will be much different than those obtained with a hollow spilt-spoon sampler.
- The use of drilling mud instead of water can increase the penetration resistance significantly.
- The penetration resistance is not significantly affected by the size and weight of the drilling rods used.
- When hollow stem augers are used, the penetration resistance can be affected by loosened ground in the bottom of the borehole.
- Aging effects (in sands) can lead to an overestimation of relative density from the SPT method.

Table 4. Estimates of the change in N-values due to some common factors (from Broms and Flodin, 1988)

Cause		Estimated % by Which Cause Can Change N
Basic	Detailed	
Effective Stresses at bottom of borehole (sands)	Use drilling mud versus casing and water	+100%
	Use hollow-stem auger versus casing and water	±100%
	Small-diameter hole (3 in.) versus large diameter (18 in.)	50%
Dynamic energy reaching sampler (all soils)	2 to 3 turn rope-cathead versus free drop	+100%
	Large versus small anvil	+50%
	Length of rods	
	Less than 10 feet	+50%
	30 to 80 feet	0%
more than 100 feet	+10%	
	Variations in height drop	±10%
	A-rods versus NW-rods	±10%
Sampler design	Larger ID for liners, but no liners	-10% (sands) -30% (insensitive clays)
Penetration interval	$N_{0 \text{ to } 12 \text{ in.}}$ instead of $N_{6 \text{ to } 18 \text{ in.}}$	-15% (sands) -30% (insensitive clays)
	$N_{12 \text{ to } 24 \text{ in.}}$ instead of $N_{6 \text{ to } 18 \text{ in.}}$	+15% (sands) +30% (insensitive clays)

+ = measured value of N is too high

- = measured value of N is too low

**Tokimatsu (1988)** as compiled the following factors that influence SPT N-values in sand:

Table 5. Estimates of the change in N-values due to various factors (from Tokimatsu, 1988)

Cause		Estimated % change in N
Basic	Detailed	
Effective Stresses at bottom of borehole	Casing and water versus drilling mud	-50%
	Allow head imbalance	+100%
	Large versus small borehole	-35%
Dynamic energy reaching sampler	Rope-cathead versus free drop	+100%
	Large versus small anvil	+50%
	Short versus long rod	+30%
Sampler design	Large ID for liners, but no liners vs. standard	±10-20%
Blow count rate	Slow versus standard	+10%
Penetration resistance count	0-12 in. versus 6-18 in.	-15%
	12-24 in. versus 6-18 in.	+15%

+ = measured value of N is too high

- = measured value of N is too low

Tokimatsu (1988) also identified the following limitations of the SPT:

1. It does not provide continuous information of soil resistance with depth. Thin layers of weak material may be missed.
2. Its apparatus and procedure have not been completely standardized.

**Decourt (1990)** presents the following factors that cause variations in SPT N-values:

Table 6. Changes in N-values due to faulty equipment and non-standard procedures (from Decourt, 1990)

Factor	Effect on N-value
Variation in drop height from exactly 30 inches	either
Failure of the driller to completely release the tension on the rope	increase
Use of wire line rather than manila rope	increase
Insufficient lubrication of the pulley	increase
Attitude of operators	either
Use of incorrect weight	either
Not striking the anvil concentrically	increase
Not using a guide rod	increase
Incorrectly reading or recording blowcounts	either
Failure to maintain sufficient hydraulic head	decrease
Borehole diameter greater than 6 inches	decrease
Using a boring pump of too high capacity	increase
Using drilling mud instead of casing (in sands)	increase
Using a deformed sampler	increase
Driving the sampler above the bottom of the casing (in sands)	increase
Sampler plugged with gravel	increase
Penetration interval:	
0-12 inches instead of 6-18 inches	decrease
12-24 inches instead of 6-18 inches	increase

**Kulhawy and Trautmann (1996)** summarized the effects of the following SPT testing variables:

Table 7. Changes in N-values due to various factors (from Kulhawy and Trautmann, 1996)

SPT Variable		
Group	Item	Relative Effect on Test Results
Equipment	Non-standard sampler	moderate
	Deformed or damaged sampler	moderate
	Rod diameter/weight	minor
	Rod length	minor
	Deformed drill rods	minor
	Hammer type	moderate to significant
	Hammer drop system	significant
	Hammer weight	minor
	Anvil size	moderate to significant
	Drill rig type	minor
Procedural / Operator	Borehole size	moderate
	Method of maintaining hole	minor to significant
	Borehole cleaning	moderate to significant
	Insufficient hydrostatic head	moderate to significant
	Seating of sampler	moderate to significant
	Hammer drop method	moderate to significant
	Error in counting blows	minor

## Corrections to Measured Blow Counts

In order for field measured blow counts to be used in geotechnical engineering applications, they should be adjusted for the effects of hammer energy, overburden pressure, and, in some cases, various other factors that influence the results. Measured blow counts can be normalized to  $N_{60}$  or  $N_{1,60}$  where  $N_{60}$  is the blow count corrected to 60% of the theoretical free-fall hammer energy and  $N_{1,60}$  is the blow count corrected to 1 tsf of effective overburden pressure and 60% of the theoretical free-fall hammer energy. The most general equations for  $N_{60}$  and  $N_{1,60}$  are as follows:

$$N_{60} = N_{\text{field}} C_E C_R C_B C_S C_A C_{BF} C_C$$

$$N_{1,60} = N_{\text{field}} C_N C_E C_R C_B C_S C_A C_{BF} C_C$$

where

$N_{60}$  = blow count corrected to 60% of the theoretical free-fall hammer energy

$N_{1,60}$  = blow count corrected to 1 tsf of overburden pressure and 60% of theoretical free-fall hammer energy

$N_{\text{field}}$  = blow count measured in the field

$C_N$  = overburden correction factor. Note that the subscript of "N" is used here because the overburden correction was one of the original correction factors. It is often used by itself to correct N, therefore it is denoted  $C_N$ .

$C_E$  = energy correction factor

$C_R$  = rod length correction factor

$C_B$  = borehole diameter correction factor

$C_S$  = liner correction factor

$C_A$  = anvil correction factor

$C_{BF}$  = blow count frequency correction factor

$C_C$  = hammer cushion correction factor

For most geotechnical applications, the last six correction factors list above are not used. In some cases, they may be used to provide better data. In most cases,  $N_{60}$  and  $N_{1,60}$  are defined as:

$$N_{60} = N_{\text{field}} C_E$$

$$N_{1,60} = N_{\text{field}} C_E C_N$$

## Overburden Correction Factor - $C_N$

In order to compare blow counts measured at different depths, measured blow counts should be adjusted to a standard overburden pressure of 1 tsf. The penetration resistance of cohesionless materials (sands) depends heavily on the confining pressure. For the same sand, an SPT performed at a shallow depth will have a lower blow count than for an SPT performed at a great depth. By multiplying  $N_{\text{field}}$  by  $C_N$ , the effects of confining pressure are compensated. Recommended values of  $C_N$  are summarized in Table 8. These equations are plotted together in Figure 8. Figure 9 shows values of  $C_N$  recommended by Seed et al. (1985) which are based on effective overburden pressure and relative density ( $D_r$ ).

Table 8. Overburden correction factors ( $C_N$ ) (after Carter and Bentley, 1991)

Reference	Correction Factor ( $C_N$ )	Units of overburden pressure ( $\sigma_v'$ )
Peck and Bazaraa (1969)	$C_N = \begin{cases} \frac{4}{1+2\sigma_v'} & \sigma_v' \leq 1.5 \\ \frac{4}{3.25+0.5\sigma_v'} & \sigma_v' > 1.5 \end{cases}$	ksf
Peck et al. (1974)	$C_N = 0.77 \log_{10} \frac{20}{\sigma_v'}$	kg/cm <sup>2</sup> or tsf
Tokimatsu and Yoshimi (1983)	$C_N = \frac{1.7}{0.7 + \sigma_v'}$	kg/cm <sup>2</sup> or tsf
Liao and Whitman (1986)	$C_N = \sqrt{\frac{1}{\sigma_v'}}$	kg/cm <sup>2</sup> or tsf
Skempton (1986)	$C_N = \begin{cases} \frac{2}{1 + \sigma_v'} & \text{For fine sands of medium relative density} \\ \frac{3}{2 + \sigma_v'} & \text{For dense, coarse sands when normally consolidated} \\ \frac{1.7}{0.7 + \sigma_v'} & \text{For overconsolidated fine sands} \end{cases}$	kg/cm <sup>2</sup> or tsf



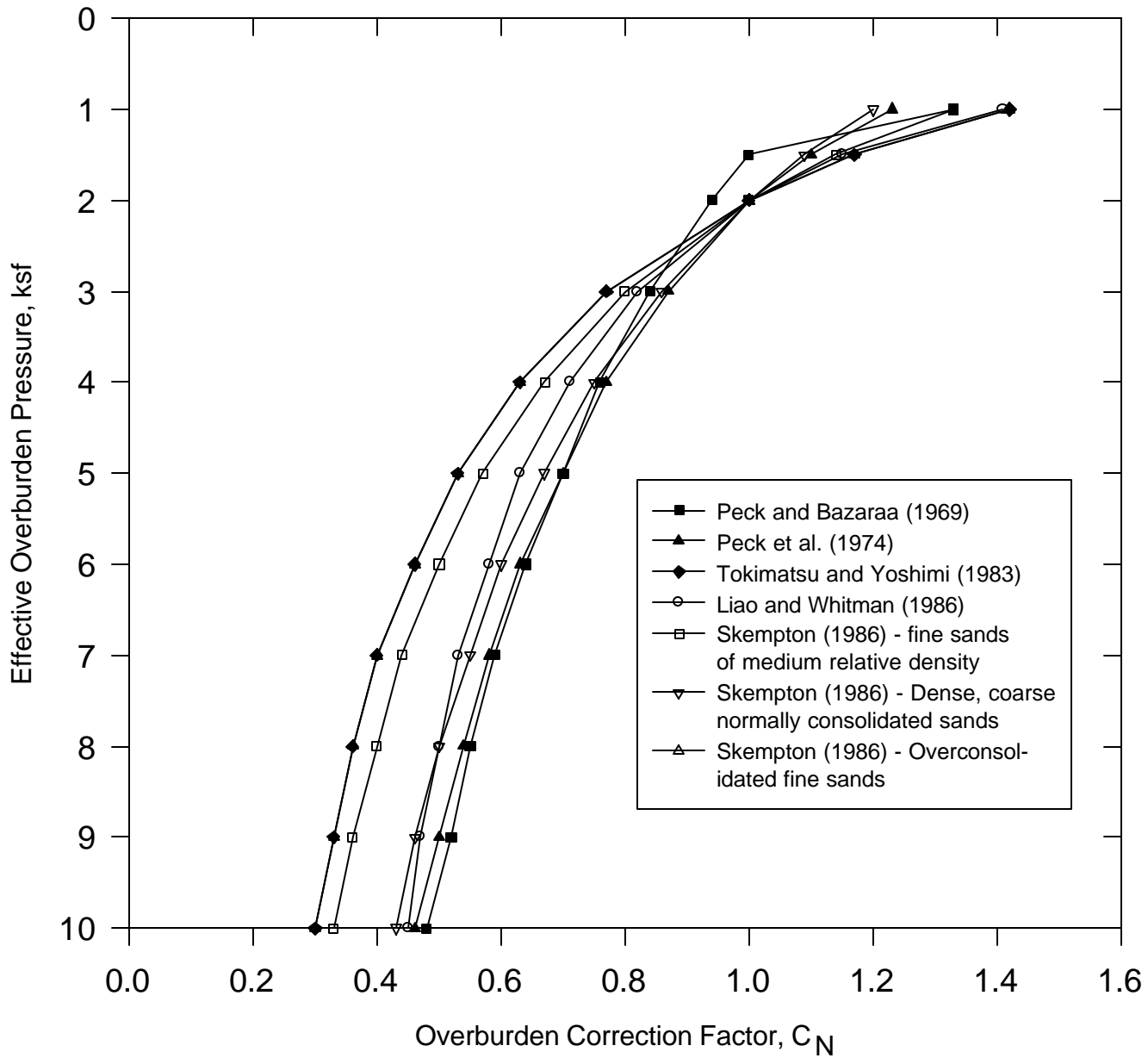


Figure 8. Overburden correction factors

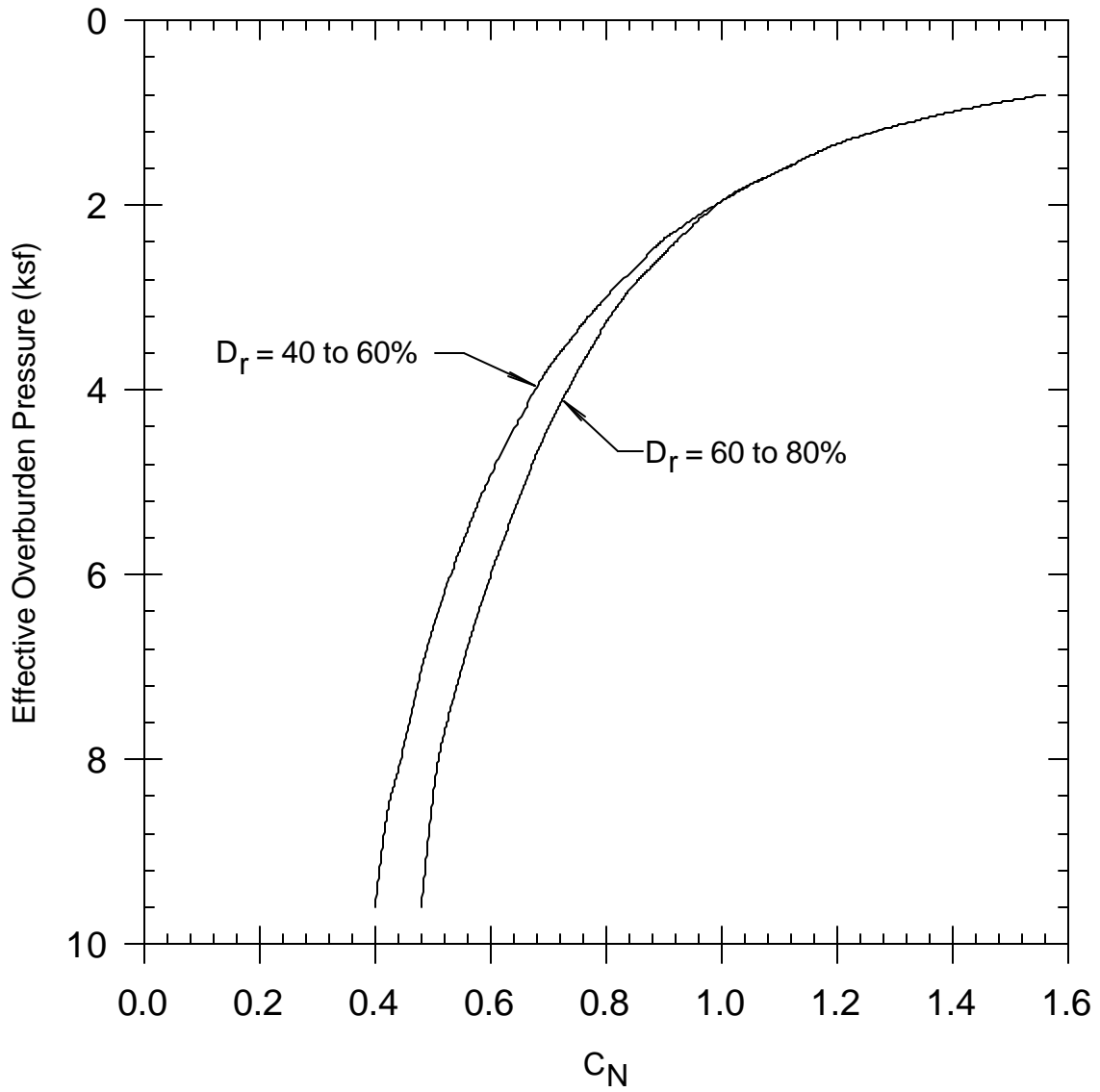


Figure 9. Chart for values of  $C_N$  (after Seed et al., 1985)

## Energy Correction Factor - $C_E$

One of the most important corrections to be made to  $N_{field}$  is for the energy delivered to the drill rods. The energy delivered from the hammer depends on the way the hammer is lifted and released, and on the design of the hammer. Theoretically, a 140 lb. hammer falling 30 inches should produce 4200 in-lbs of energy. Due to losses (friction, lack of free-fall), the actual energy delivered to the drill rods is less than 4200 in-lbs. The objective of applying the energy correction factor is to adjust the blow count to the value that would have been measured if a hammer imparting 60% of the theoretical energy had been used in the test. The correction factor is defined as:

$$C_E = \frac{ER}{60}$$

where

$C_E$  = hammer energy correction factor

ER = hammer system energy ratio expressed as a percentage of the theoretical energy of a 140-lb. hammer falling 30 inches

Each type of hammer has a value of  $C_E$ , as shown in Table 9.

Table 9. Energy correction factors ( $C_E$ ) (from Seed et al., 1985)

Hammer Type	ER (%)	$C_E$
Donut	45	0.75
Safety	60	1.0
Trip	100	1.67

Youd and Idriss (1997) propose a range of  $C_E$  values for each hammer due to variations in drilling and testing equipment, as shown in Table 10.

Table 10. Ranges of energy correction factors ( $C_E$ ) (from Youd and Idriss, 1997)

Hammer Type	$C_E$
Donut	0.5 to 1.0
Safety	0.7 to 1.2
Automatic-trip Donut	0.8 to 1.3

Alternatively, the energy ratio may be measured directly following procedures outlined in ASTM D 6066-96, *Standard Practice for Determining Normalized Penetration Resistance of Sands for Evaluation of Liquefaction Potential*.

### Rod Length Correction Factors ( $C_R$ )

The energy delivered to the sampler is affected to some extent by the length of the drill rod, and measured blow counts are sometimes corrected for this factor. Tables 11 and 12 summarize values of  $C_R$  recommended by Seed et al. (1985), Skempton (1986), and Youd and Idriss (1997).

Table 11. Rod length correction factors ( $C_R$ ) (after Tokimatsu, 1988)

Rod length	$C_R$	
	Seed et al. (1985)	Skempton (1986)
< 10 feet	0.75	-
10 - 13 feet	1.0	0.75
13 - 20 feet	1.0	0.85
20 - 30 feet	1.0	0.95
> 30 feet	1.0	1.0

Youd and Idriss (1997) recommended the following rod length correction factors:

Table 12. Rod length correction factors ( $C_R$ ) (after Youd and Idriss, 1997)

Rod length	$C_R$
10-13 feet	0.75
13 - 20 feet	0.85
20 -30 feet	0.95
30 -100 feet	1.0
> 100 feet	< 1.0

### Borehole Diameter Correction Factors ( $C_B$ )

Measured SPT N-values are sometimes corrected if they are made in boreholes larger than 4.5 inches. When boreholes are larger than 4.5 inches, stress relaxation occurs and measured N-values are lower than they would be for a smaller-diameter hole. This effect can be significant in sands, but is probably negligible in cohesive soils (Sanglerat and Sanglerat, 1982). Table 13 provides values of the borehole size correction factor,  $C_B$ .

Table 13. Borehole diameter correction factors ( $C_B$ ) (after Skempton, 1986)

Borehole diameter	$C_B$
2.5 to 4.5 inches	1.0
6 inches	1.05
8 inches	1.15

### Liner Correction Factors ( $C_S$ )

The SPT may be performed with or without sample liners. An illustration of the sample liner configuration is shown in Figure 10. Liners are often omitted in practice and the inside diameter of the sampling tube is thereby increased from 1-3/8 inches to 1-1/2 inches. The increase in inside diameter reduces the friction on the inside of the sampler and reduces the measured penetration resistance of the soil. Youd and Idriss (1997) have proposed a range of corrections due the absence of liners in Table 14.

Table 14. Liner correction factors ( $C_S$ ) (after Youd and Idriss, 1997)

Sampler Configuration	$C_S$
Standard sampler (with liners)	1.0
U.S. sampler without liners	1.1 to 1.3

### Anvil Correction Factors ( $C_A$ )

When the hammer falls during the SPT, it strikes an anvil attached to the drill rod stem. See Figures 1 and 2. The anvil is usually metallic and can vary in shape, size, and weight. The amount of energy transferred to the drill rods depends on the weight of the anvil (Tokimatsu, 1988). Table 15 provides correction factors to  $N_{field}$  based on hammer type and anvil weight.

Table 15. Anvil correction factors ( $C_A$ ) (after Tokimatsu, 1988)

Hammer	Anvil	$C_A$
Donut	Small (4.4 lbs)	0.85
	Large (26.5 lbs)	0.70
Safety	5.5 lbs	0.90

Note that Table 15 provides no  $C_A = 1.0$ . For the safety hammer,  $C_A = 1.0$  is commonly used.

### Blow count Frequency Correction Factors ( $C_{BF}$ ) (only for sands below the water table)

The rate at which blows are applied to the drill rods can affect the measured N-value. The correction factor  $C_{BF}$  accounts for pore pressure effects in sands below the water table. The value of  $C_{BF}$  is dependent on the value of  $N_{1,60}$ . Table 16 lists blow

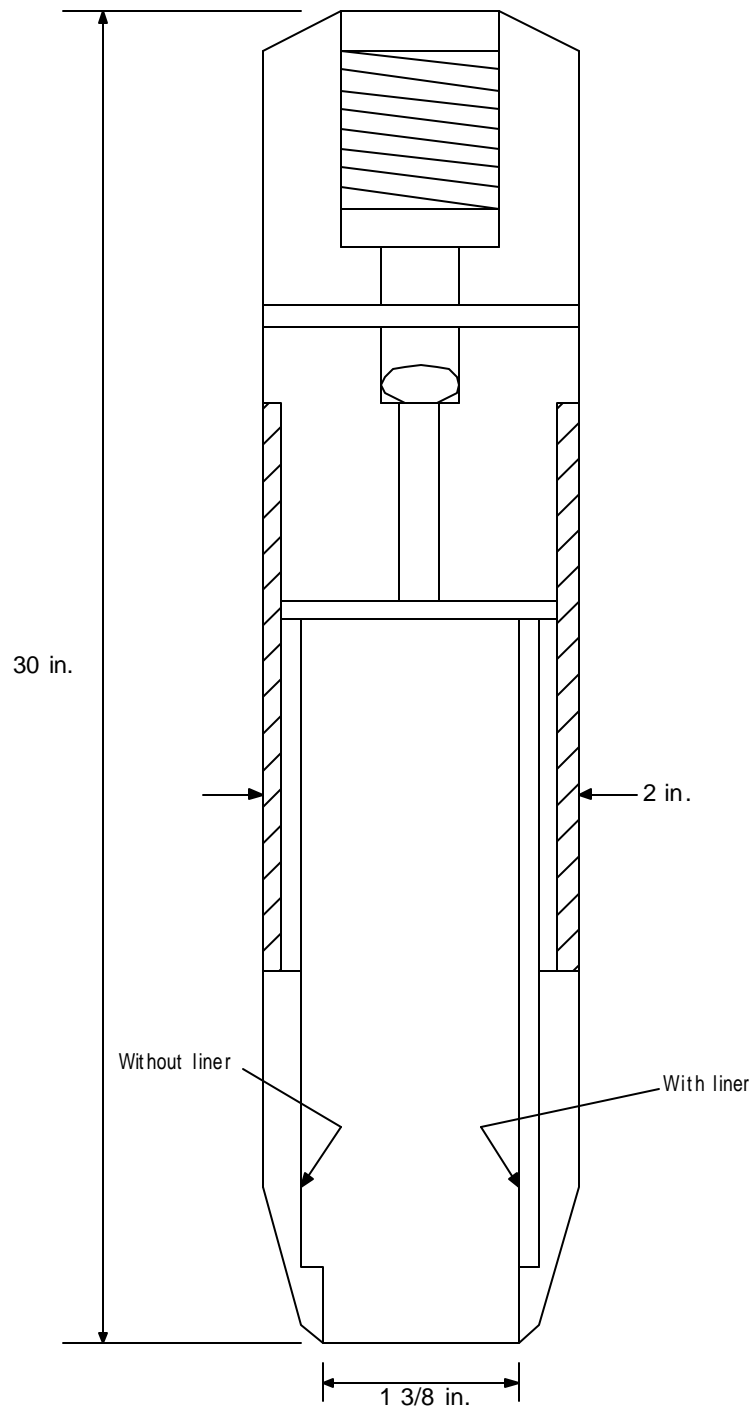


Figure 10. Sampler liner configuration. Note that the right side of the sampler contains a liner and is at a constant diameter. The left side contains no liner and has a varying diameter. (after Al-Khafaji and Andersland, 1992)

count frequency correction factors. If the frequency of hammer blows is 30 - 40 blows per minute, use  $C_{BF} = 1.0$ .

Table 16. Blow count frequency correction factors ( $C_{BF}$ ) (after Decourt, 1990)

$N_{1,60}$	Frequency of hammer blows	$C_{BF}$
< 20	10 - 20 blows per minute	0.95
> 20	10 -20 blows per minute	1.05

Hammer Cushion Correction Factors ( $C_C$ )

Some hammers have a hard wood cushion block on the anvil striking surface. The block absorbs energy and increases the measured N-value. These N-values should be adjusted with the factors shown in Table 17.

Table 17. Hammer cushion correction factors ( $C_C$ ) (after Decourt, 1990)

Type of hard wood cushion block	$C_C$
none	1.0
new	0.95
used	0.90

Corrections for saturated very fine or silty sand:

When the SPT is performed in saturated very fine or silty sand, the measured N-values need to be corrected for dynamic pore pressure effects (Meyerhof, 1956). Correction is only necessary for measured blow counts greater than 15.

$$N = 15 + \frac{(N' - 15)}{2} \quad \text{for } N' > 15$$

where

$N'$  = measured blow count

$N$  = corrected blow count

## Becker Penetration Test (BPT) Correlations with the SPT

In soils containing gravels and/or cobbles, the SPT can be unreliable, and can produce unconservative results. BPT blow counts are regarded by some investigators as more reliable than SPT N-values in gravelly soils (Campanella and Sy, 1994). The Becker Penetration Test (BPT) results have been correlated to equivalent SPT N-values. These equivalent SPT blow counts have been used to predict liquefaction in gravelly soils.

The BPT consists of driving a double-walled pipe (casing) into the ground with a double-acting diesel pile hammer. The casing can be driven open (for drilling and sampling), or close-ended (as a large-scale penetration test used to evaluate density and pile driveability). While the pipe is being driven, the driving resistance or blow count per 12 inches of penetration is recorded. The Becker penetration resistance is defined as the number of hammer blows required to drive the casing through an increment of 12 inches. Figure 11 shows a schematic drawing of the Becker sampling operation.

BPT-SPT correlations are not always accurate and may be uncertain for three reasons:

1. The diesel hammer used in the BPT has a variable energy output. It inherently gives lower energy in soft ground driving conditions, and higher energy in hard driving conditions (Sy 1997).
2. Shaft friction acting on the BPT pipe during driving is significant, especially at depths greater than 100 feet.
3. Variations in equipment and procedures used to perform the SPT cause variations in results (Harder and Seed, 1986).

The BPT has not been standardized (Youd and Idriss, 1997) and test equipment varies. The casings (pipes) are available in 8 or 10-foot lengths and the following sizes:

- 5.5 inch O.D. with 3.3 inch I.D. (original size)
- 6.6 inch O.D. with 4.3 inch I.D.
- 9.0 inch O.D. with 6.0 inch I.D.

Sy (1997) notes that the BPT is performed with one of two basic drill rig types:

- The older and more compact HAV180, or
- The newer and more elaborate AP1000.



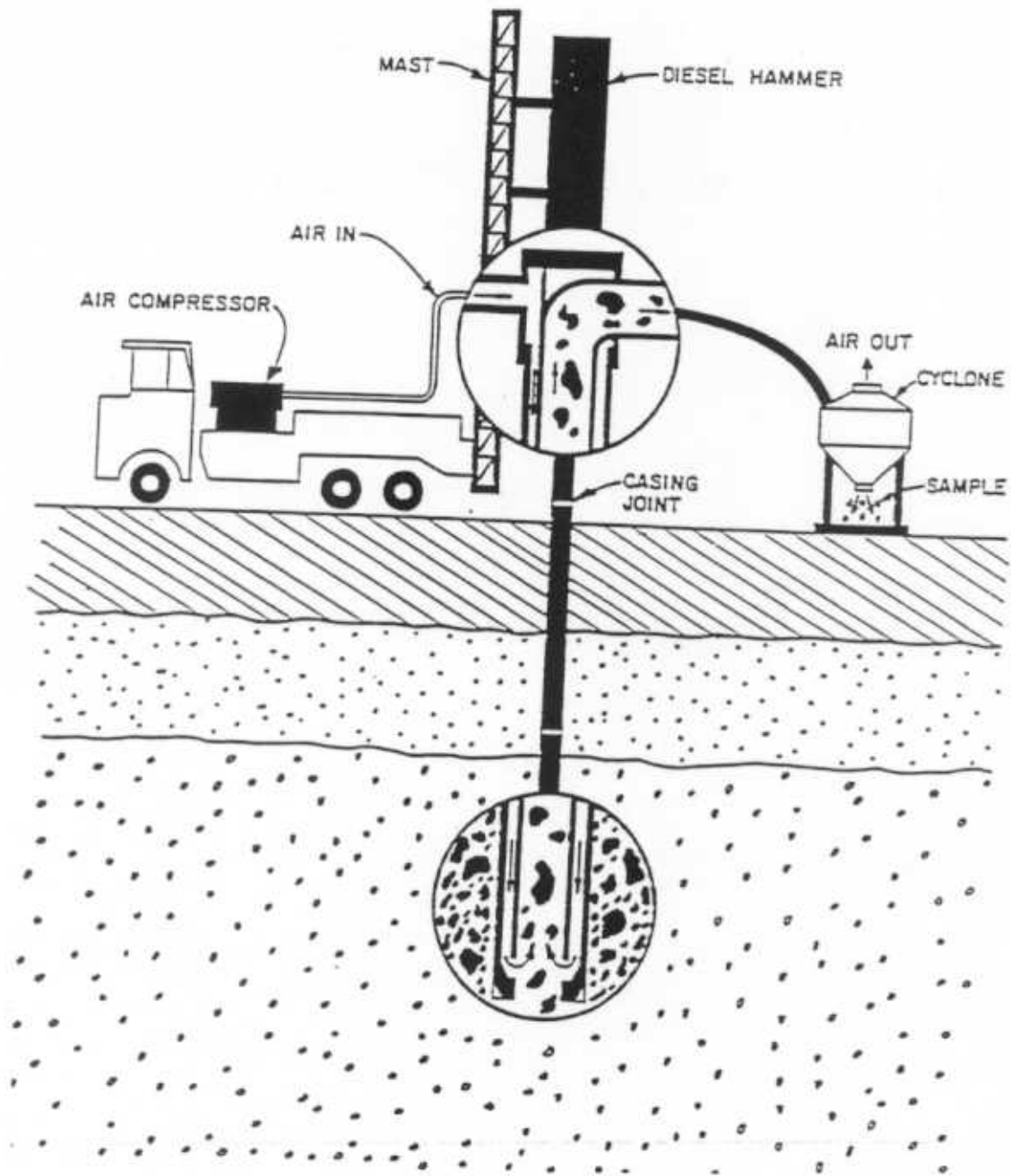


Figure 11. Schematic diagram of Becker sampling operation (from Harder, 1997)

Both of these drill rigs use an International Construction Equipment (ICE) Model 180 double-acting atomized fuel injection diesel pile hammer with a manufacturer's rated energy of 8100 ft•lbs. A blow rate of 90 to 95 blows per minute (at maximum stroke) is typical (Campanella and Sy, 1994). The hammer is closed at the top and part of its energy is developed by compression of air in the hammer cylinder (Harder and Seed, 1986). Figure 12 illustrates the operating principle of a double-acting diesel pile hammer. By measuring the pressure in the top chamber (the bounce chamber pressure), the driving energy of the hammer can be estimated.

The Becker penetration resistance is strongly affected by the bounce chamber pressure in the diesel hammer. As the energy output of the hammer changes due to temperature, pressure, or air-fuel mixture, so does the kinetic energy at impact. Sy and Campanella (1994) note that the kinetic energy, not the potential energy, of the ram appears to control the resulting blow count.

The BPT suffers from the same lack of standardization as the SPT. Due to specifications that are subject to individual interpretation, some guidance or standard procedure is desirable. The following authorities have offered recommendations and guidance for the BPT:

**Harder and Seed (1986)** recommend using AP1000 drill rigs equipped with supercharged diesel hammers, 6.6-inch O.D. casing, and a plugged bit.

**Youd and Idriss's (1997)** recommendations are similar to Harder and Seed's (1986) and include:

1. Use AP1000 drill rigs equipped with supercharged diesel hammers, and a plugged 6.6-inch O.D. casing.
2. Bounce chamber pressures should be used to adjust measured BPT blow counts to  $N_{bc}$  (corrected Becker blow count) to account for variations in diesel hammer combustion efficiency.
3. The influence of casing friction is intrinsically accounted for in the Harder and Seed (1986) BPT-SPT correlation. This correlation should not be used for depths greater than 100 feet or for sites with thick, dense deposits overlying loose sands or gravels.

**Sy and Campanella (1994)** recommend the following procedure for estimating SPT  $N_{60}$  values from the BPT performed with a 6.6-inch O.D. Becker pipe:

1. Monitor BPT with a pile driving analyzer in accordance with ASTM D4945-89, which governs high-strain dynamic testing of piles. Correct the recorded blow counts to  $N_{b30}$  using:

$$N_{b30} = N_b \frac{ENTHRU}{30}$$

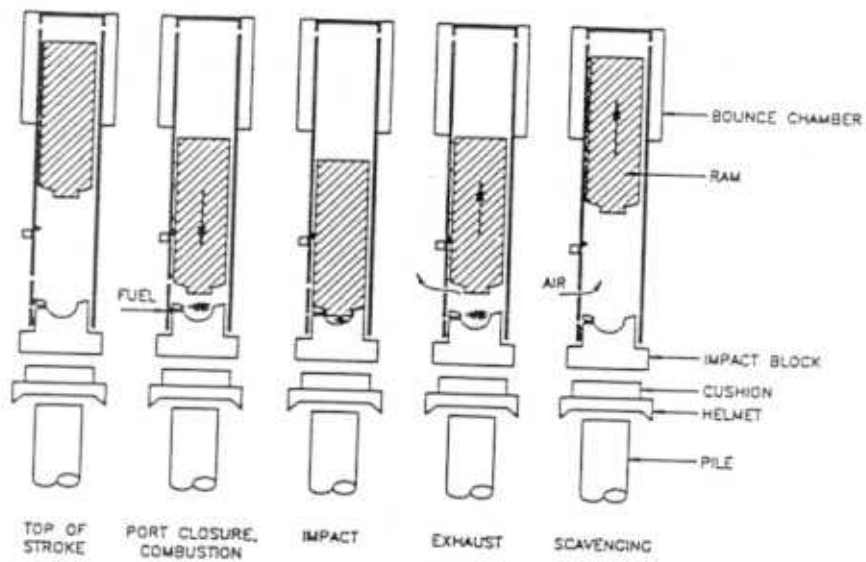


Figure 12. Operating principle of double-acting atomized fuel injection diesel pile hammer (from Sy and Campanella, 1993)

where

$N_{b30}$  = BPT blow count normalized to the 30% reference energy level

$N_b$  = measured Becker blow count

ENTHRU = measured maximum transferred energy expressed as a percentage of the rated hammer energy of 8100 ft-lbs.

2. Select representative blows for CAPWAP analysis to determine the total shaft resistance ( $R_s$ ) at specific depths and estimate or interpolate between computed  $R_s$  values for other depths.

CAPWAP is a complex numerical procedure for interpreting pile driving data.

3. With the energy-corrected BPT  $N_{b30}$  and  $R_s$  values, estimate equivalent SPT  $N_{60}$  from Figure 13.

**Harder and Seed (1986)** developed a BPT-SPT correlation by standardizing the BPT blow counts to a constant combustion condition by measuring peak pressure in the bounce chamber of the diesel hammer. Their correlation involves 2 steps:

Step 1: The field measured (uncorrected) BPT blow count,  $N_B$  is corrected to a reference combustion condition using Figure 14.

Step 2: The corrected BPT blow count,  $N_{BC}$  is used to estimate the equivalent SPT  $N_{60}$  using Figure 16.

The procedure for using Figure 14 is as follows:

1. Plot the bounce chamber pressure at sea level with the uncorrected Becker blow count,  $N_B$ .
2. From this point, follow the blow count correction curves for reduced combustion efficiencies down to the constant combustion rating curve AA.
3. The point on curve AA is then used to obtain the corrected Becker blow count,  $N_{BC}$ .

Harder and Seed (1986) provide the following examples to clarify the use of Figure 14:

Example 1: An uncorrected blow count,  $N_B$  was measured as 43. It was obtained at sea level with a bounce chamber pressure of 18 psig. Using Figure 15, the corrected Becker blow count would be 30.

If the BPT is conducted at an elevation higher than sea level, the bounce chamber pressure needs to be corrected. Using Table 18, the bounce chamber pressure is corrected to sea level conditions. Example 2 clarifies the use of Table 18.

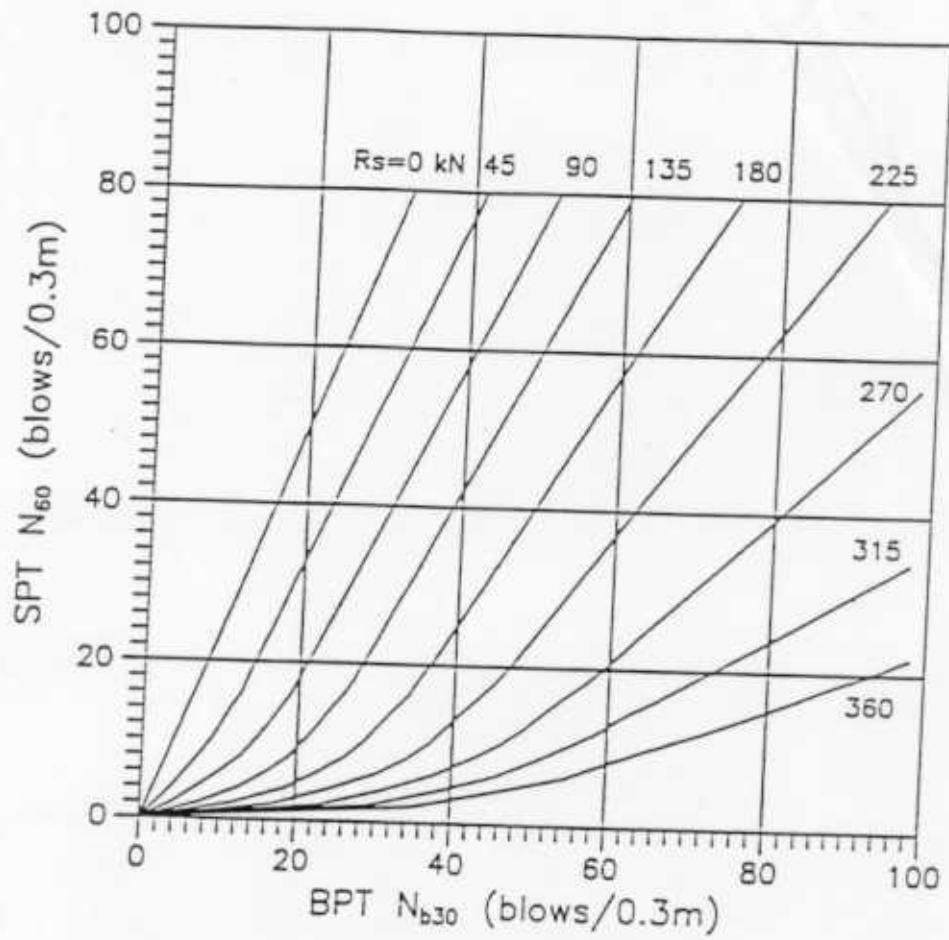


Figure 13. Computed BPT vs. SPT correlation for different BPT casing shaft resistance (from Sy and Campanella, 1994)

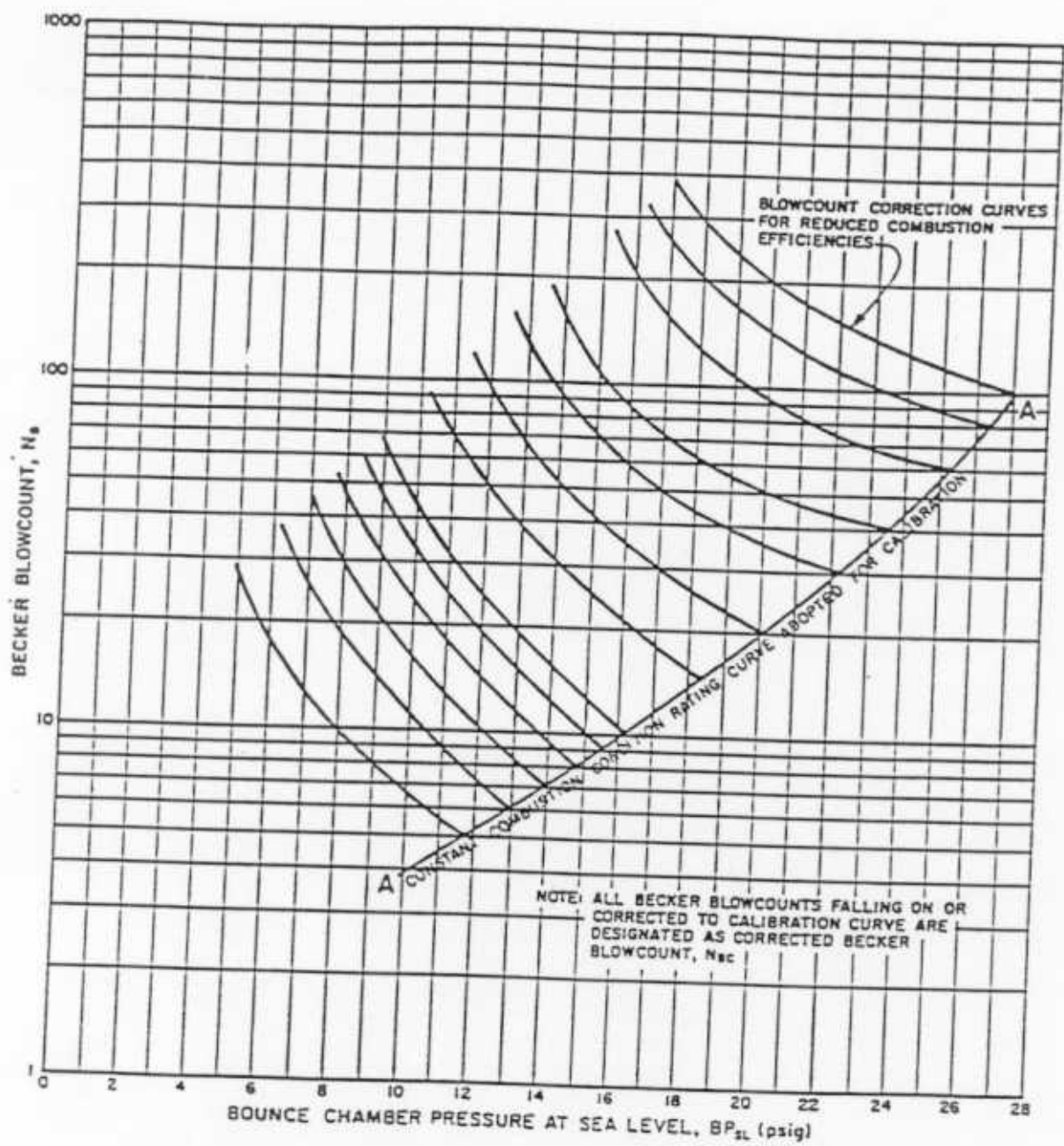


Figure 14. Correction curves adopted to correct Becker blow counts to constant combustion curve adopted for correlation (from Harder and Seed, 1986)

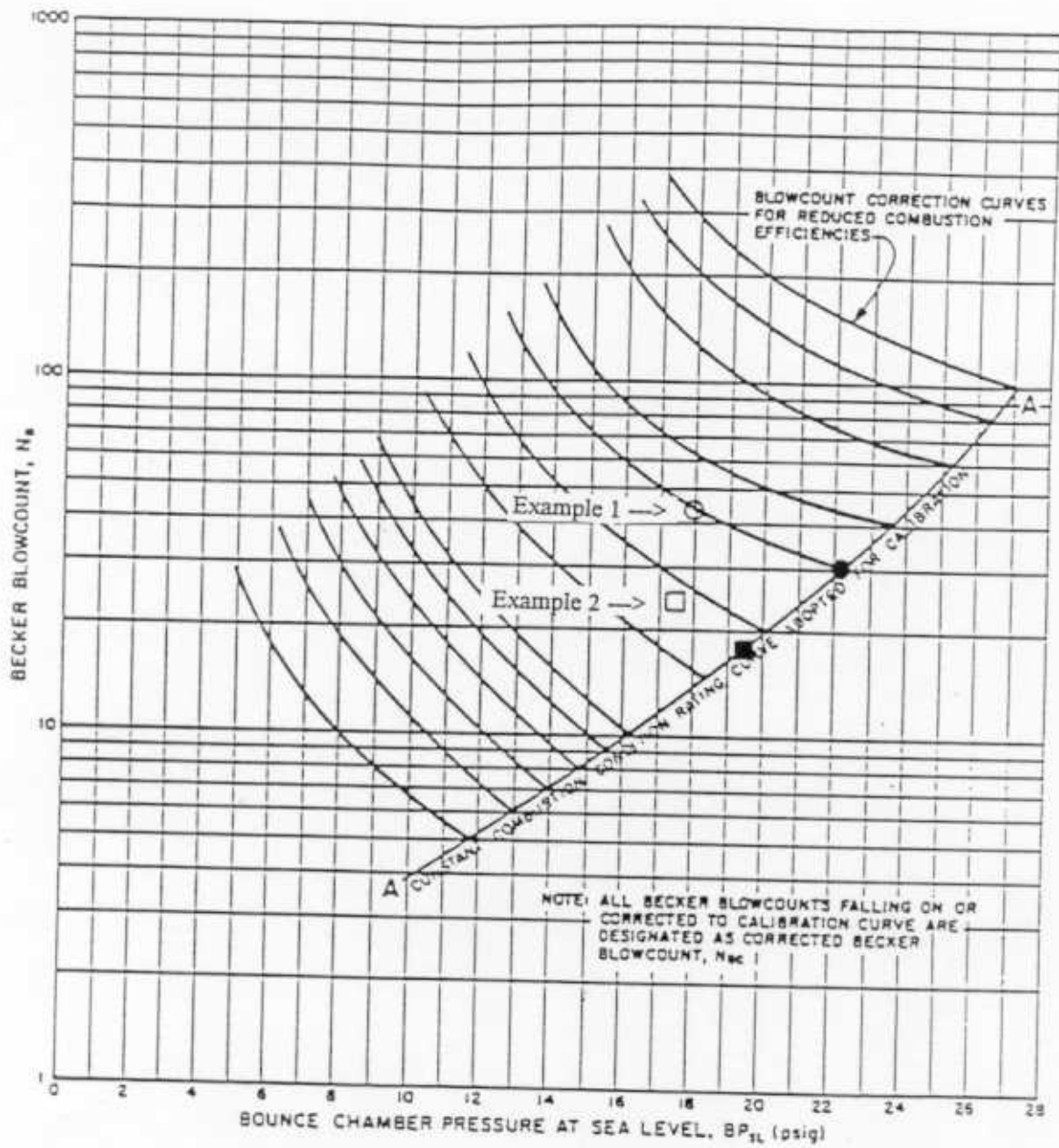


Figure 15. Examples illustrating the use of the correction curves in Figure 14. The circles correspond to Example 1 and the squares correspond to Example 2. (after Harder and Seed, 1986)

Table 18. Elevation Corrections for Bounce Chamber Pressures (in psig) (data from Harder and Seed, 1986)

Elevation (feet)	Measured Bounce Chamber Pressure (psig)			
	10	15	20	25
0 (Sea Level)	0	0	0	0
1000	0.8	0.9	1.1	1.1
2000	1.5	1.8	2.1	2.2
3000	2.3	2.8	3.2	3.2
4000	3.0	3.7	4.2	4.3
5000	3.8	4.6	5.3	5.4
6000	4.5	5.5	6.3	6.5
7000	5.3	6.4	7.4	7.6
8000	6.0	7.4	8.4	8.7



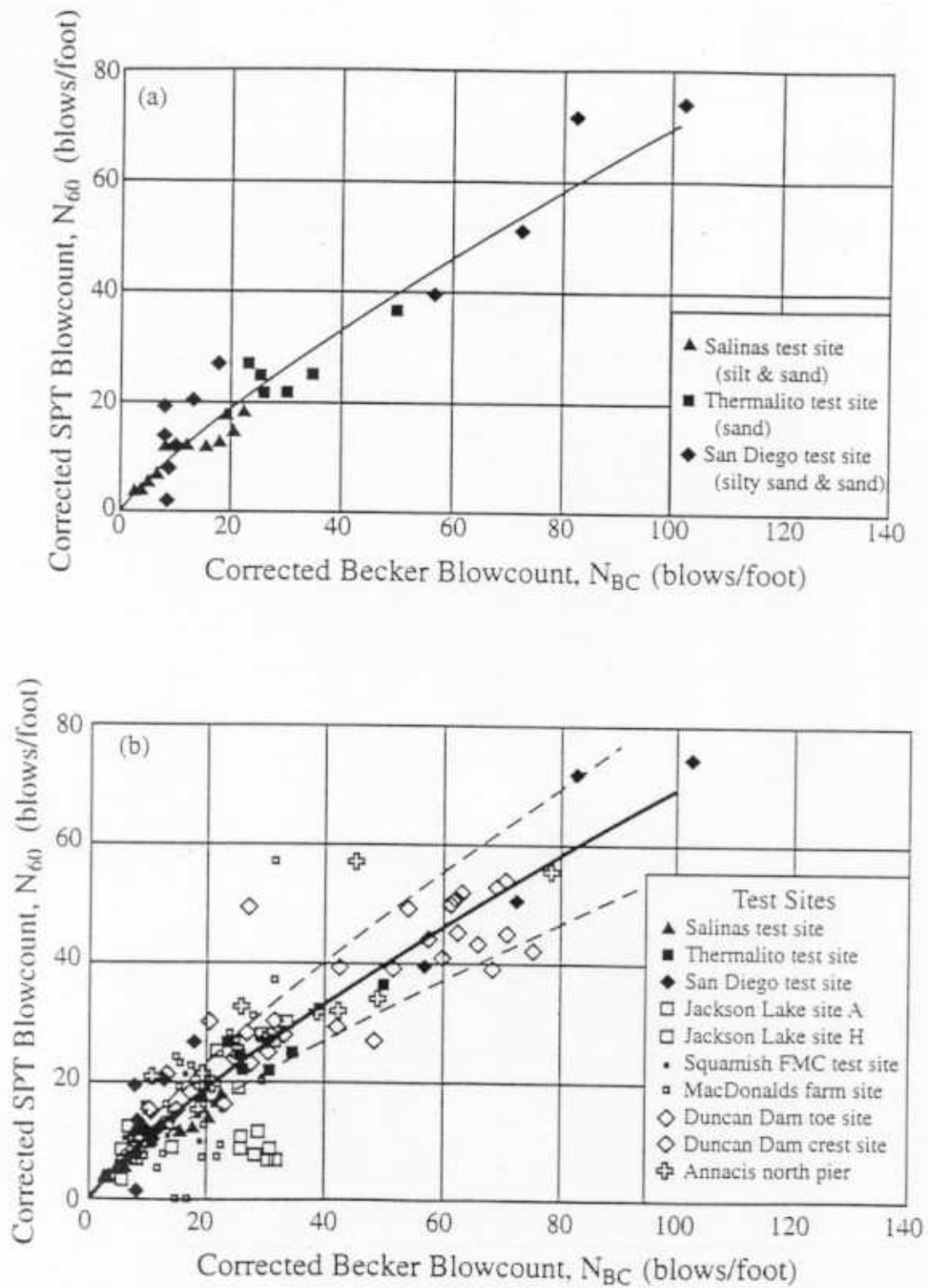


Figure 16. Correlation between corrected Becker and SPT blow counts (from Harder and Seed, 1986)

Example 2: An uncorrected blow count,  $N_B$  of 24 was measured at an elevation of 6000 feet with a bounce chamber pressure of 12.5 psig. Using Table 18 and interpolating between bounce chamber pressures of 10 and 15, the bounce chamber pressure correction is 5.0 psig (corrected bounce chamber pressure = 12.5 + 5.0 = 17.5 psig). From Figure 15, an  $N_B = 24$  and a corrected bounce chamber pressure = 17.5 psig yields an  $N_{BC} = 18$ .

Sy (1997) made the following comments about the Harder and Seed approach:

- Peak bounce chamber pressure can easily be measured in the field.
- Reference combustion line (A-A) is specific for the particular hammer used - this approach cannot be applied to different Becker rigs or hammers (Sy and Campanella, 1993).
- This approach does not consider soil friction on the Becker casing.

Sy (1993) used the complex CAPWAP analysis procedure to calculate the shaft resistance ( $R_s$ ) along the Becker casing. The measured  $R_s$  values and  $N_{b30}$  were then used to find the equivalent SPT  $N_{60}$  as seen in Figure 13.

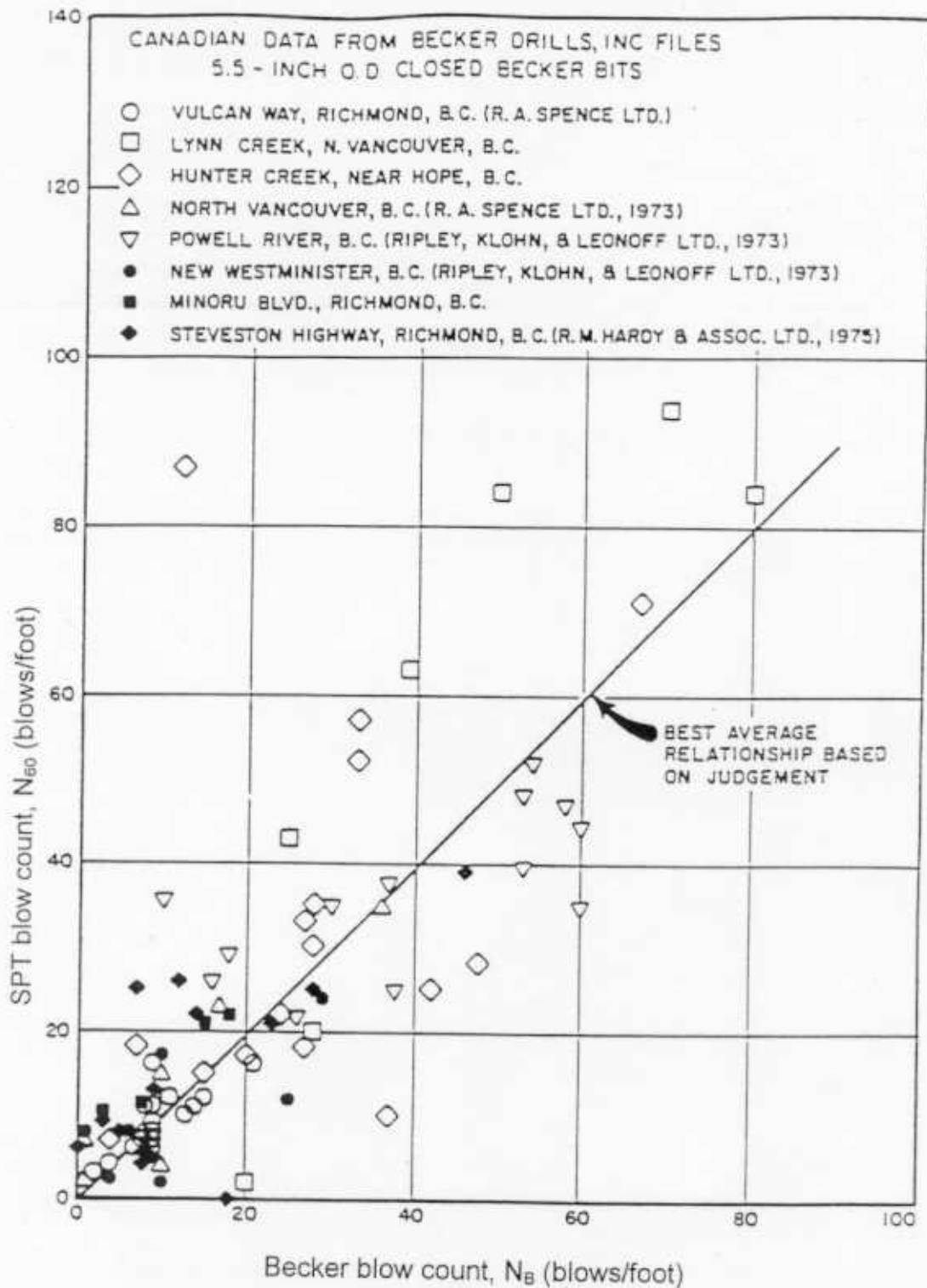
While the BPT is generally used in gravelly soils, some BPT correlations with SPT have been developed for other soil types. Table 19 provides a list of BPT-SPT correlations for different types of soil. Figures 17-21 show the correlations listed in Table 19 in plot form. Figure 21 is a summary of Figures 17-20 and shows all correlations on one plot. It can be seen that the suggested relationships cover an extremely wide range.

Table 19. Correlations between Becker and SPT blow counts (after Harder and Seed, 1986)

Reference and Job Location	Soil Type	Casing O.D. (inches)	Drill Bit Configuration	Figure
1. Canadian Data from Becker Drills, Inc. Files A. Vulcan Way, Richmond, BC (R.A. Spence Ltd.) B. Lynn Creek, N. Vancouver, BC C. Hunter Creek, Near Hope, BC D. North Vancouver, BC (R. A. Spence Ltd.)	Silty & Clayey Silts Gravelly Sands Sands & Gravels Gravelly & Silty Sands	5.5 5.5 5.5 5.5	Closed Closed Closed Closed	17 17 17 17
E. Powell River, BC (Ripley, Klohn, & Leonoff Ltd.) F. New Westminster, BC (Ripley, Klohn, & Leonoff, Ltd.) G. Minoru Blvd., Richmond, BC (R.M. Hardy & Assoc., Ltd.)	Gravelly Sands Sands & Silts Sands & Silts	5.5 5.5 5.5	Closed Closed Closed	17 17 17
2. Sargent, Hauskins, & Beckwith (1973) (Salt River Valley, Arizona)	Gravels ( $D_{50} = 10-30$ mm)	6.6	Open	18
3. Geotechnical Consultants, Inc. (1981, 1983) A. Santa Felicia Dam Foundation, CA B. Vern Freeman Diversion Structure, CA	Gravels ( $D_{50} = 4-10$ mm) Sands & Gravels	6.6 6.6	Open Open	19 19
4. Jones and Christensen (1982) A. Great Western Malting Facility, Pocatello, ID B. Northern Engineering & Testing, Inc. Files	Silts and Gravels Sands, Gravels, Baked Shale	6.6 5.5	Open Open	20 20

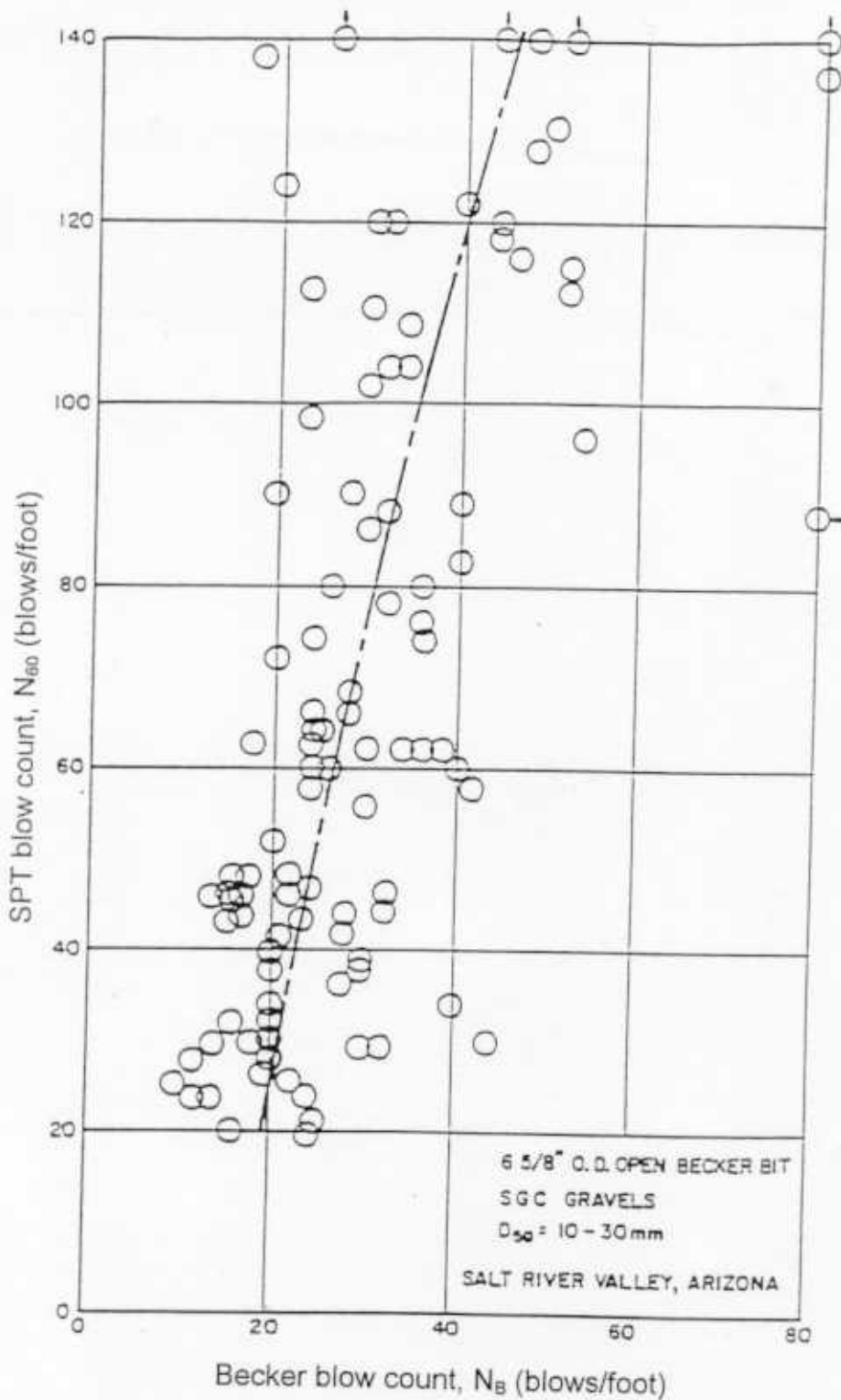
Foundex Explorations, Ltd. and Klohn Leonoff, Ltd. have developed the Foundex Becker penetration test (FBPT) that uses a mud-injection system to reduce casing friction. As bentonite mud is pumped through a series of holes (Figure 22), the side friction on the casing is reduced. The reduction in casing friction can be measured using a pile driving analyzer.

Sy and Lum (1997) have developed FBPT-SPT correlations for both the 6.6-inch diameter casing (Figure 23a) and the 9.0-inch casing (Figure 23b). These correlations eliminate the need for determining casing friction and offer a quick and approximate method for determining SPT  $N_{60}$  from FBPT  $N_{b30}$ .



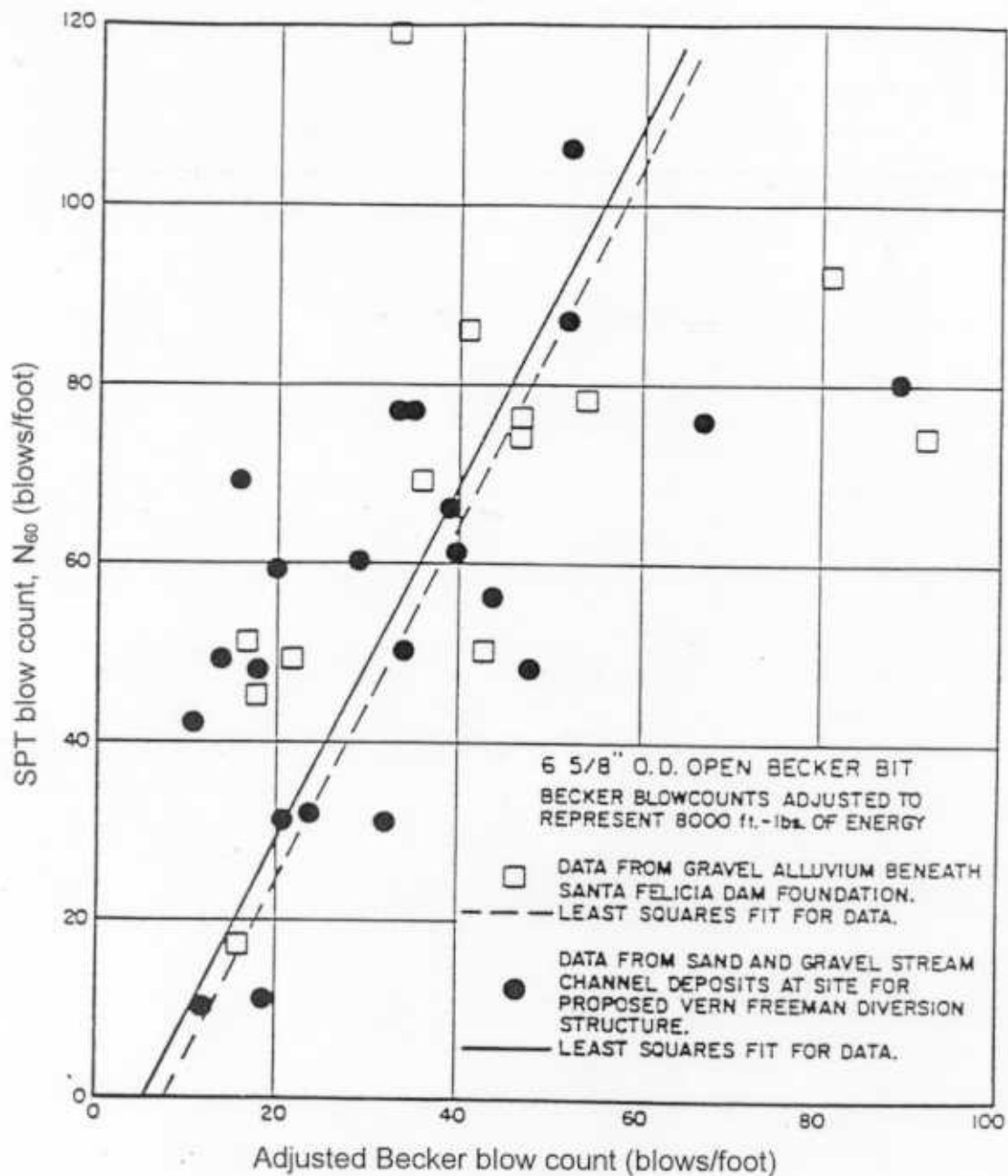
Note: As originally proposed, this correlation used the uncorrected SPT blowcount,  $N$ . However, hammers delivering 60% of the theoretical energy have been the most commonly used hammers for SPT tests, and it seems likely that the data on which the correlation was based was obtained primarily from tests with such hammers. It therefore seems logical to use  $N_{60}$  with this correlation, and it is the recommendation of this report that this be done.

Figure 17. Correlation between Becker and SPT blowcounts developed from Canadian data obtained from Becker Drills, Inc. files (from Harder and Seed, 1986)



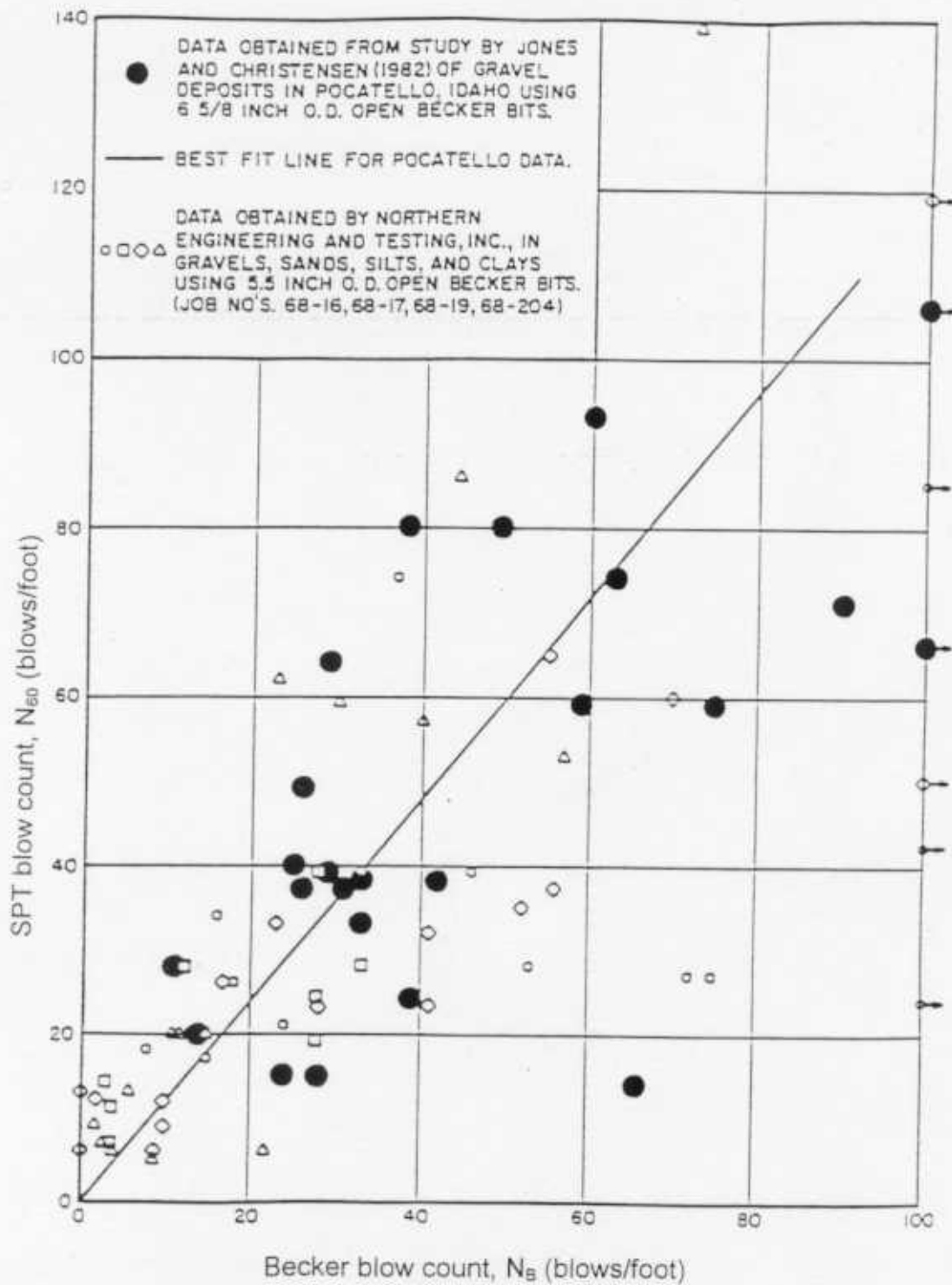
Note: As originally proposed, this correlation used the uncorrected SPT blowcount,  $N$ . However, hammers delivering 60% of the theoretical energy have been the most commonly used hammers for SPT tests, and it seems likely that the data on which the correlation was based was obtained primarily from tests with such hammers. It therefore seems logical to use  $N_{60}$  with this correlation, and it is the recommendation of this report that this be done.

Figure 18. Correlation between Becker and SPT blowcounts developed by Sergent, Hauskins, & Beckwith (1973) (from Harder and Seed, 1986)



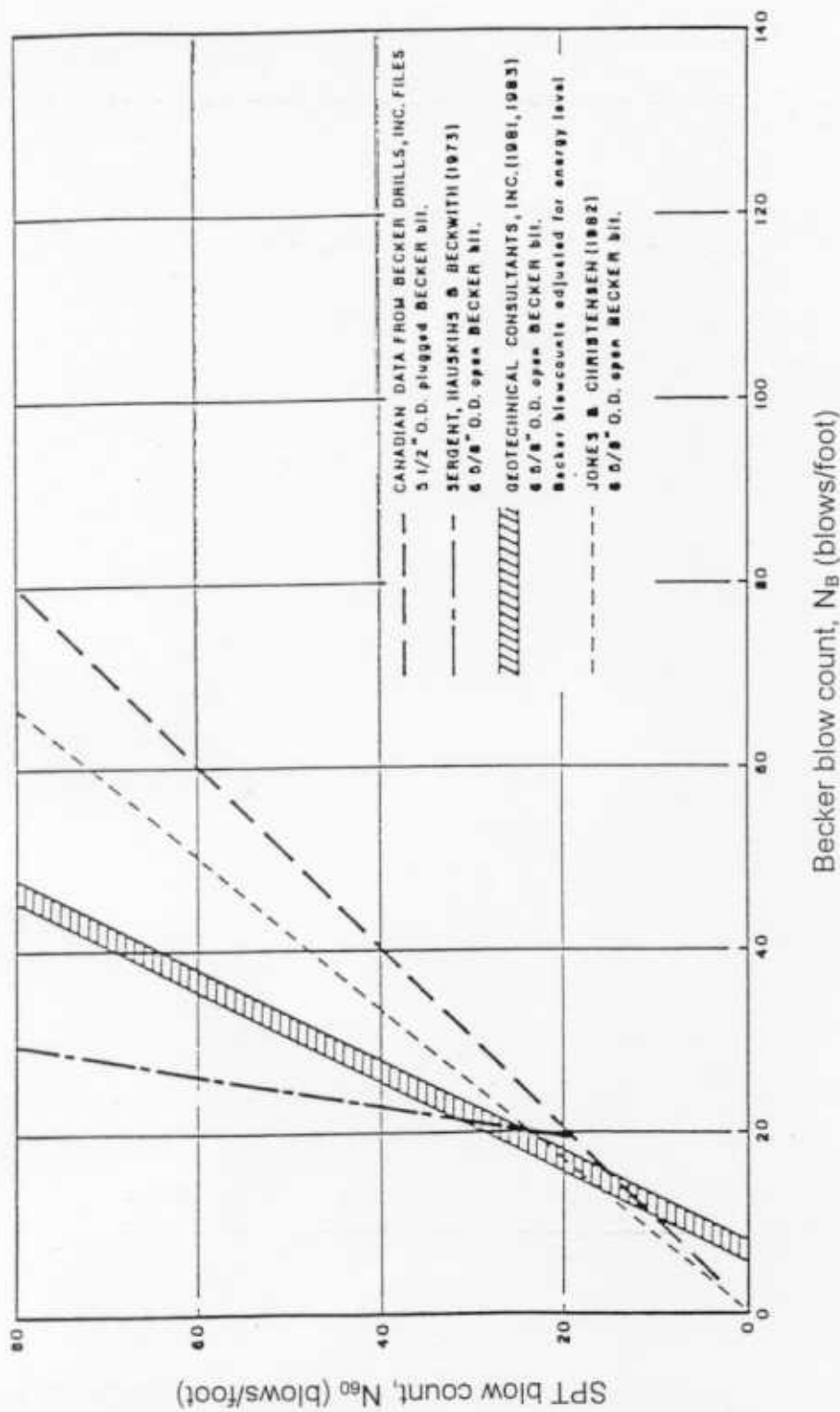
Note: As originally proposed, this correlation used the uncorrected SPT blowcount,  $N$ . However, hammers delivering 60% of the theoretical energy have been the most commonly used hammers for SPT tests, and it seems likely that the data on which the correlation was based was obtained primarily from tests with such hammers. It therefore seems logical to use  $N_{60}$  with this correlation, and it is the recommendation of this report that this be done.

Figure 19. Correlations between Becker and SPT blowcounts developed by Geotechnical Consultants, Inc. (1981, 1983) (from Harder and Seed, 1986)



Note: As originally proposed, this correlation used the uncorrected SPT blowcount,  $N$ . However, hammers delivering 60% of the theoretical energy have been the most commonly used hammers for SPT tests, and it seems likely that the data on which the correlation was based was obtained primarily from tests with such hammers. It therefore seems logical to use  $N_{60}$  with this correlation, and it is the recommendation of this report that this be done.

Figure 20. Correlation between Becker and SPT blowcounts developed by Jones and Christensen (1982) (from Harder and Seed, 1986)



Note: As originally proposed, this correlation used the uncorrected SPT blowcount,  $N$ . However, hammers delivering 60% of the theoretical energy have been the most commonly used hammers for SPT tests, and it seems likely that the data on which the correlation was based was obtained primarily from tests with such hammers. It therefore seems logical to use  $N_{60}$  with this correlation, and it is the recommendation of this report that this be done.

Figure 21. Summary of correlations between Becker and SPT blow counts (Figures 17-20) (from Harder and Seed, 1986)



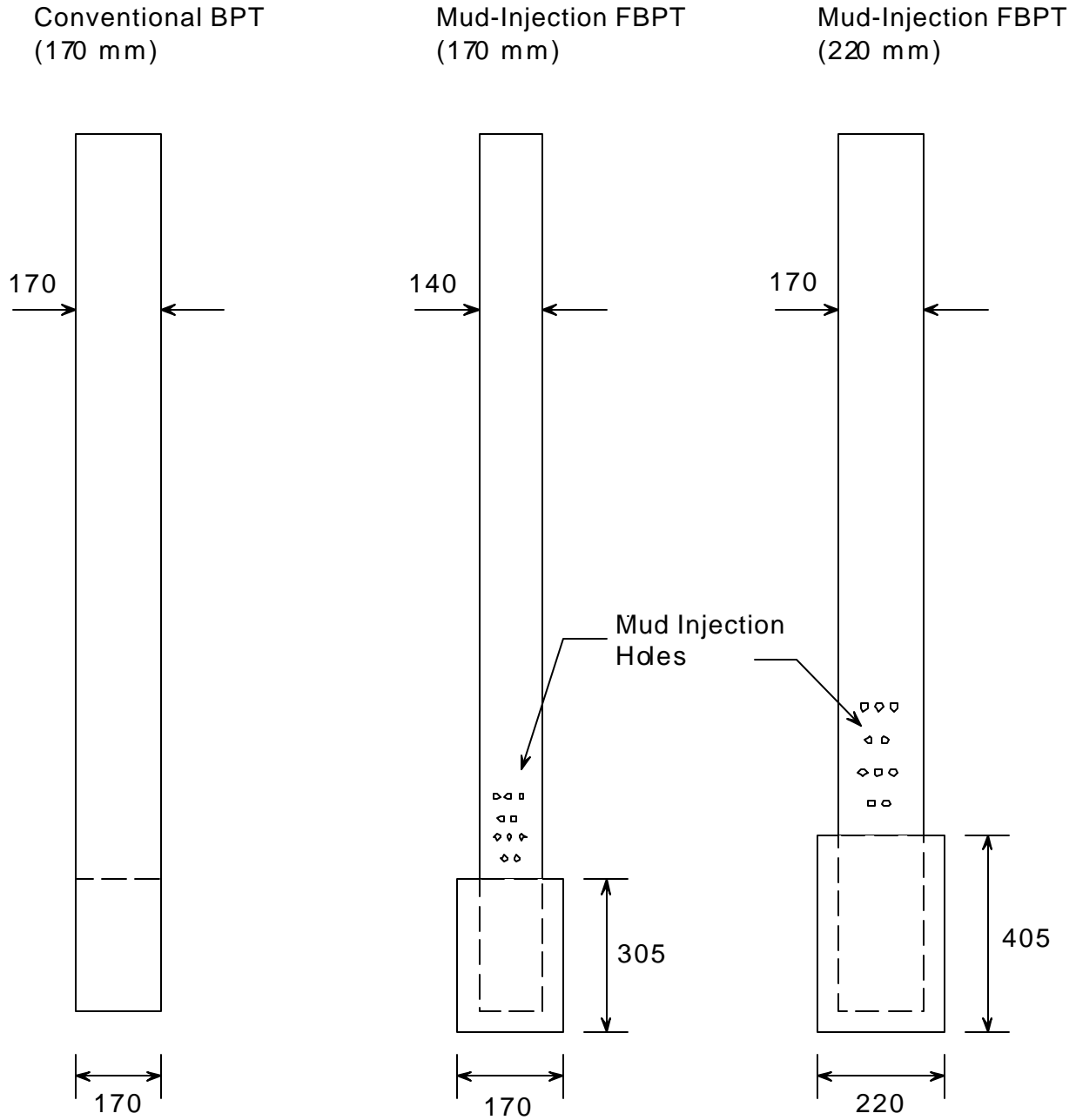


Figure 22. Conventional BPT mud-injection FBPT casing configurations. All dimensions in millimeters (after Syand Lum, 1997)

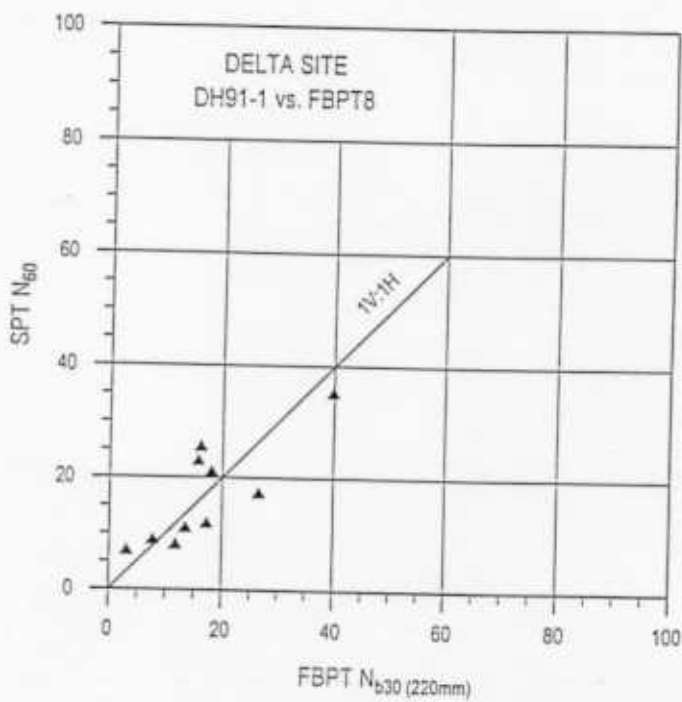
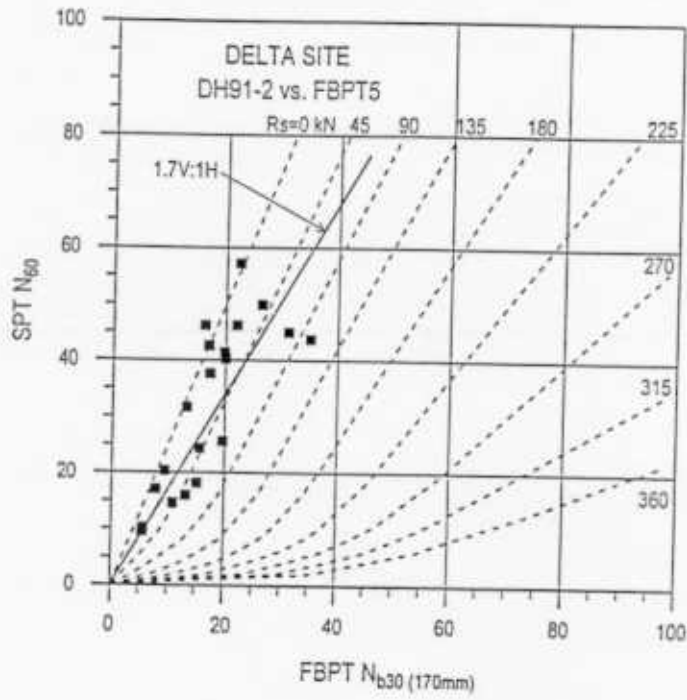


Figure 23. FBPT-SPT correlations for (a) 170 mm diameter shoe and (b) 220 mm diameter shoe (from Sy and Lum, 1997)

## Correlations Between SPT and Soil Properties

The SPT is widely used for estimating in situ properties of soils. It is most useful for estimating the properties of sands, but can also be used to estimate properties of silts and clays. This section provides the following correlations between the SPT and soil properties:

Relative Density of Sands

Friction Angles ( $\phi$ ) of Sands and Silts

Undrained Shear Strength ( $S_u$ ) of Clay

Undrained Residual Steady State Strengths ( $S_r$ ) of Sands After Liquefaction

Soil Modulus Values

These correlations are approximate and their use requires the exercise of engineering judgment regarding the inevitable uncertainties in estimated property values.

## Relative Density of Sands

SPT blow count can be used to estimate relative density values for sands. Because blow count depends on effective overburden pressure as well as relative density, both  $\sigma_v'$  and N should be considered in estimating  $D_r$ .

Table 20 lists equations relating  $D_r$  to N and  $\sigma_v'$  that have been suggested by various authorities. Their recommendations are shown in graphical form in Figures 24 through 30.

Table 21 provides descriptive estimates of relative density based on standard penetration resistance.

Figures 31 and 32 show correlations compiled by Mitchell et al. (1978) and NAVFAC (1982).

Table 20. Correlations of relative density and SPT N-values

Soil Type	Relative Density ( $D_r$ )	Parameters and Units	Reference
Normally consolidated sands	$D_r = \sqrt{\frac{N}{1.7(10 + \sigma_v')}} \quad (\text{See Note})$	$\sigma_v'$ = effective vertical stress in psi	Gibbs and Holtz (1957) Figure 24
Normally consolidated silica sand	$D_r = \left( \frac{N}{0.234\sigma_v' + 16} \right)^{0.5} \quad (\text{See Note})$	N = SPT blowcount in blows/foot  $\sigma_v'$ = effective overburden stress in kN/m <sup>2</sup> at depth of test	Meyerhof (1956) Figure 25
Coarse sands	$D_r = \left( \frac{N}{0.773\sigma_v' + 22} \right)^{0.5} \quad \text{for } \sigma_v' < 75 \text{ kPa}$ $D_r = \left( \frac{N}{0.193\sigma_v' + 66} \right)^{0.5} \quad \text{for } \sigma_v' \geq 75 \text{ kPa}$ (See Note)	$\sigma_v'$ = effective overburden stress in kN/m <sup>2</sup> at depth of test	Peck and Bazaraa (1969) Figure 26
Ottawa sand	$D_r = 8.6 - 0.83 \left[ \frac{N + 10.4 - 3.2(\text{OCR}) - 0.24(\sigma_v')}{0.0045} \right]^{0.5}$ (See Note)	$\sigma_v'$ = effective vertical stress in psi  OCR = overconsolidation ratio	Marcuson and Bieganousky (1977)
Normally consolidated sands	$D_r = \left( \frac{N_{60}}{a\sigma_v' + b} \right)^{0.5}$  If sand is overconsolidated, increase b by a factor $C_f$ : $C_f = \frac{1 + K}{1 + 2K_{\text{onc}}}$ where: $K_0$ = ratio of effective horizontal stress to vertical stress for overconsolidated sand  $K_{\text{onc}}$ = ratio of effective horizontal stress to vertical stress for the normally consolidated sand $\approx 1 - \sin \phi$	$N_{60}$ = blowcount corrected to 60% of the theoretical maximum energy  a = 0.3 (mean value)  b = 30 (mean value)	Skempton (1986)
Gravelly soils	$D_r = 22N^{0.57} \sigma_v'^{-0.14} \quad (\text{fine sand})$ $D_r = 18N^{0.57} \sigma_v'^{-0.14} \quad (\text{gravel fraction 25\%})$ $D_r = 25N^{0.44} \sigma_v'^{-0.13} \quad (\text{gravel fraction 50\%})$ $D_r = 25N^{0.46} \sigma_v'^{-0.12} \quad (\text{average for all sands})$ (See Note)	$\sigma_v'$ = effective vertical stress in kPa	Yoshida and Ikemi (1988) Figures 27-30

Note: As originally proposed, this correlation used the uncorrected SPT blowcount, N. However, hammers delivering 60% of the theoretical energy have been the most commonly used hammers for SPT tests, and it seems likely that the data on which the correlation was based was obtained primarily from tests with such hammers. It therefore seems logical to use  $N_{60}$  with this correlation, and it is the recommendation of this report that this be done.

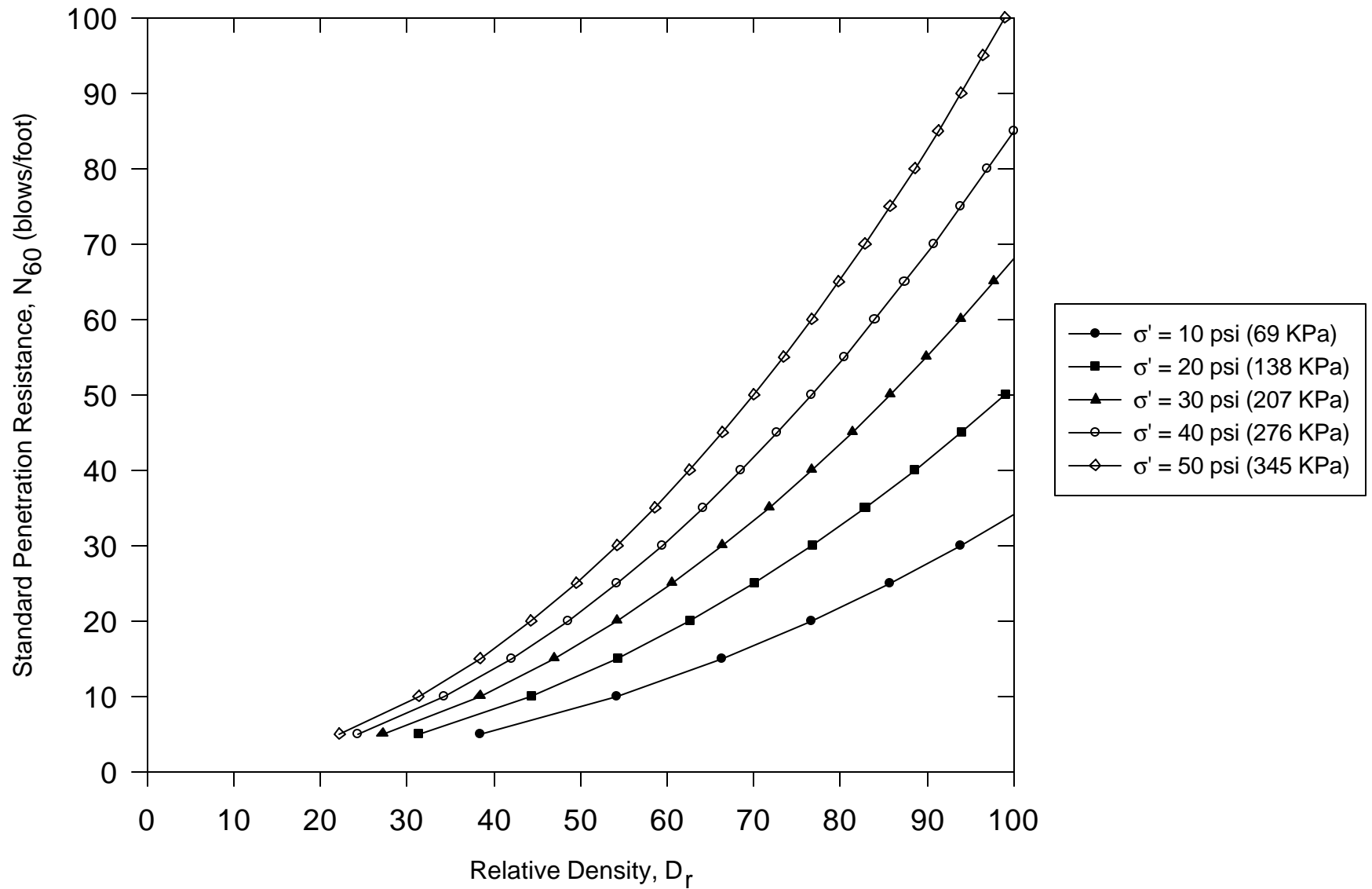


Figure 24. Variations of relative density with penetration resistance at different overburden pressures (after Gibbs and Holtz, 1957)

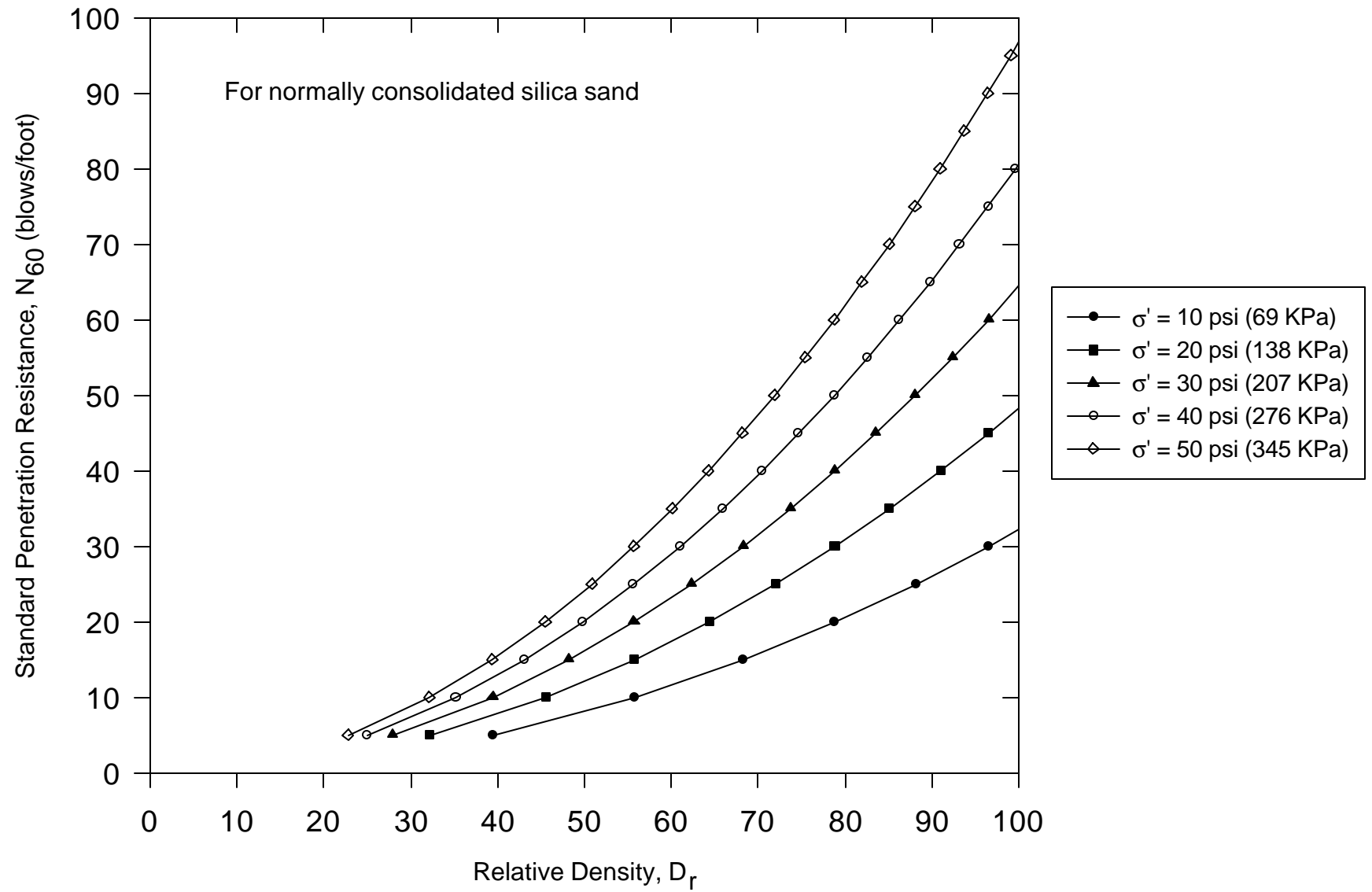


Figure 25. Variations of relative density with penetration resistance at different overburden pressures (after Meyerhof, 1956)

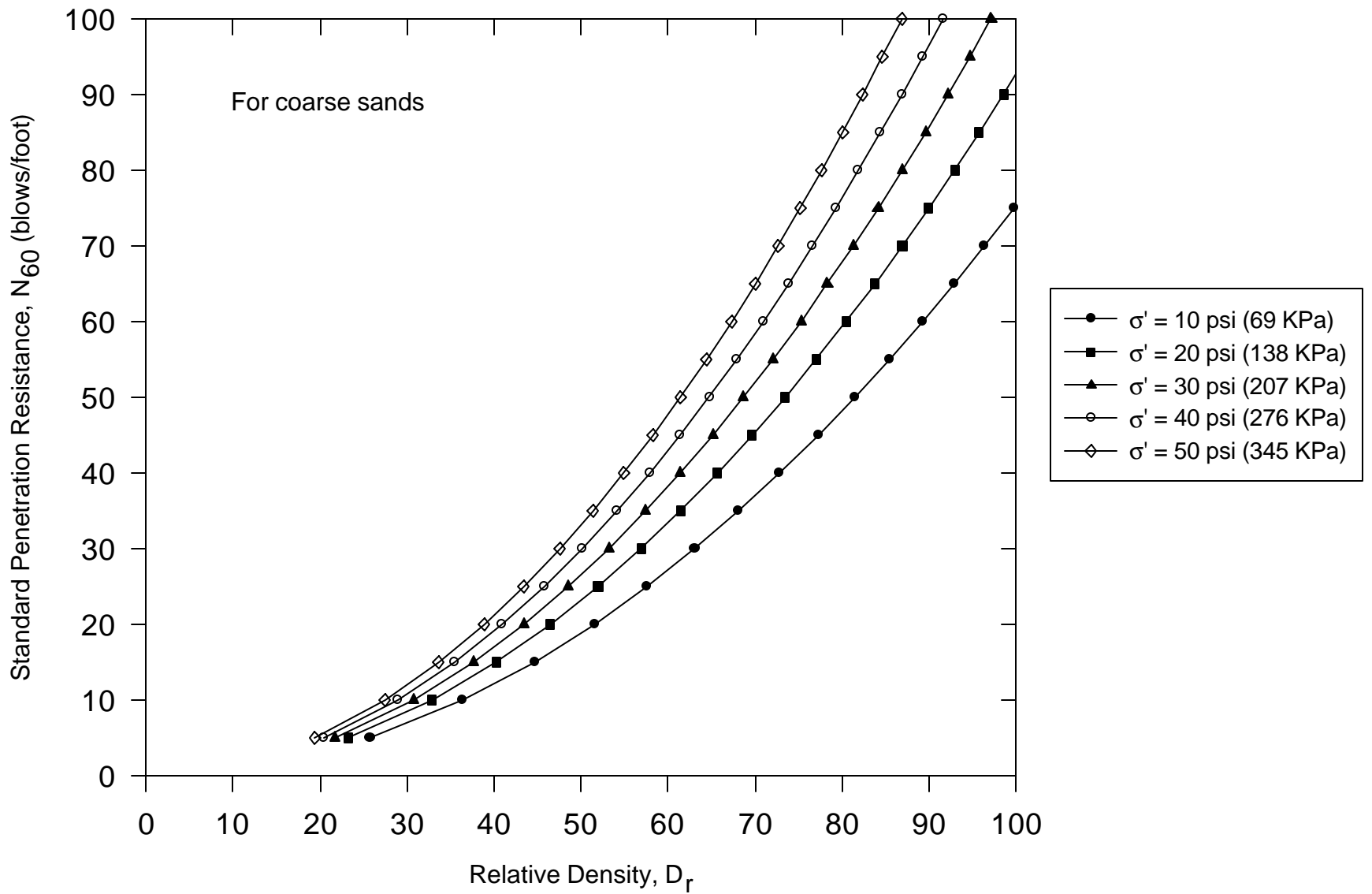


Figure 26. Variations of relative density with penetration resistance at different overburden pressures (after Peck and Bazaraa, 1969)



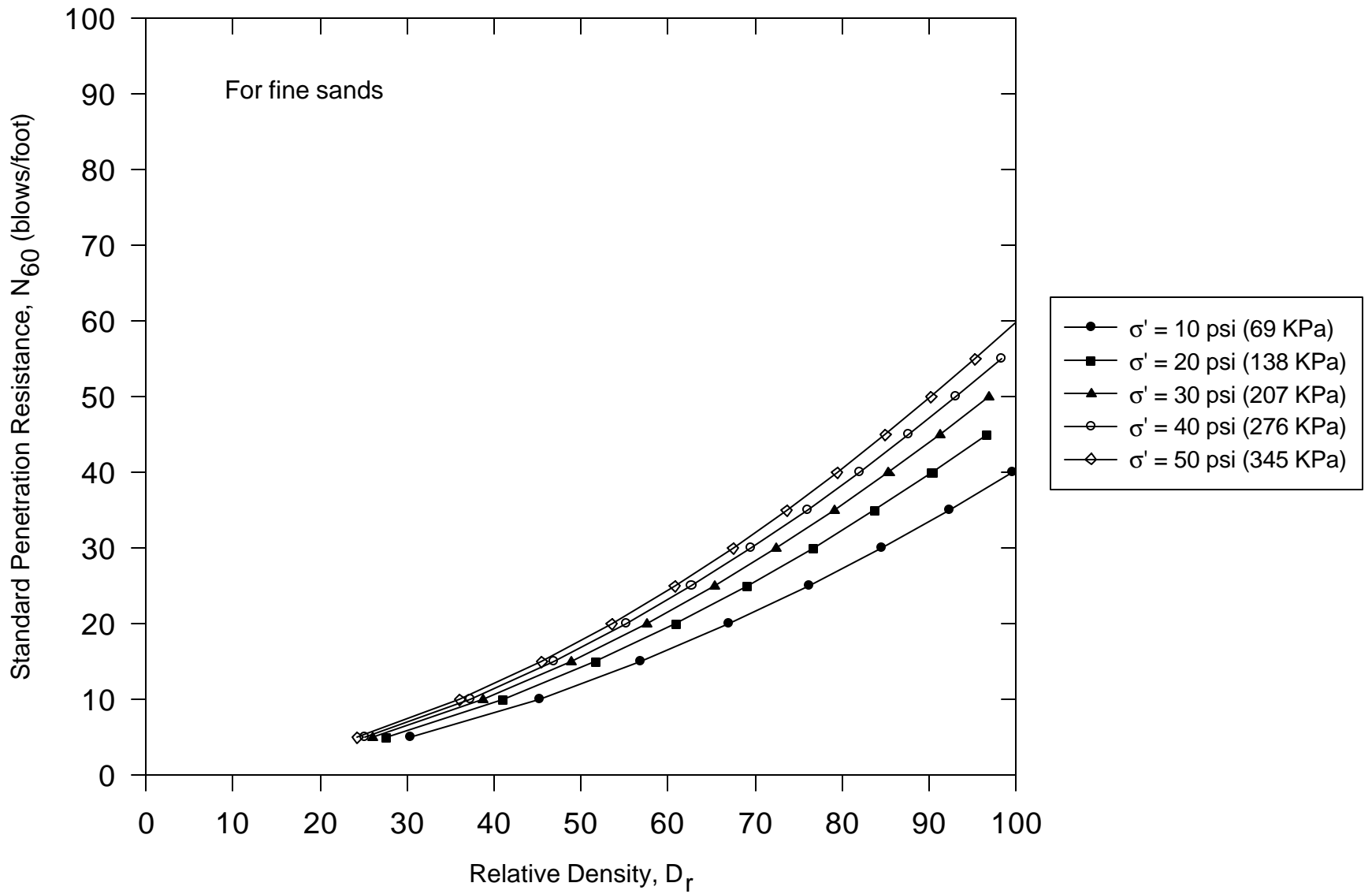


Figure 27. Variations of relative density with penetration resistance at different overburden pressures (after Yoshida and Ikemi, 1988)

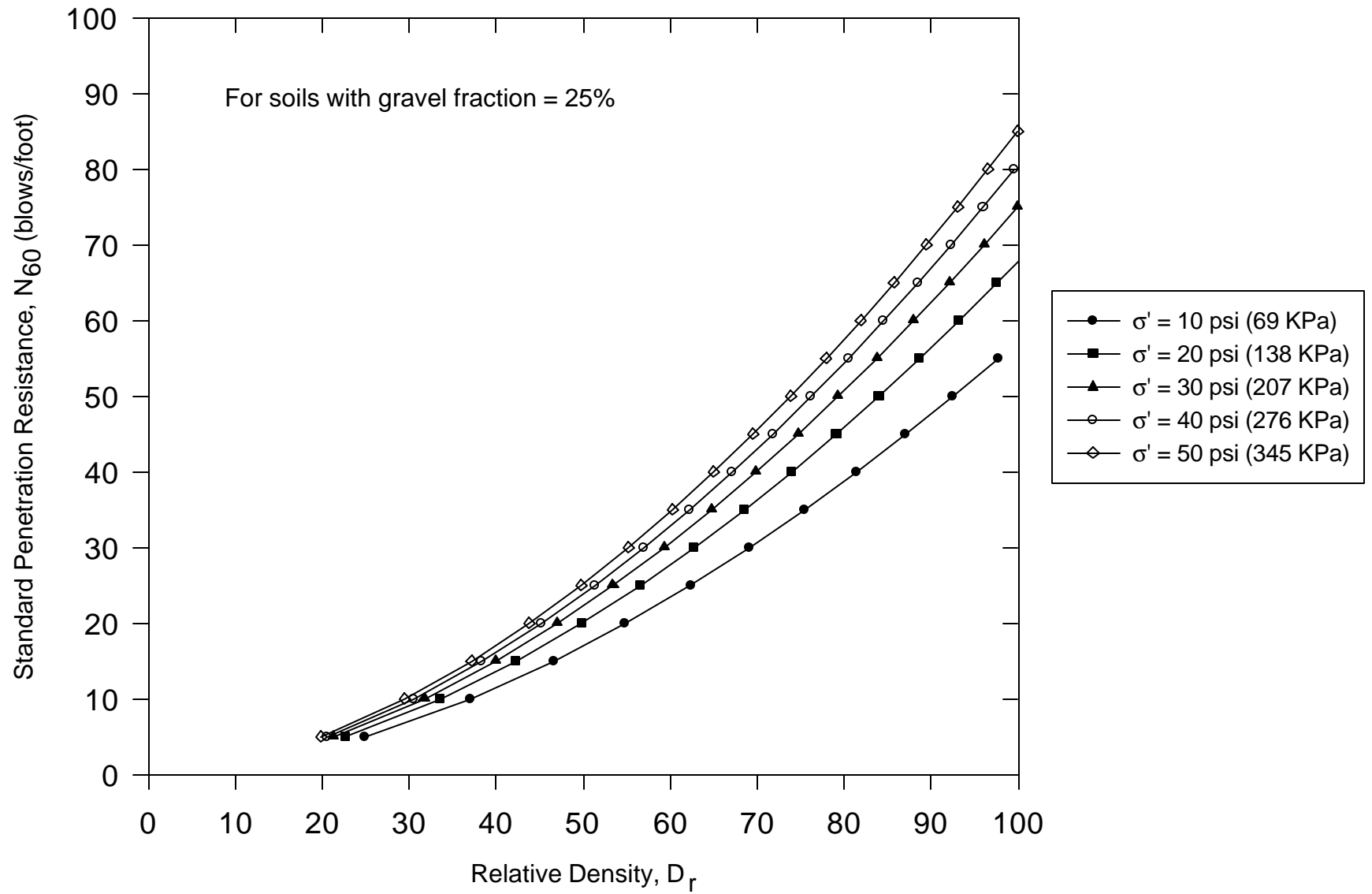


Figure 28. Variations of relative density with penetration resistance at different overburden pressures (after Yoshida and Ikemi, 1988)

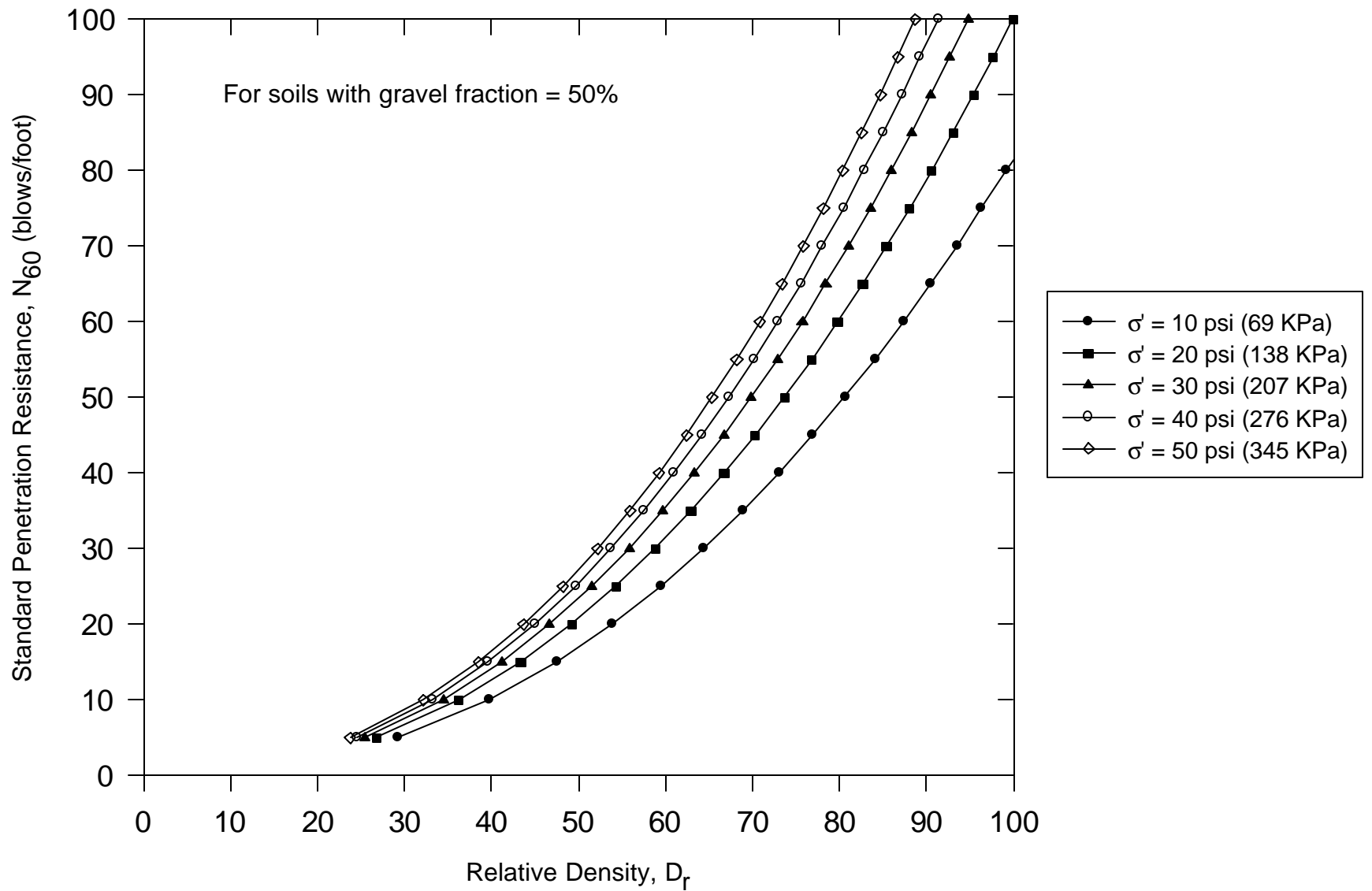


Figure 29. Variations of relative density with penetration resistance at different overburden pressures (after Yoshida and Ikemi, 1988)

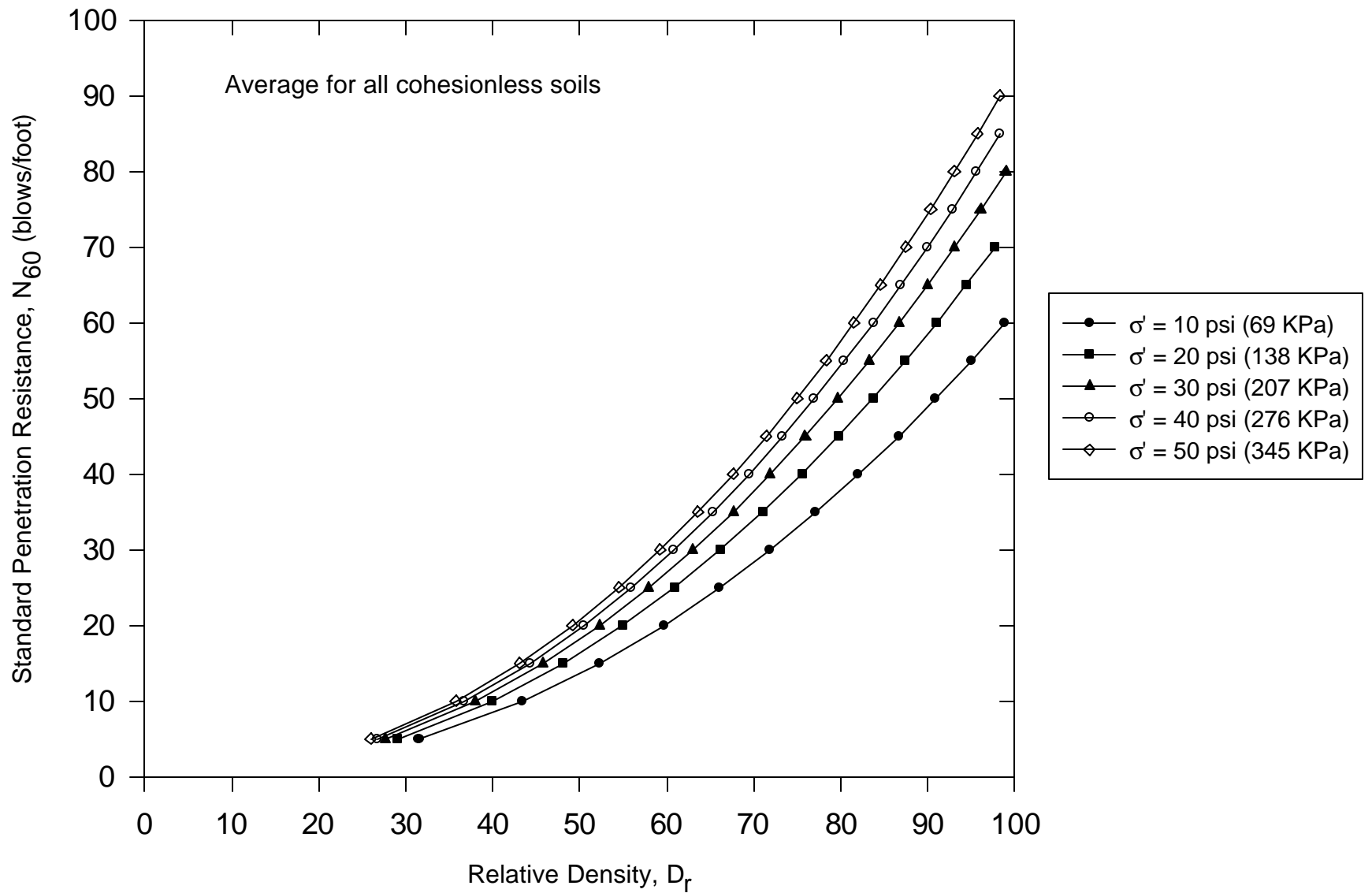


Figure 30. Variations of relative density with penetration resistance at different overburden pressures (after Yoshida and Ikemi, 1988)

Table 21. Relationship among relative density, penetration resistance, dry unit weight, and angle of internal friction of cohesionless soils (after Duncan and Buchignani, 1976)

Descriptive Relative Density	Relative Density **	Standard Penetration Resistance $N_1$ (see Note) *	Static Cone Resistance $q_c$	Angle of Internal Friction $\phi$	Dry Unit Weight
	%	blows/foot	tsf or kgf/cm <sup>2</sup>	degrees	KN/m <sup>3</sup>
Very Loose	< 15	< 4	< 50	< 30	< 14
Loose	15 - 35	4 - 10	50 - 100	30 - 32	14 - 16
Medium Dense	35 - 65	10 - 30	100 - 150	32 - 35	16 - 18
Dense	65 - 85	30 - 50	150 - 200	35 - 38	18 - 20
Very Dense	85 - 100	> 50	> 200	> 38	> 20

\*  $N_1 = N$  -value corrected to an effective vertical overburden pressure of 1.0 tsf or 100 kPa

\*\* Freshly deposited, normally consolidated sand

Note: As originally proposed, this correlation used the uncorrected SPT blowcount,  $N_1$ . However, hammers delivering 60% of the theoretical energy have been the most commonly used hammers for SPT tests, and it seems likely that the data on which the correlation was based was obtained primarily from tests with such hammers. It therefore seems logical to use  $N_{1,60}$  with this correlation, and it is the recommendation of this report that this be done.

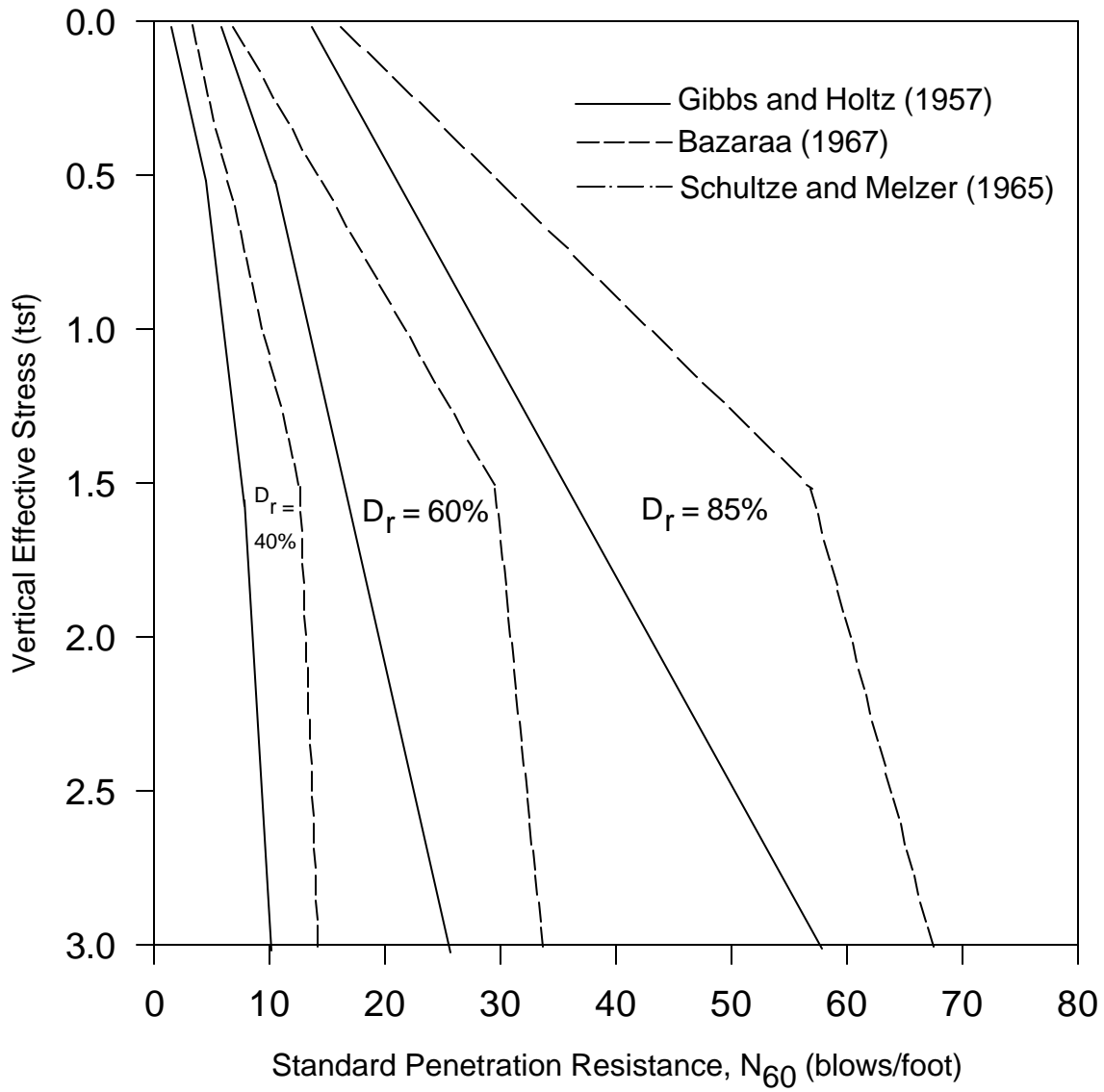
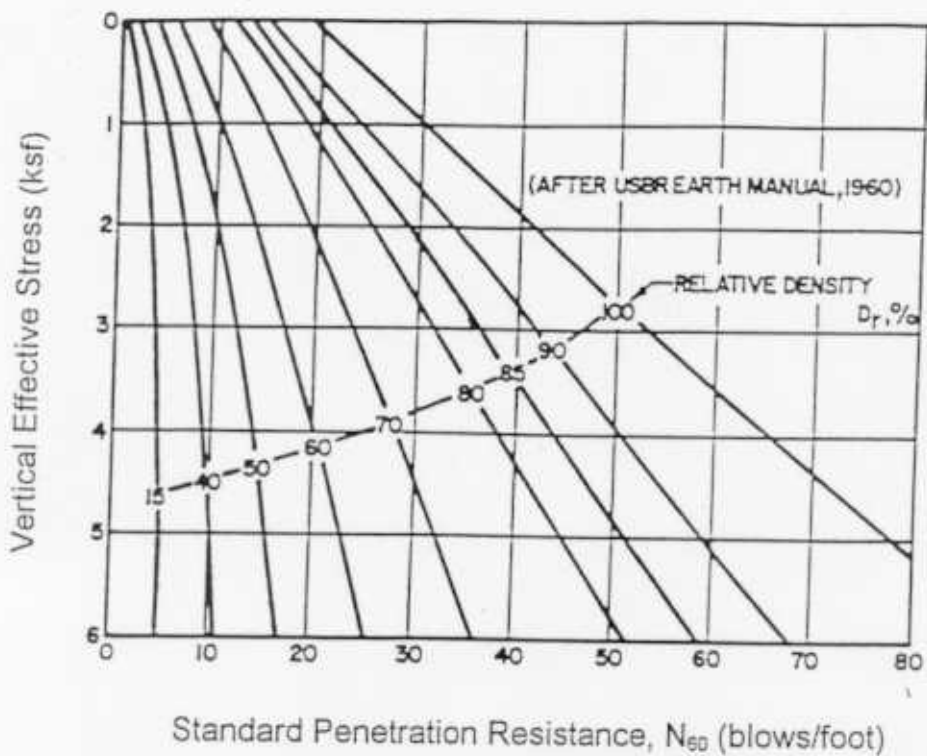


Figure 31. Correlations between relative density and standard penetration resistance (after Mitchell et al., 1978)



Note: As originally proposed, this correlation used the uncorrected SPT blowcount,  $N$ . However, hammers delivering 60% of the theoretical energy have been the most commonly used hammers for SPT tests, and it seems likely that the data on which the correlation was based was obtained primarily from tests with such hammers. It therefore seems logical to use  $N_{60}$  with this correlation, and it is the recommendation of this report that this be done.

Figure 32. Correlations between relative density and standard penetration resistance (from NAVFAC, 1982)

## Friction Angles ( $\phi$ ) of Sands and Silts

The SPT can be used to estimate the in-situ angle of internal friction ( $\phi$ ) for sands and silts. In situ tests such as the SPT and cone penetration tests are commonly used to estimate the properties of cohesionless soils due to the difficulty in obtaining undisturbed samples.

Equations relating  $\phi$  to SPT N-values for sandy and granular soils have been summarized in Table 22 and plotted together in Figure 33.

Bowles (1968) summarized empirical values for  $\phi$ , relative density ( $D_r$ ), and unit weights of granular soils based on SPT N-values as shown in Table 23.

Terzaghi et al. (1996) suggested the relationship between  $N_{1,60}$  and  $\phi$  for fine-grained and coarse-grained soils shown in Figure 34. Fine-grained sands are defined as sands passing the #40 sieve and retained on the #200 sieve. Coarse-grained sands are defined as sands passing the #4 sieve and retained on the #10 sieve.

Carter and Bentley (1991) have developed a plot of  $\phi$  versus N with corresponding descriptions of relative density in Figure 35.

Relationships between the angle of internal friction and relative density for different types of sands and gravels are shown in Figure 36 (Decourt, 1990).

Relationships between  $\phi$ , SPT N-values, and overburden pressure from Mitchell et al. (1978) are shown in Figure 37.

Duncan et al. (1997) correlated values of  $\phi$  from UU tests on unsaturated silts and clays from five locations in Virginia with SPT blow counts, as shown in Figure 38. Note that the undrained strength envelopes for these soils have cohesion intercepts varying from 150 psf to 400 psf.



Table 22. Correlations of internal friction angle and SPT N-values (data from Hatanaka and Uchida (1996) and Broms and Flodin (1988))

Soil Type	$\phi$ (degrees)	Reference
Angular and well-grained soil particles	$\phi = (12N)^{0.5} + 25$ (See Note)	Dunham (1954) (#1)
Round and well-grained or angular and uniform-grained soil particles	$\phi = (12N)^{0.5} + 20$ (See Note)	Dunham (1954) (#2)
Round and uniform-grained soil particles	$\phi = (12N)^{0.5} + 15$ (See Note)	Dunham (1954) (#3)
Sandy	$\phi = (20N)^{0.5} + 15$ (See Note)	Ohsaki et al. (1959)
Granular	$\phi = 20 + 3.5(N)^{0.5}$ (See Note)	Muromachi et al. (1974)
Sandy	$\phi = (15N)^{0.5} + 15 \leq 45$ (N > 5) (See Note)	Japan Road Association (1990)
Sandy	$\phi = (20N_1)^{0.5} + 20$  N <sub>1</sub> = N-value normalized to 1 tsf of overburden pressure using the Liao and Whitman (1986) equation. It is the recommendation of this report to use N <sub>1,60</sub> with this correlation.	Hatanaka and Uchida (1996)

Note: As originally proposed, these correlations used the uncorrected SPT blowcount, N. However, hammers delivering 60% of the theoretical energy have been the most commonly used hammers for SPT tests, and it seems likely that the data on which these correlations were based was obtained primarily from tests with such hammers. It therefore seems logical to use N<sub>60</sub> with these correlations, and it is the recommendation of this report that this be done.

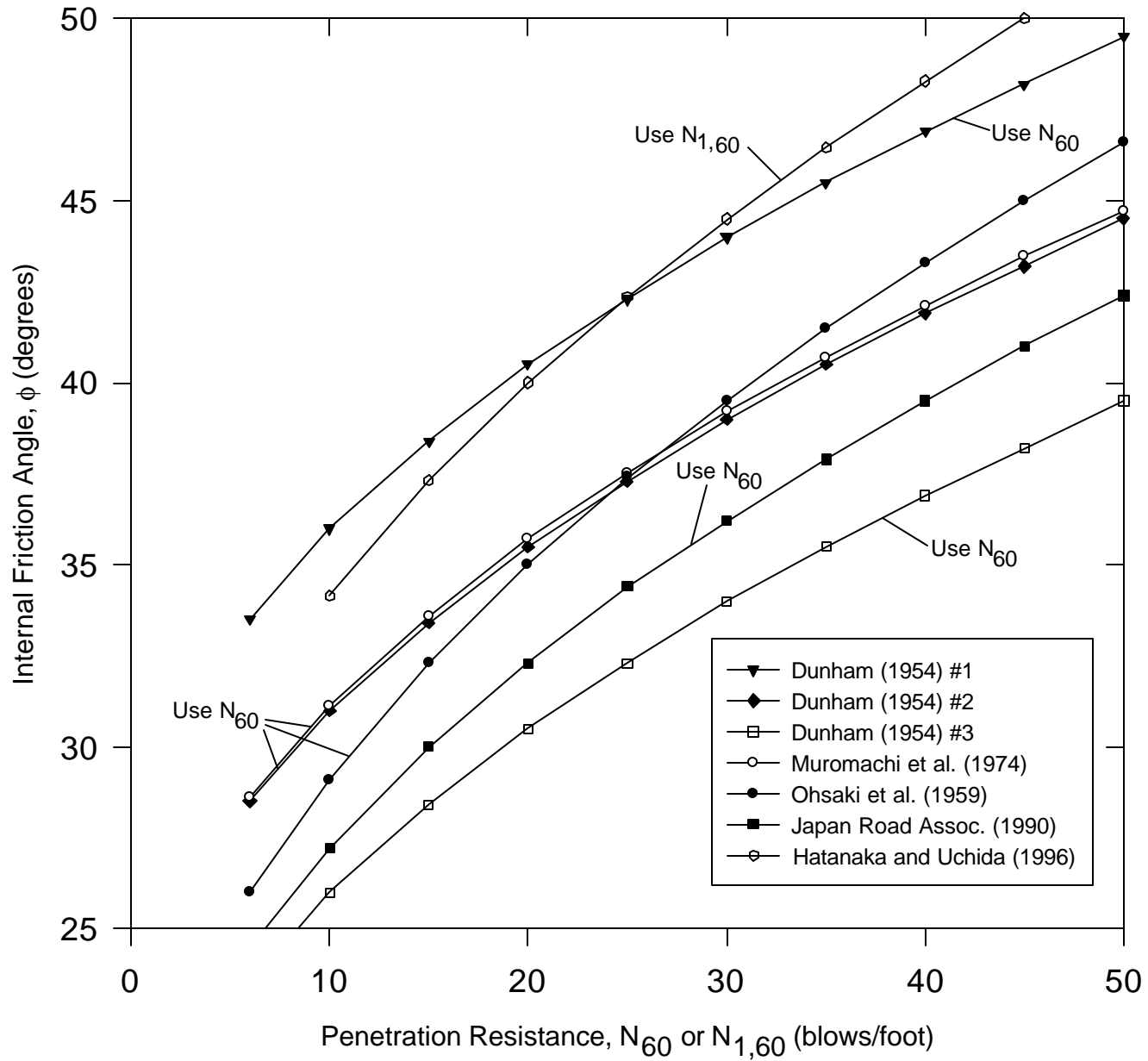


Figure 33. Correlations between internal friction angle and penetration resistance

Table 23. Empirical values for  $\phi$ ,  $D_r$ , and unit weight of granular soils based on the standard penetration number with corrections for depth and for fine saturated sands (from Bowles, 1968)

Description	Very loose	Loose	Medium	Dense	Very dense	
Relative density $D_r$	0	0.15	0.35	0.65	0.85	1.00
Standard penetration no. $N$		4	10	30	50	
Approx. angle of internal friction $\phi^{\dagger}$	25°-30°	27-32°	30-35°	35-40°	38-43°	
Approx. range of moist unit weight, ( $\gamma$ ) pcf	70-100‡	90-115	110-130	110-140	130-150	

† After Meyerhof [9].  $\phi = 25 + 0.15D_r$ , with more than 5 percent fines and  $\phi = 30 + 0.15D_r$ , with less than 5 percent fines. Use larger values for granular material with 5 percent or less fine sand and silt.

‡ It should be noted that excavated material or material dumped from a truck will weigh 70 to 90 pcf. Material must be quite dense and hard to weigh much over 130 pcf. Values of 105 to 115 pcf for nonsaturated soils are common.

Note: As originally proposed, this correlation used the uncorrected SPT blowcount,  $N$ . However, hammers delivering 60% of the theoretical energy have been the most commonly used hammers for SPT tests, and it seems likely that the data on which the correlation was based was obtained primarily from tests with such hammers. It therefore seems logical to use  $N_{60}$  with this correlation, and it is the recommendation of this report that this be done.

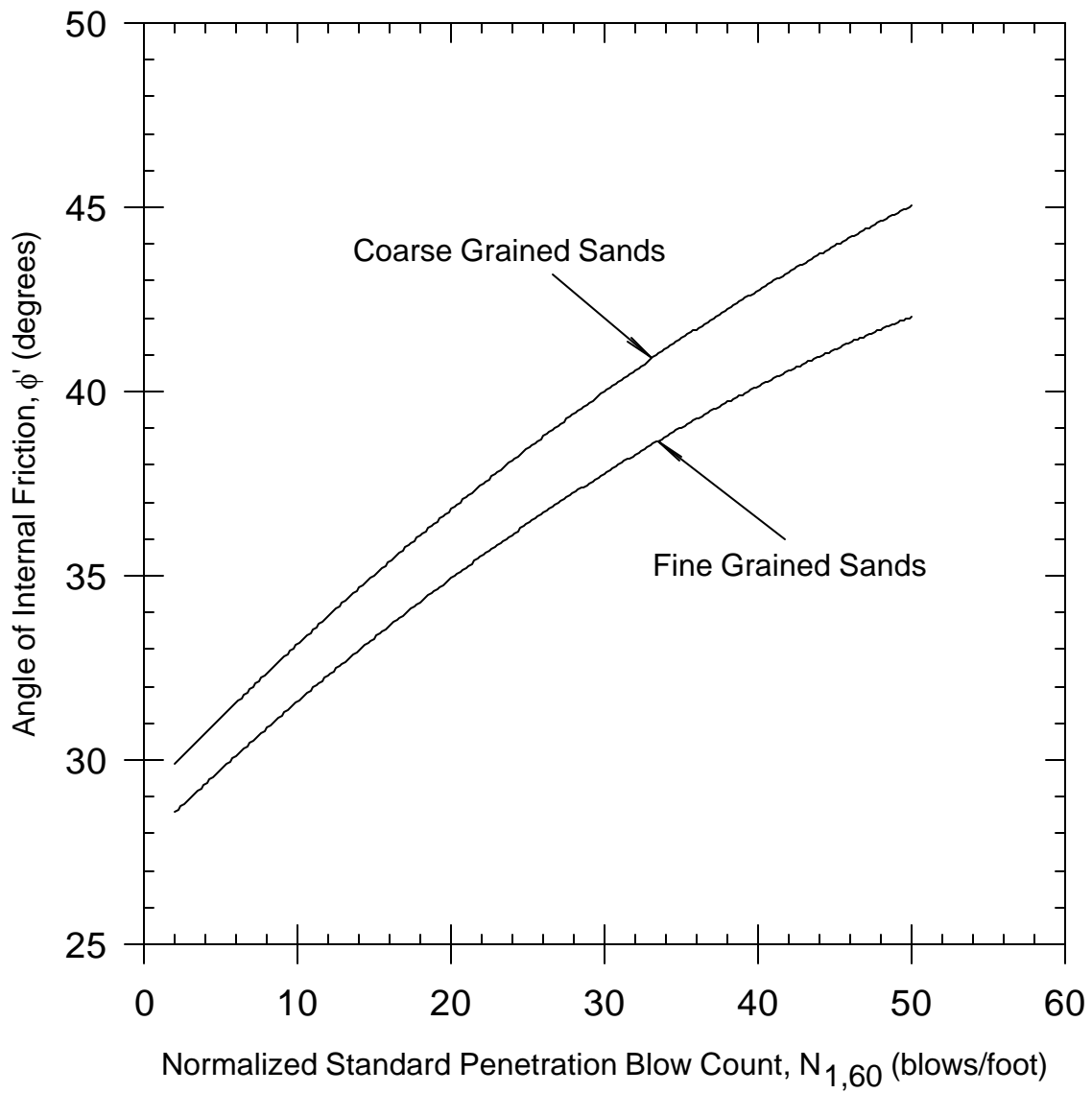


Figure 34. Empirical correlation between friction angle of sands and normalized standard penetration blow count (after Terzaghi et al., 1996)

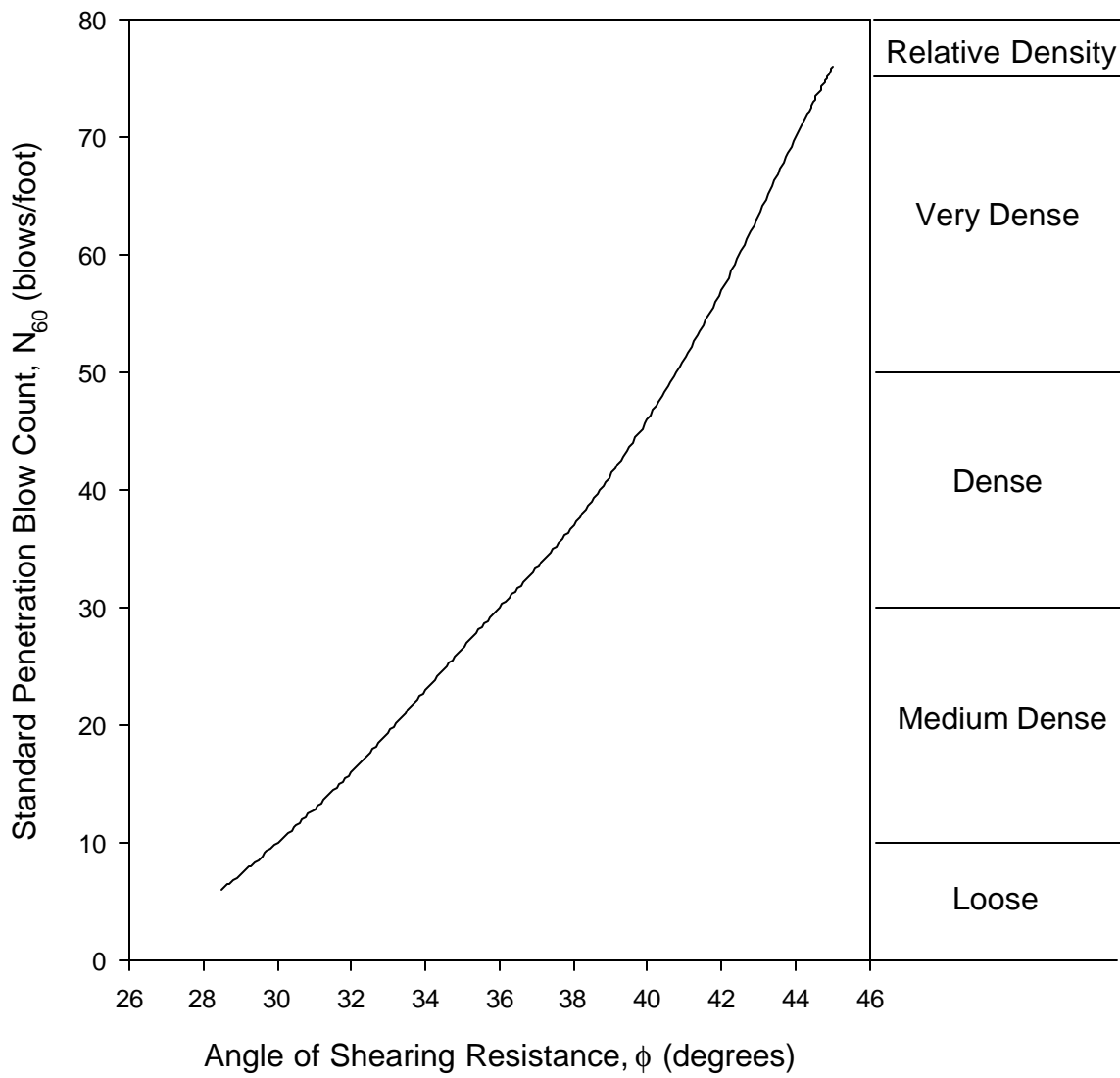


Figure 35. Estimation of the angle of shearing resistance of granular soils from standard penetration test results (Originally from Peck et al., 1974, modified by Carter and Bentley, 1991).

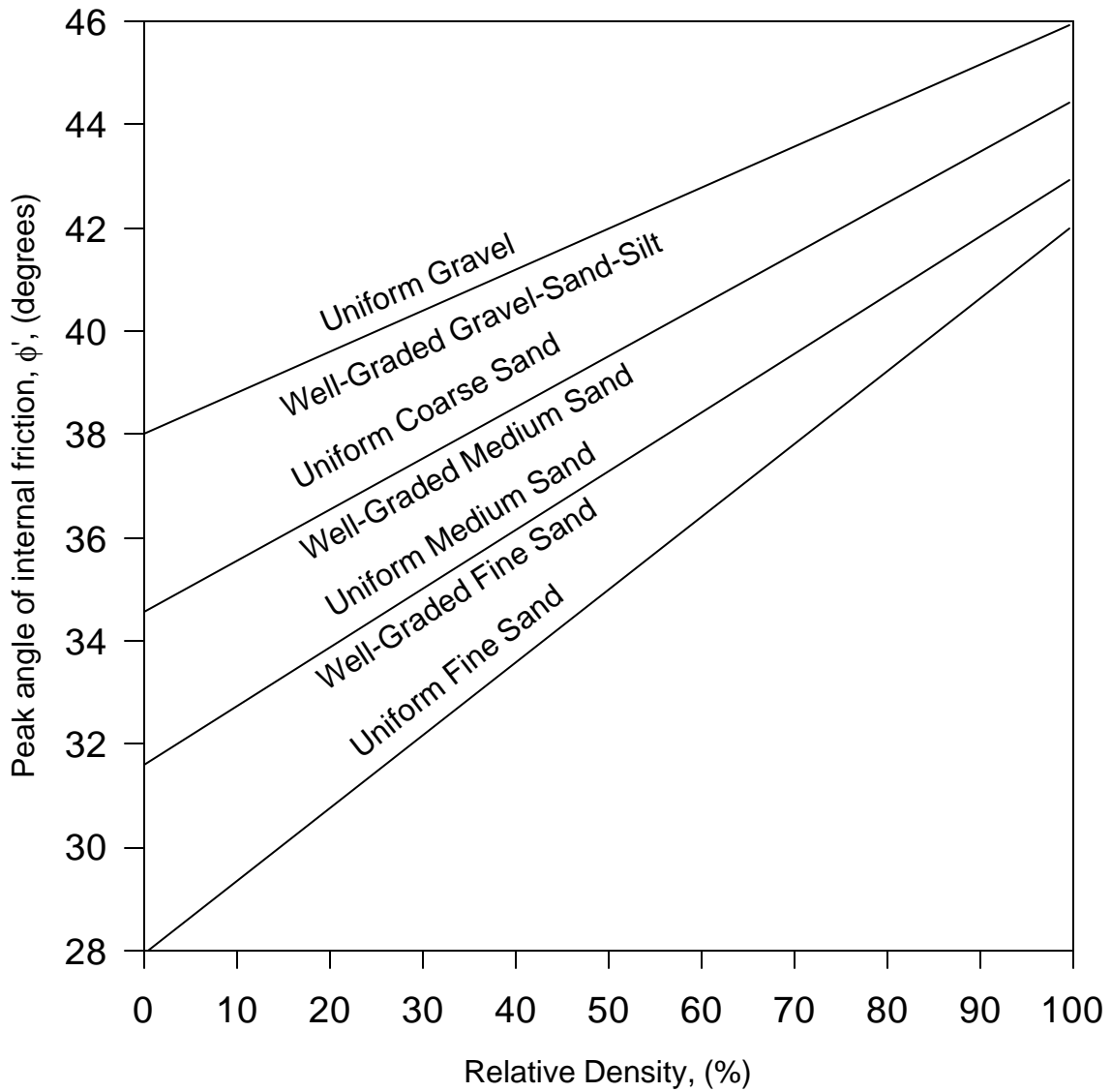


Figure 36. Angle of internal friction as a function of relative density for different types of sand and gravel (after Decourt, 1990)

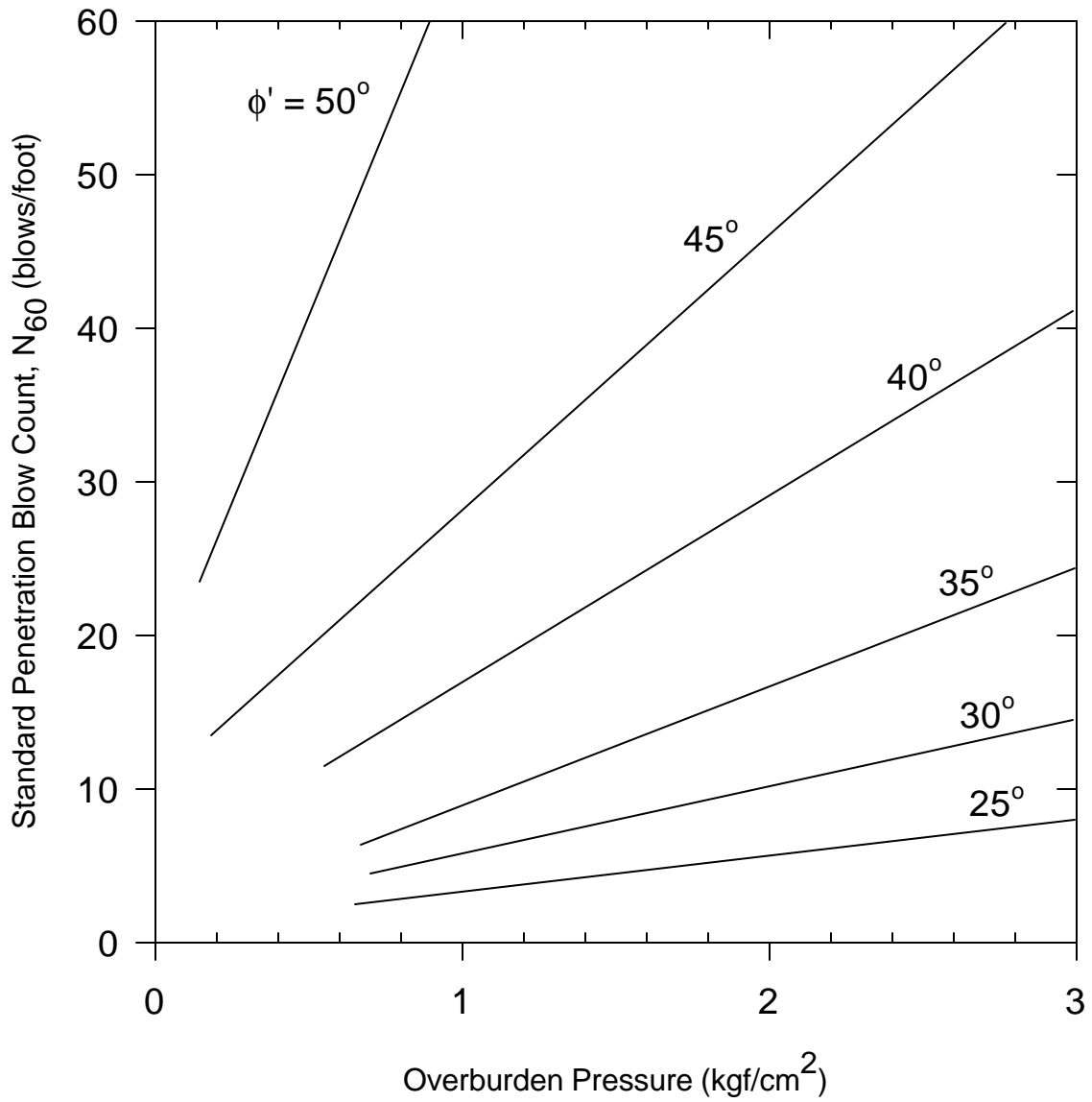


Figure 37. Method for estimating effective friction angle ( $\phi'$ ) from SPT blow count ( $N$ ) (after Mitchell et al., 1978)

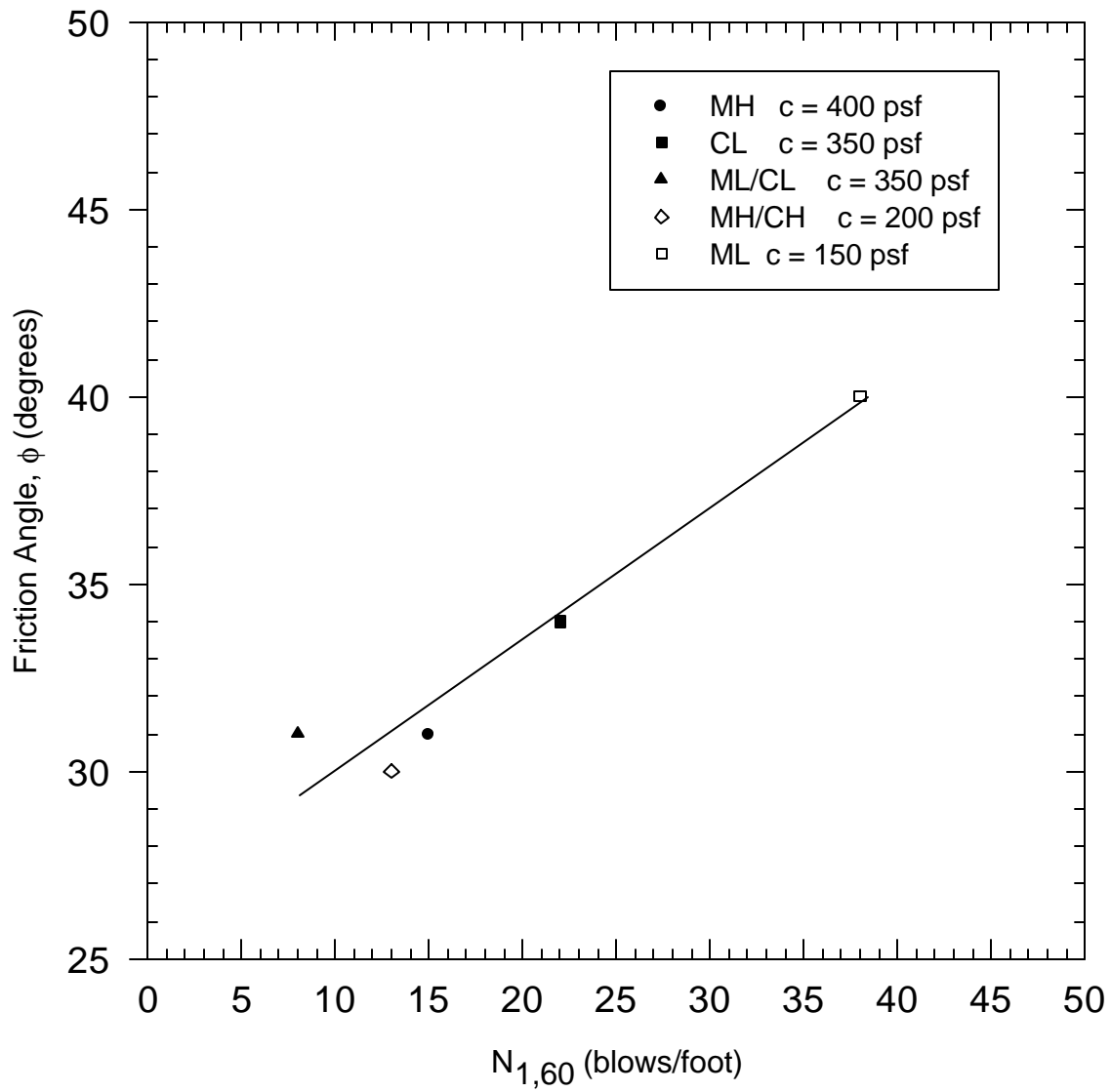


Figure 38. Variations of friction angle with  $N_{1,60}$  for silts and clays (data from Duncan et al., 1997)



## Undrained Shear Strength ( $S_u$ ) of Clays

The SPT can be used to estimate undrained shear strengths ( $S_u$ ) for clays. Ladd et al. (1977) in Robertson (1986) caution that  $S_u$  values obtained from SPT N-values are of little value unless the clay is relatively stiff and insensitive. Casagrande (1966), de Mello (1971), Schmertmann (1971) and Mitchell et al. (1978) note that clay sensitivity may cause lower blow counts for a given undisturbed strength due to strength loss during sampler penetration (see Figures 42 and 43).

Suggested relationships between  $S_u$  and N are shown in Tables 24, 25, and 26.

A correlation between  $S_u$ , N and plasticity index for clays (Stroud, 1974) is shown in Figure 39.

Correlations between N and  $S_u$  are shown in Figure 40, and correlations between N and  $q_u$  are shown in Figures 41 and 43.

Table 24. Approximate values of undrained shear strength for cohesive soils based on SPT blow count N-values (from Terzaghi and Peck, 1967)

Soil Consistency	SPT N (See Note)	S <sub>u</sub> (psf)
Very Soft	< 2	< 250
Soft	2 - 4	250 - 500
Medium	4 - 8	500 - 1000
Stiff	8 - 15	1000 - 2000
Very Stiff	15 - 30	2000 - 4000
Hard	> 30	> 4000

Table 25. Approximate undrained shear strength for cohesive soils based on SPT blow counts (from Tschebotarioff, 1973 and Parcher and Means, 1968)

SPT N (See Note)	S <sub>u</sub> (kgf/cm <sup>2</sup> )		S <sub>u</sub> (psf)	
	Ref. a	Ref b.	Ref a.	Ref b.
< 2	0.15	< 0.12	300	-
2 - 4	0.15 - 0.3	0.12 - 0.25	300 - 600	250 - 500
4 - 8	0.3 - 0.6	0.25 - 0.5	600 - 1200	500 - 1000
8 - 15	0.6 - 1.2	0.5 - 1.0	1200 - 2400	1000 - 2000
15 - 30	1.2	1.0 - 2.0	2400	2000 - 4000
> 30	> 2.25	> 2.0	> 4500	> 4000

Ref. (a) Tschebotarioff (1973)

(b) Parcher and Means (1968)

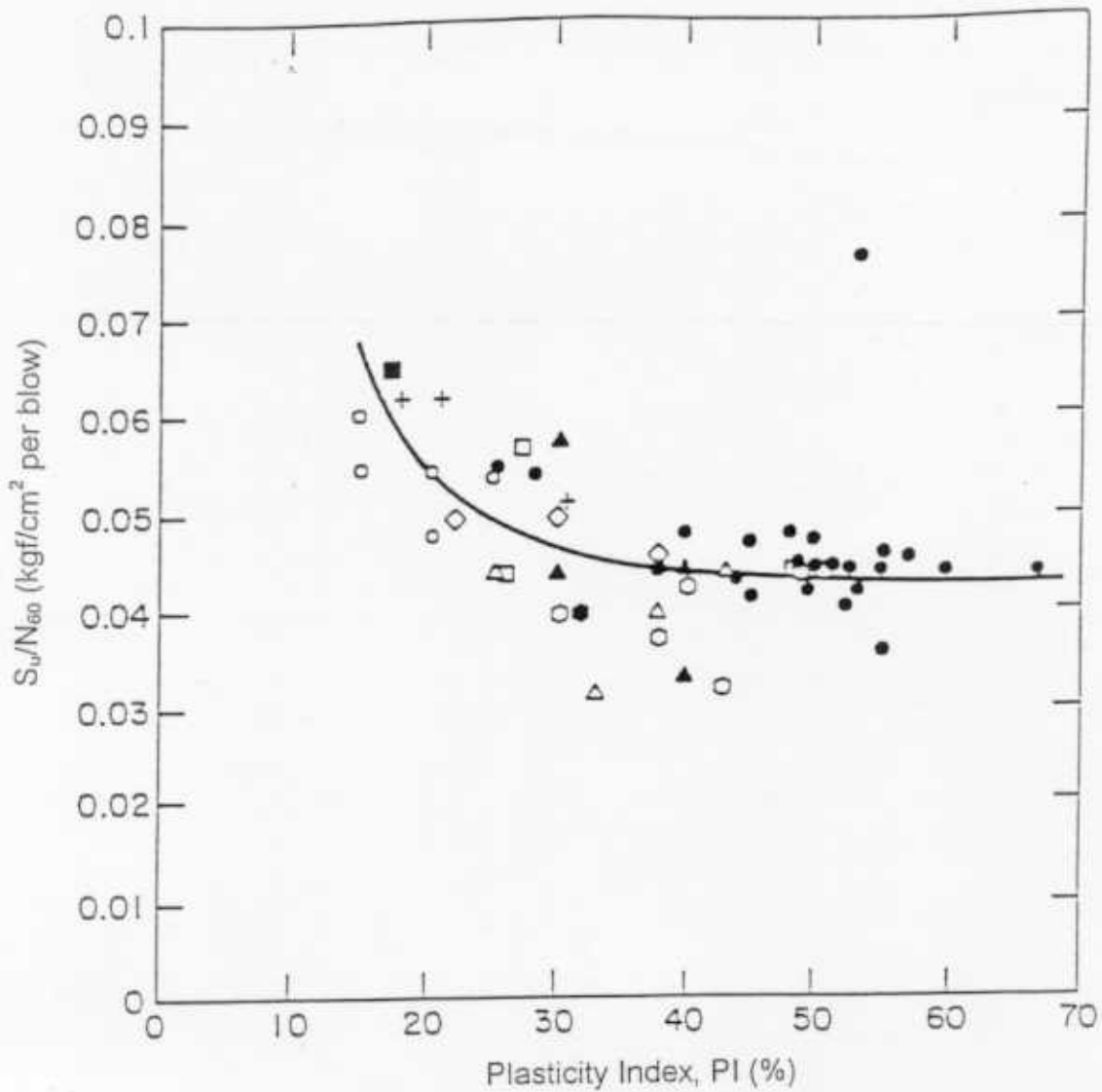
Note: As originally proposed, this correlation used the uncorrected SPT blowcount, N. However, hammers delivering 60% of the theoretical energy have been the most commonly used hammers for SPT tests, and it seems likely that the data on which the correlation was based was obtained primarily from tests with such hammers. It therefore seems logical to use N<sub>60</sub> with this correlation, and it is the recommendation of this report that this be done.

Table 26 - Empirical values for  $q_u$  \* and consistency of cohesive soils based on the standard penetration number (After Bowles, 1968)

Consistency	Very Loose	Loose	Medium	Dense	Very Dense	
$q_u$ , ksf	0	0.5	1.0	2.0	4.0	8.0
N, Standard Penetration Resistance	0	2	4	8	16	32
$\gamma_{sat}$ , pcf	100-120		110-130		120-140	

\* These values should be used as a guide only. Local cohesive samples should be tested, and the relationship between N and the unconfined compressive strength  $q_u$  established as  $q_u = KN$ .

Note: As originally proposed, this correlation used the uncorrected SPT blowcount, N. However, hammers delivering 60% of the theoretical energy have been the most commonly used hammers for SPT tests, and it seems likely that the data on which the correlation was based was obtained primarily from tests with such hammers. It therefore seems logical to use  $N_{60}$  with this correlation, and it is the recommendation of this report that this be done.

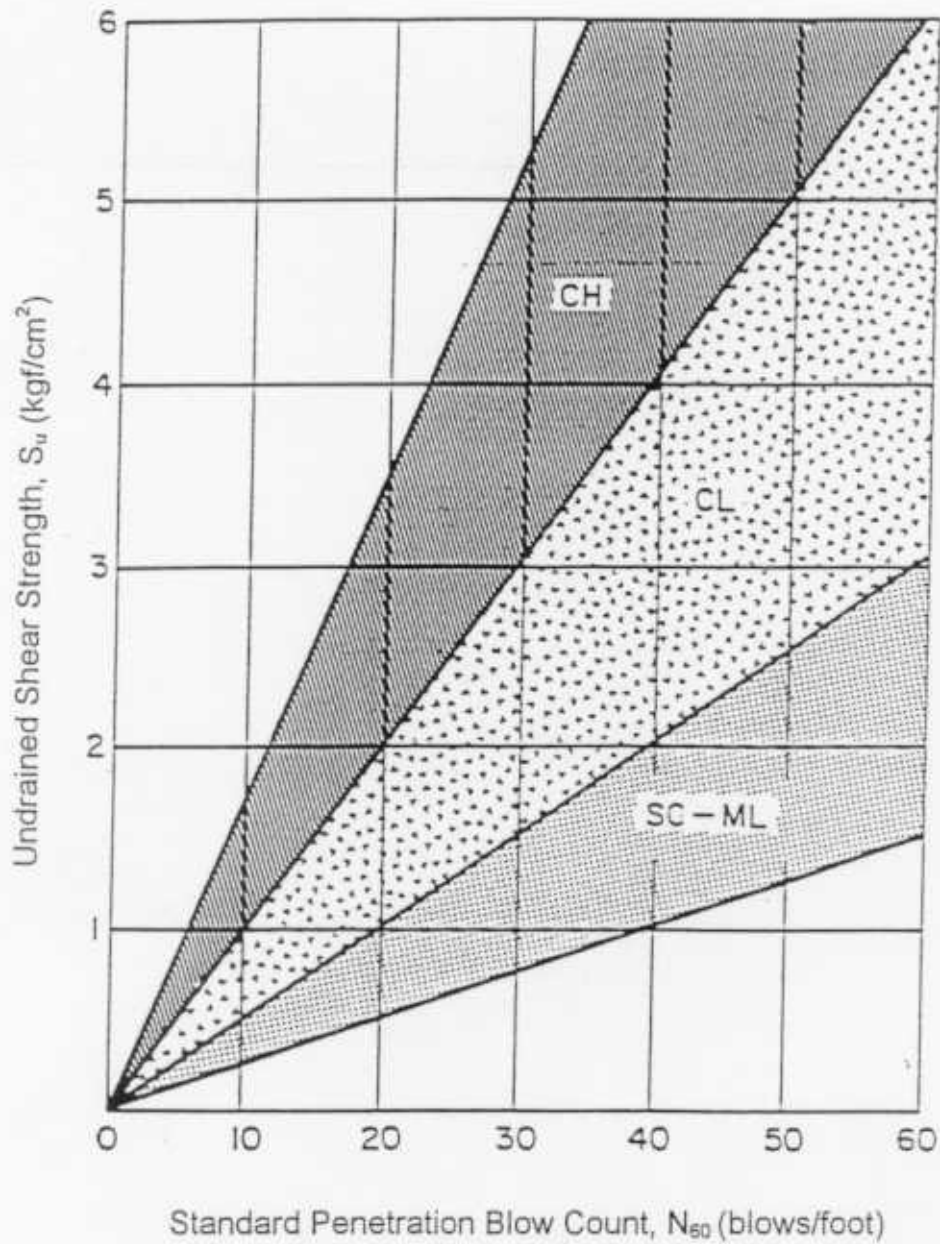


Legend :

- |                      |                          |
|----------------------|--------------------------|
| ● London Clay        | } less strongly fissured |
| ○ Boulder Clay       |                          |
| ◇ Laminated Clay     |                          |
| □ Bracklesham Beds   |                          |
| + Keuper Marl        |                          |
| ■ Flinz              |                          |
| ▲ Oxford Clay        | } more strongly fissured |
| △ Kimmeridge Clay    |                          |
| ○ Woolwich & Reading |                          |
| ● Upper Lias Clay    |                          |

Note: As originally proposed, this correlation used the uncorrected SPT blowcount,  $N$ . However, hammers delivering 60% of the theoretical energy have been the most commonly used hammers for SPT tests, and it seems likely that the data on which the correlation was based was obtained primarily from tests with such hammers. It therefore seems logical to use  $N_{60}$  with this correlation, and it is the recommendation of this report that this be done.

Figure 39. The variation of  $S_u/N$  with plasticity index, PI. (after Stroud, 1974)



Note: As originally proposed, this correlation used the uncorrected SPT blowcount,  $N$ . However, hammers delivering 60% of the theoretical energy have been the most commonly used hammers for SPT tests, and it seems likely that the data on which the correlation was based was obtained primarily from tests with such hammers. It therefore seems logical to use  $N_{60}$  with this correlation, and it is the recommendation of this report that this be done.

Figure 40. Relationship between standard penetration blow count,  $N$  and undrained shear strength,  $S_u$  (after Sowers, 1979)

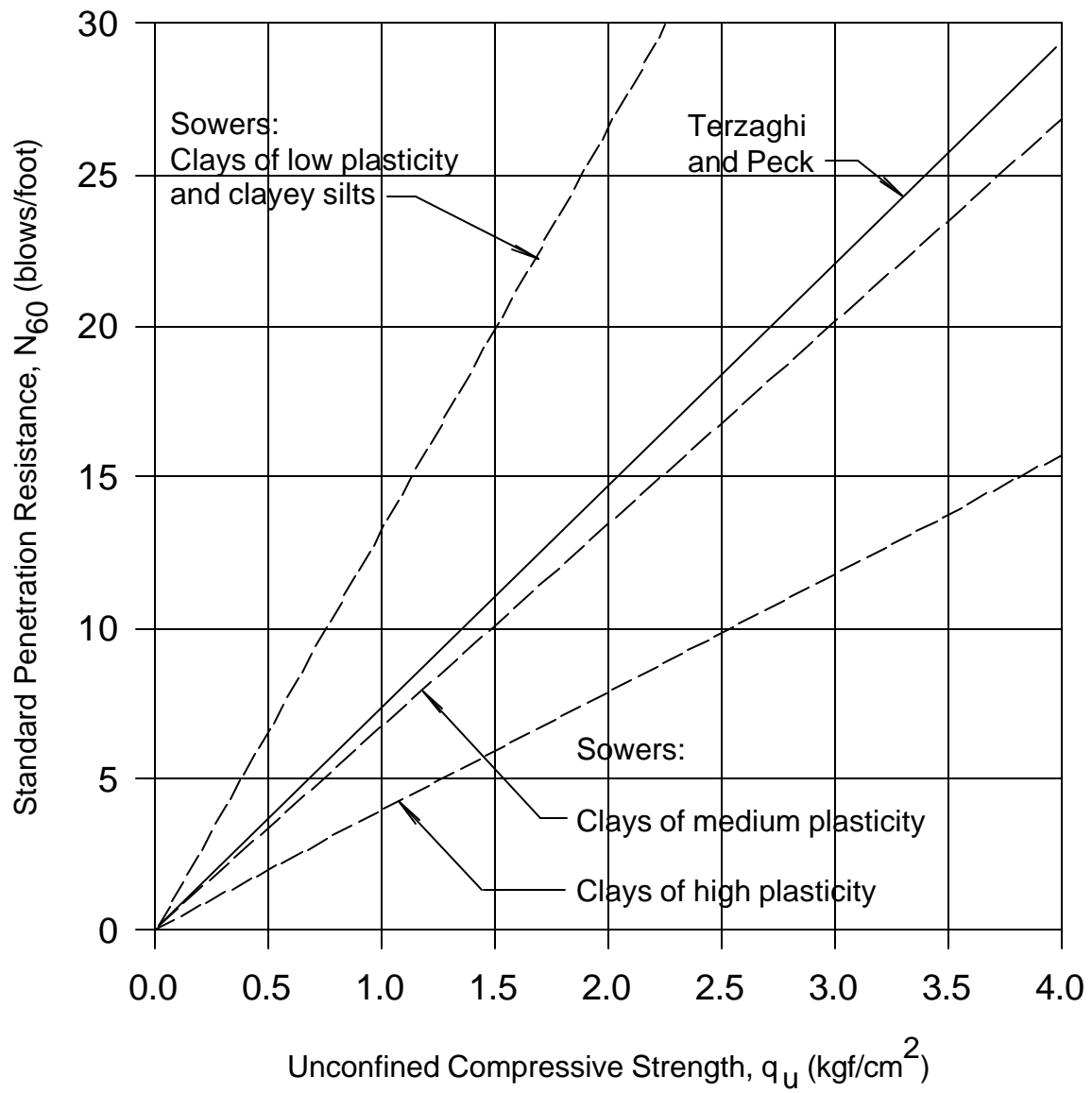


Figure 41. Relationship between standard penetration resistance,  $N_{60}$ , and unconfined compressive strength,  $q_u$  (after NAVFAC, 1982)

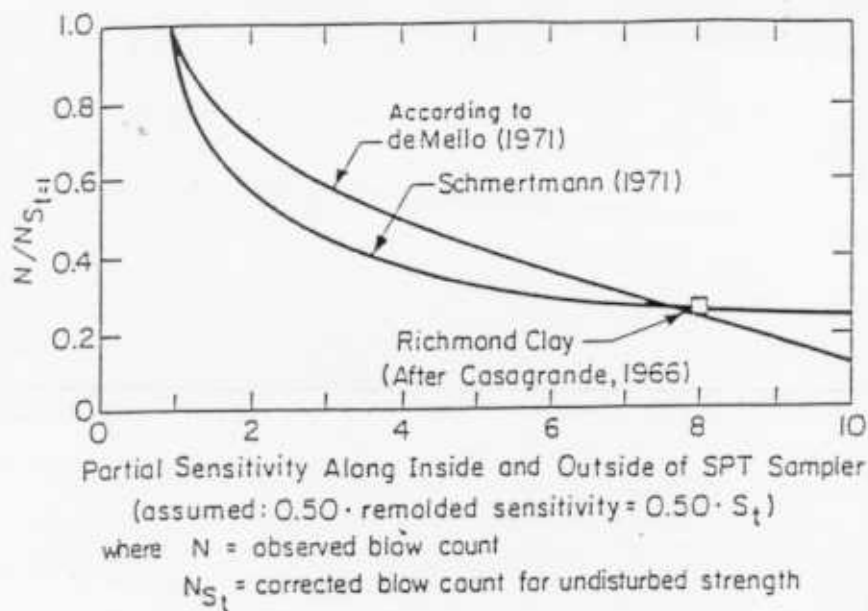
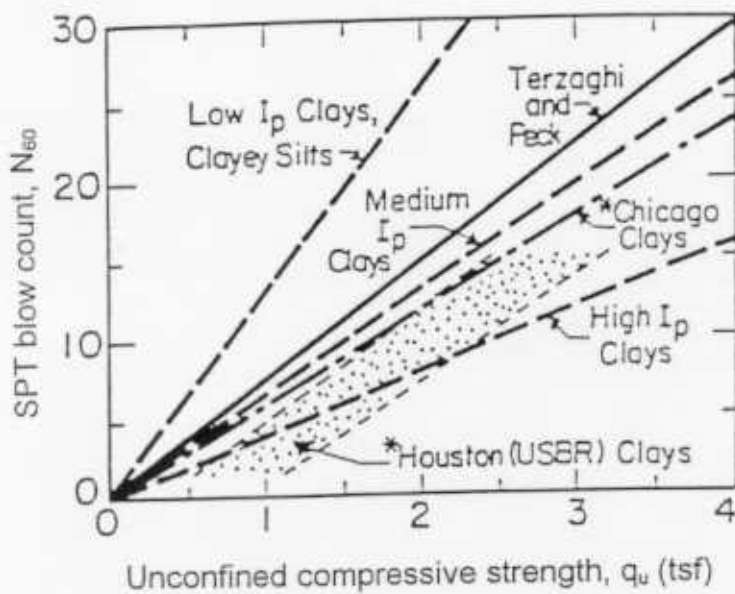


Figure 42. Estimated decrease in standard blow count with increasing clay sensitivity at constant undrained strength (originally from Schmertmann, 1975) (from Mitchell et al., 1978)



Note: As originally proposed, this correlation used the uncorrected SPT blowcount,  $N$ . However, hammers delivering 60% of the theoretical energy have been the most commonly used hammers for SPT tests, and it seems likely that the data on which the correlation was based was obtained primarily from tests with such hammers. It therefore seems logical to use  $N_{60}$  with this correlation, and it is the recommendation of this report that this be done.

Figure 43. Some correlations between SPT blow count ( $N$ ) and unconfined compressive strength ( $q_u$ ) in clays (originally from Schmertmann, 1975) (from Mitchell et al., 1978)

## Undrained Residual Steady State Strengths ( $S_r$ ) of Sands After Liquefaction

The SPT has been used to estimate residual steady-state strengths of soils after liquefaction. When soils are liquefied, or sheared to very large strains under undrained conditions, they reach a residual condition at which further shearing causes no additional change in strength, volume, or pore pressure (Casagrande, 1936). This “steady-state” strength is used to estimate post-liquefaction strengths and stability of soils. Figure 44 (Seed and Harder 1990) shows variations of residual undrained shear strength ( $S_r$ ) and equivalent clean sand SPT blow count ( $N_{1,60 - cs}$ ). The residual strengths in this figure were back-calculated from flow slides and slope failures. SPT tests were conducted at these sites to find the corresponding penetration resistances. The equivalent clean sand SPT blow count is calculated as follows:

$$N_{1,60 - cs} = N_{1,60} + N_{corr}$$

where

$N_{1,60 - cs}$  = equivalent clean sand SPT blow count (for use in Figure 44)

$N_{1,60}$  = SPT blow count normalized to 1 tsf of overburden pressure and 60% of the maximum free-fall hammer energy

$N_{corr}$  = correction factor based on fines content of the soil (see Table 27)

Note that Figure 44 indicates a wide range of residual shear strengths based on a limited number of case histories.



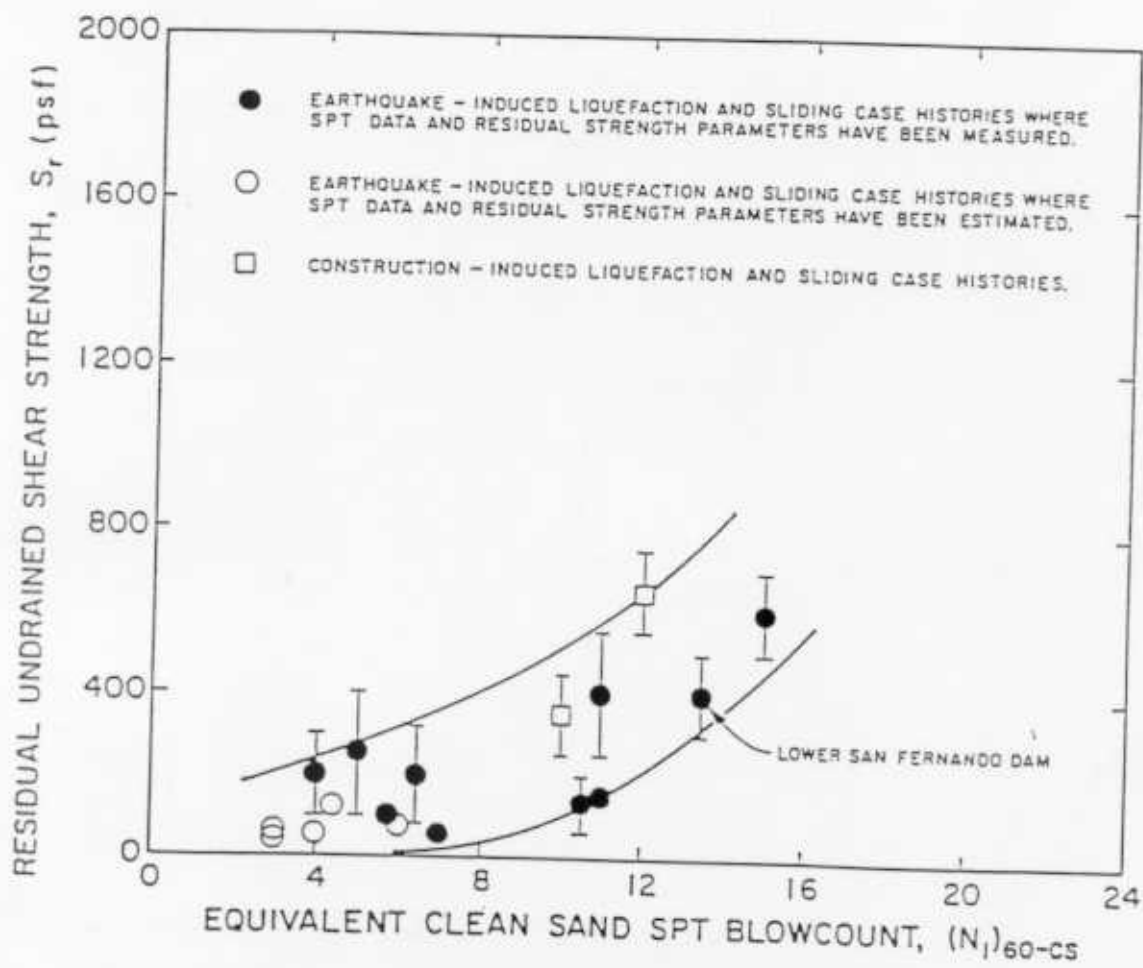


Figure 44. Relationship between corrected "clean sand" blow count,  $N_{1,60-CS}$  and undrained residual strength,  $S_r$  from case studies (from Seed and Harder, 1990)

Table 27. Recommended fines correction for estimation of residual undrained strength by Seed-Harder and Stark-Mesri Procedures (after Kramer, 1996)

Percent Fines	$N_{corr}$ (blows/foot)	
	Seed-Harder	Stark-Mesri
0	0	0
10	1	2.5
15	--	4
20	--	5
25	2	6
30	--	6.5
35	--	7
50	4	7
75	5	7

## Soil Modulus Values

The SPT can be used to estimate in-situ modulus values for soils. Constrained modulus ( $M$ ) and Young's modulus ( $E$  or  $E_s$ ) can be estimated using correlations with N-values. Summaries of correlations between moduli and SPT N-values are found in Table 28 (Tan et al. 1991) and plotted in Figure 46. Mitchell and Gardner (1975) warn that it is difficult to be certain which relationship applies to a particular soil, if any. Figure 45 shows variations of  $E_s$  with N summarized by Mitchell and Gardner (1975).

Relationships between modulus of compressibility ( $M$ ) and N-values for preloaded sand and normally loaded sand or sand and gravel are shown in Figure 47 (Tan et al. 1991).

Young's modulus ( $E$ ) can be related to the constrained modulus ( $M$ ) as follows:

$$E \approx 0.65M \text{ for loose sand}$$

$$E \approx 0.85M \text{ for dense sand}$$

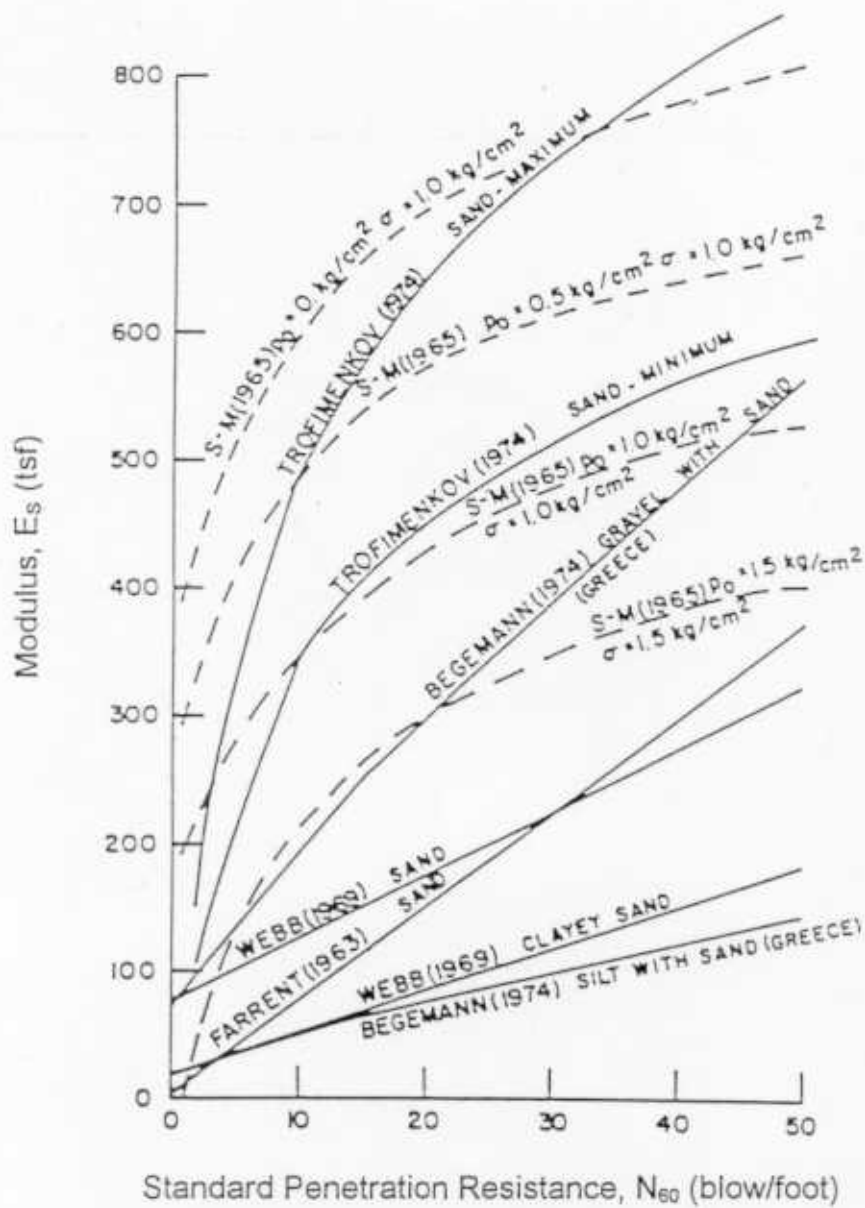
A correlation between small-strain shear modulus with uncorrected N-value, from NAVFAC (1982), is shown in Figure 48.

Table 28. Equations for stress-strain modulus by the SPT method (after Tan et al., 1991)

Soil	Stress-Strain Modulus, $E_S$ * (See Note)
Normally consolidated sand	$E_S = 500(N_{60} + 15)$ #1 $E_S = (15000 \text{ to } 22000) \ln N_{60}$ #2
Over-consolidated sand	$E_S = 18000 + 750N_{60}$ $E_{S,OCR} = E_{S,NC} (OCR)^{0.5}$
Gravelly sand and gravel	$E_S = 600(N_{60} + 6)$ $N_{60} \leq 15$ $E_S = 600(N_{60} + 6) + 2000$ $N_{60} > 15$
Clayey sand	$E_S = 320(N_{60} + 15)$
Silty sand	$E_S = 300(N_{60} + 6)$

\* Unit of  $E_S$  is in kPa (1 tsf  $\approx$  100 kPa)

Note: As originally proposed, these correlations used the uncorrected SPT blowcount,  $N$ . However, hammers delivering 60% of the theoretical energy have been the most commonly used hammers for SPT tests, and it seems likely that the data on which these correlations were based was obtained primarily from tests with such hammers. It therefore seems logical to use  $N_{60}$  with these correlations, and it is the recommendation of this report that this be done.



Note: As originally proposed, this correlation used the uncorrected SPT blowcount,  $N$ . However, hammers delivering 60% of the theoretical energy have been the most commonly used hammers for SPT tests, and it seems likely that the data on which the correlation was based was obtained primarily from tests with such hammers. It therefore seems logical to use  $N_{60}$  with this correlation, and it is the recommendation of this report that this be done.

Figure 45. Relationship for compressibility modulus as a function of standard penetration resistance (from Mitchell and Gardner, 1975)

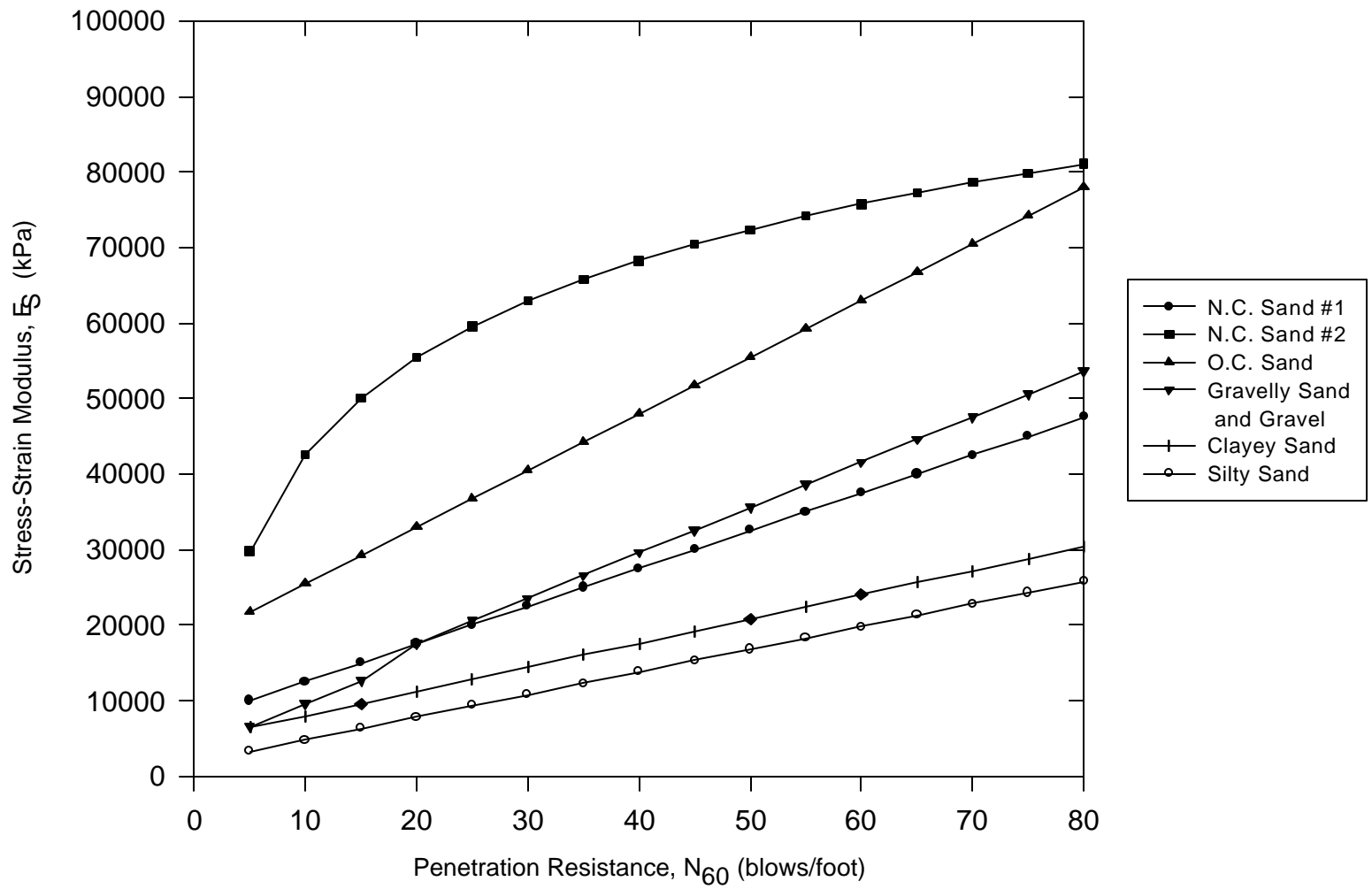
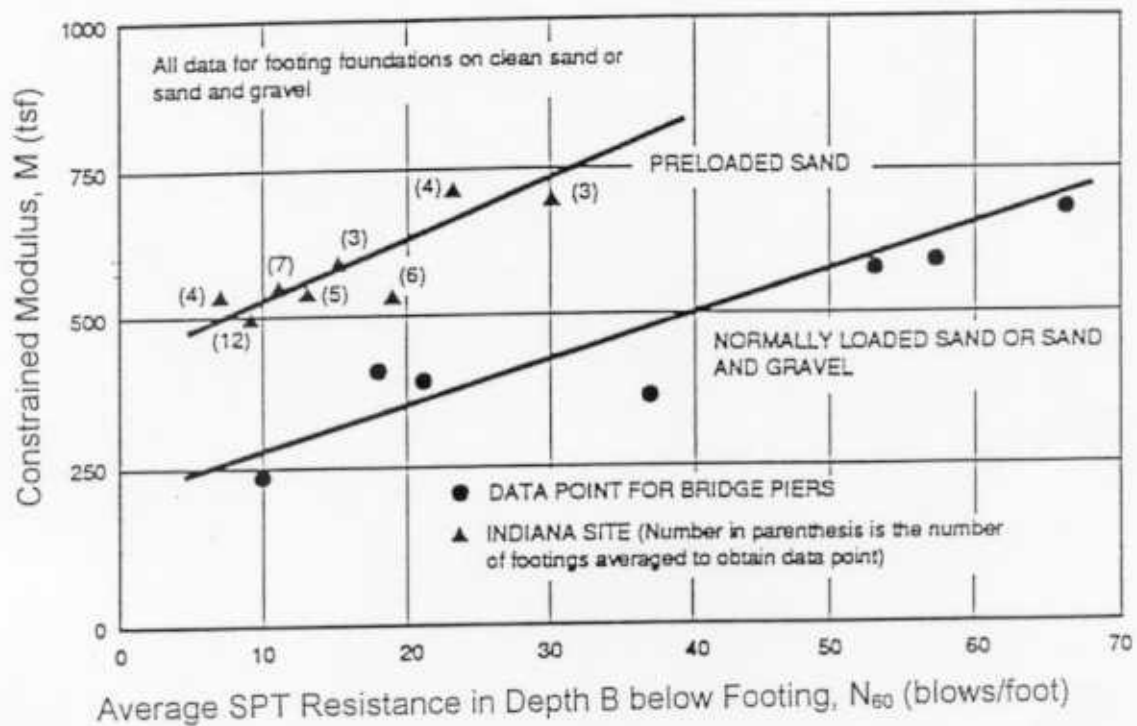
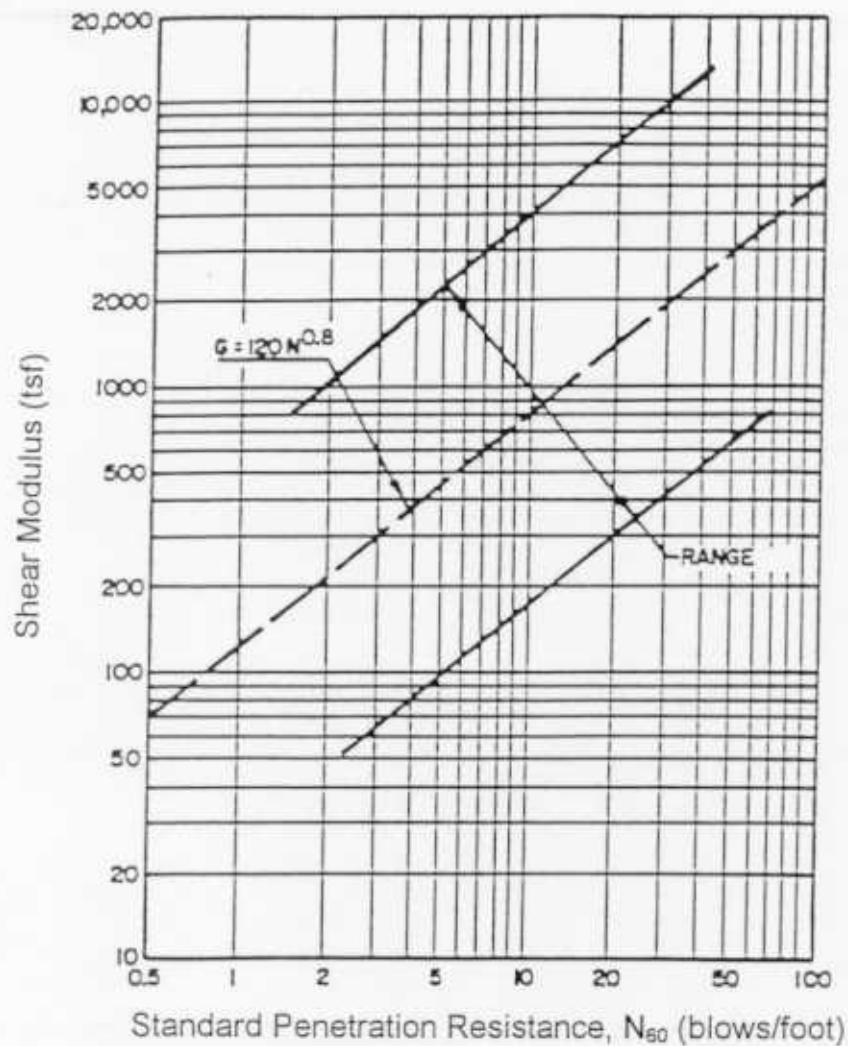


Figure 46. Correlations of stress-strain modulus and penetration resistance (data from Tan et al. , 1991)



Note: As originally proposed, this correlation used the uncorrected SPT blowcount,  $N$ . However, hammers delivering 60% of the theoretical energy have been the most commonly used hammers for SPT tests, and it seems likely that the data on which the correlation was based was obtained primarily from tests with such hammers. It therefore seems logical to use  $N_{60}$  with this correlation, and it is the recommendation of this report that this be done.

Figure 47. Correlation between constrained modulus and average value of SPT blow count (originally from D'Appolonia et al., 1970) (after Tan et al., 1991)



Note: As originally proposed, this correlation used the uncorrected SPT blowcount,  $N$ . However, hammers delivering 60% of the theoretical energy have been the most commonly used hammers for SPT tests, and it seems likely that the data on which the correlation was based was obtained primarily from tests with such hammers. It therefore seems logical to use  $N_{60}$  with this correlation, and it is the recommendation of this report that this be done.

Figure 48. Shear modulus vs.  $N$  values at very small strains (after NAVFAC, 1982)



## **Correlations Between SPT and Foundation Performance**

The SPT is often used to estimate settlement and bearing capacity of shallow foundations (mats, strips, rafts) and deep foundations (piles, drilled shafts). Both settlement and bearing capacity can be estimated directly based on SPT penetration resistance. This section provides correlations which can be used to estimate:

Settlement of Shallow Foundations on Sand

Settlement of Pile Groups in Sand

Bearing Capacity of Footings on Sand

Bearing Capacity of Pile Groups in Sand

Bearing Capacity of Drilled Shafts

## **Settlements of Shallow Foundations on Sand**

Settlement of shallow foundations on sand occurs quickly and is called immediate settlement ( $\rho$  or  $\rho_i$ ). The SPT can be used to estimate immediate settlements of foundations on sand based on modulus values estimated from SPT N-values, together with elastic settlement theories (Tan et al., 1991).

Correlations relating settlements directly to N-values have been suggested by Bazaraa (1967), Duncan and Buchignani (1976), Parry (1977), Burland and Burbridge (1985), and Terzaghi et al. (1996) as shown in Table 29.

Table 29. Correlations of settlements of footings on sand and SPT N-values

Settlement Equation	Parameters	Notes	Reference
$\rho = \rho \frac{\bar{N} \left[ \frac{B+1}{2B} \right]^2}{3}$	<p><math>\rho</math> = bearing pressure corresponding to a given magnitude of settlement (<math>\rho</math>) in tsf</p> <p><math>\rho</math> = settlement in inches</p> <p><math>\bar{N}</math> = average SPT blowcount (See Note)</p> <p>B = footing width in feet</p>		Bazaraa (1967)
$\rho_i = \frac{5p}{(N-1.5)C_B}$	<p><math>r_i</math> = maximum value of immediate settlement in inches</p> <p><math>p</math> = bearing pressure in tsf</p> <p>N = minimum average SPT blowcount * (See Note)</p> <p><math>C_B</math> = width correction factor (see Table 30)</p>	<p>* Average blowcounts for all borings over a depth B (B = footing width) below the base. Use the minimum of these values in the settlement equation. If the sand is saturated and silty with <math>N &gt; 15</math>, correct the N-value as outlined in the correction section</p>	Duncan and Buchignani (1976)
$\rho = 300 \frac{qB}{N_m}$	<p><math>r</math> = settlement in mm</p> <p>q = bearing pressure in <math>MN/m^2</math></p> <p>B = width of footing in m</p> <p><math>N_m</math> = representative SPT N-value at a depth of <math>(3/4)B</math> below foundation level (See Note)</p>	Design value of settlement	Parry (1977)

Table 29 continued

Settlement Equation	Parameters	Notes	Reference
$\rho_i = qB^{0.7}I_c$ (for NC sands)  $\rho_i = qB^{0.7} \frac{I_c}{3}$ (for OC sands)	$\rho_i$ = settlement of footing in mm  $q$ = foundation pressure in Kpa  $B$ = width of footing in m  $I_c = \frac{1.7}{N^{1.4}}$  $N$ = average SPT blowcount measured over a depth of $B^{0.75}$ (See Note)	The settlement of a NC sand is 3 times greater than that of the same sand in an OC state	Burland and Burbridge (1985)
$\rho_i = qB^{0.75}I_c$ (for NC sands)  $\rho_i = qB^{0.75} \frac{I_c}{3}$ (for OC sands)	$\rho_i$ = settlement of footing in mm  $q$ = foundation pressure in Kpa  $B$ = width of footing in m  $I_c = \frac{1.7}{N^{1.4}}$  $N$ = average SPT blowcount measured over a depth of $B^{0.75}$ (See Note)	Very similar to Burland and Burbridge	Terzaghi et al. (1996)

Note: As originally proposed, these correlations used the uncorrected SPT blowcount,  $N$ . However, hammers delivering 60% of the theoretical energy have been the most commonly used hammers for SPT tests, and it seems likely that the data on which these correlations were based was obtained primarily from tests with such hammers. It therefore seems logical to use  $N_{60}$  with these correlations, and it is the recommendation of this report that this be done.

Table 30. Width correction factor,  $C_B$  (after Duncan and Buchignani (1976))

Footing Width, B (feet)	$C_B$
$\leq 4$	1.00
6	0.95
8	0.90
10	0.85
$\geq 12$	0.80

## Settlements of Pile Groups in Sand

In-situ methods, such as the SPT, can be used to estimate settlements of pile groups. Settlements of pile groups in cohesionless soils (sands) occur rapidly and are usually complete by the end of construction.

### Piles in cohesionless soils:

Meyerhof (1976) related the settlement of pile groups ( $\rho$ ) to standard penetration resistance as:

$$\rho = \frac{2q\sqrt{B}}{N_1} I$$

where

$\rho$  = settlement of pile group on saturated sand or gravel in inches

$q$  = net foundation pressure in tsf applied at  $2D_b/3$  (see Figure 49)

$B$  = width of pile group in feet

$I$  = influence factor of effective group embedment

$$= 1 - \frac{D'}{8B} \geq 0.5$$

$D'$  = effective depth =  $2D_b/3$

$D_b$  = depth of penetration in bearing layer

$N_1$  = average corrected SPT N-value within the seat of settlement (approximately one pile group width ( $B$ ) below the equivalent footing). It is the recommendation of this report to use  $N_{1,60}$  in place of  $N_1$ .

If the pile group is in silty sand, Meyerhof (1976) suggests the following equation:

$$\rho = \frac{4q\sqrt{B}}{N_1} I$$

where all variables are the same as noted above.

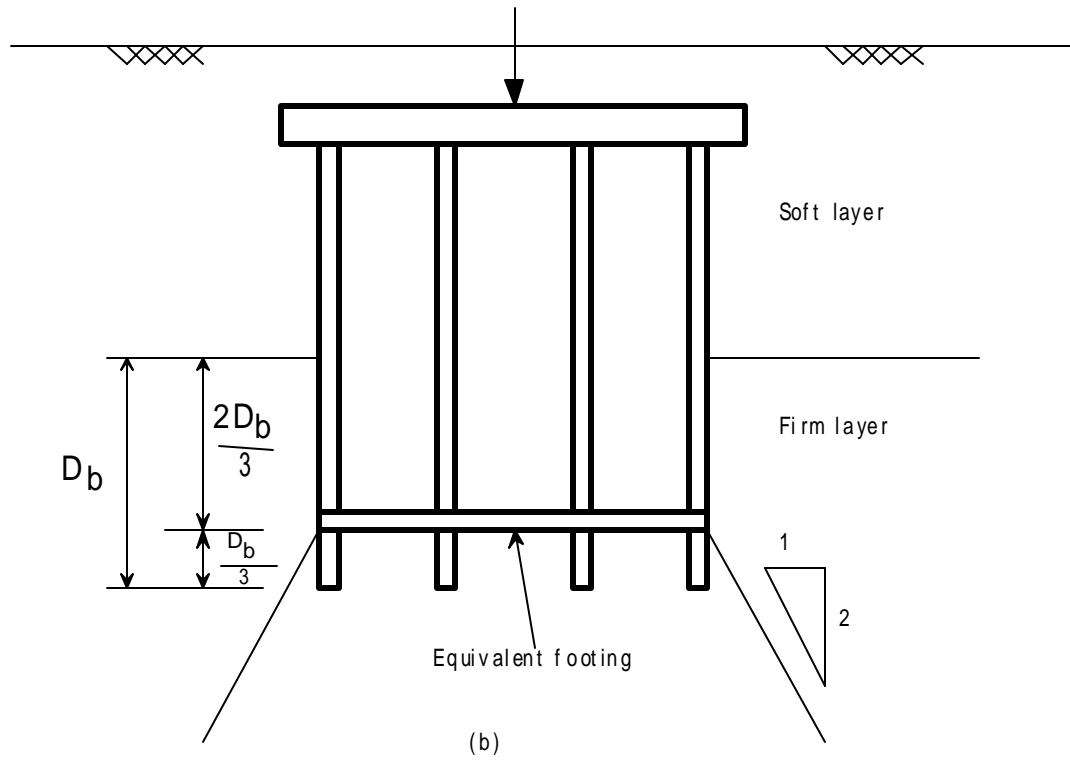
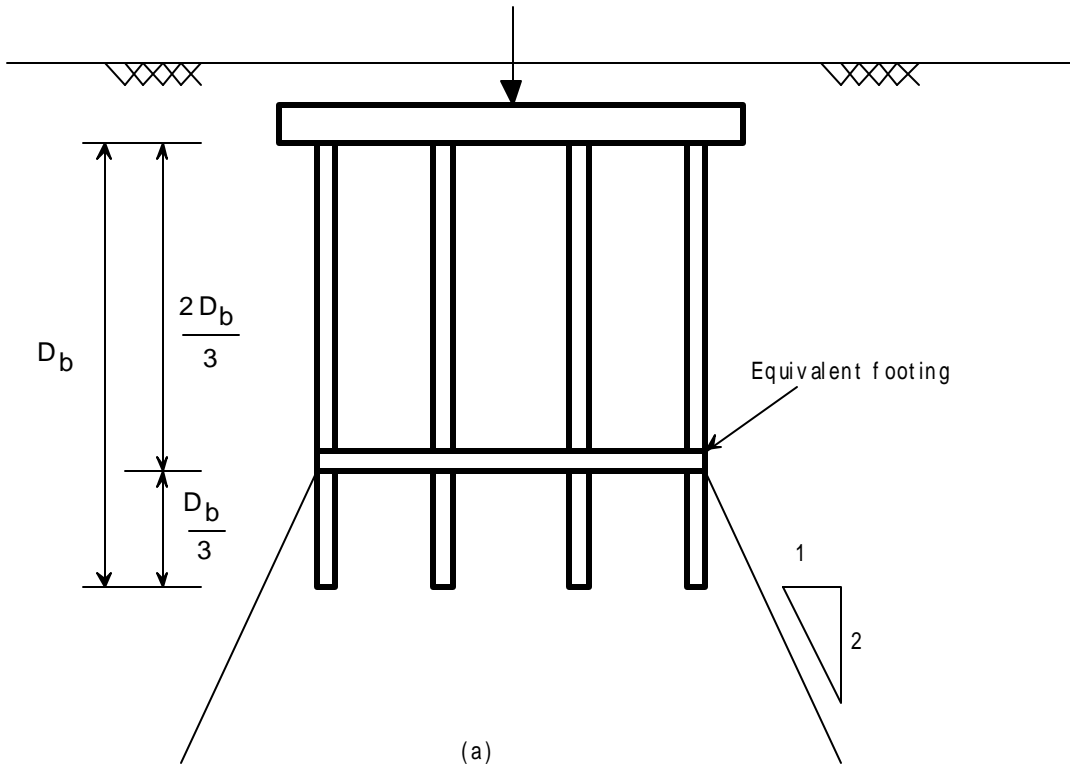


Figure 49. Location of equivalent footing (after Meyerhof, 1976)

### Piles in clay:

Pile groups in clay settle over longer time periods due to the longer time required for drainage. To estimate settlements of pile groups in clay, the group is transformed to an equivalent footing, as shown in Figure 49 (Ooi et al., 1991a). The equivalent footing is located at  $2/3$  of the depth of penetration in the bearing layer ( $2D_b/3$ ). Figure 49(a) illustrates a homogeneous bearing layer, and Figure 49(b) shows a bearing layer overlain by a soft, non-bearing soil layer.

The settlement of the equivalent footing is estimated using the same procedures as for shallow foundations. As noted by Ooi et al. (1991a), three components contribute to the total settlement of a pile group in clay:

1. immediate settlement
2. consolidation settlement and
3. secondary compression settlement.



## Bearing Capacity of Footings on Sand

The SPT can be used two ways to estimate the bearing capacity of footings on sand:

1. The SPT can be used to estimate the angle of internal friction angle ( $\phi$ ) for the sands, and this can be used with bearing capacity theories to estimate bearing capacity.
2. The bearing capacity can be estimated directly using the equation suggested by Meyerhof (1956) and modified by Tan et al. (1991):

$$q_{ult} = \frac{\bar{N}B}{10} \left( C_{w1} + C_{w2} \frac{D_f}{B} \right) R_i$$

where

$q_{ult}$  = ultimate bearing capacity in tsf

$\bar{N}$  = the average blow count corrected for submergence in saturated very fine or silty sand as shown in Section 5.  $N$  is averaged over a depth  $1.5B$  below the footing (Meyerhof, 1956). It is the recommendation of this report to use  $N_{60}$  with this correlation.

$B$  = footing width (least dimension) in feet

$D_f$  = embedment depth (depth from ground surface to base of footing) in feet

$C_{w1}$ ,  $C_{w2}$  = water table correction factors ( $D_w$  = distance from the ground surface to the water table)

$C_{w1} = C_{w2} = 1.0$  for  $D_w \geq D_f + 1.5B$

$C_{w1} = 0.5$  and  $C_{w2} = 1.0$  for  $D_w = D_f$

$C_{w1} = 0.5$  and  $C_{w2} = 0.5$  for  $D_w = 0$

$R_i$  = load inclination factor from Table 31a or 31b

Values of  $C_{w1}$  and  $C_{w2}$  for other positions of the water table (between  $D_w = 0$  and  $D_w = D_f + 1.5B$ ) can be determined by interpolation (Tan et al., 1991).

Table 31. Load inclination factors ( $R_i$ ) (after Tan et al., 1991)

Table 31a. For square footings

H/V = horizontal load / vertical load	Load Inclination Factor ( $R_i$ )		
	D <sub>i</sub> /B = 0	D <sub>i</sub> /B = 1	D <sub>i</sub> /B = 5
0.10	0.75	0.80	0.85
0.15	0.65	0.75	0.80
0.20	0.55	0.65	0.70
0.25	0.50	0.55	0.65
0.30	0.40	0.50	0.55
0.35	0.35	0.45	0.50
0.40	0.30	0.35	0.45
0.45	0.25	0.30	0.40
0.50	0.20	0.25	0.30
0.55	0.15	0.20	0.25
0.60	0.10	0.15	0.20

Table 31b. For rectangular footings

H/V = horizontal load / vertical load	Load Inclination Factor ( $R_i$ )					
	Load Inclined in Width Direction			Load Inclined in Length Direction		
	D <sub>i</sub> /B = 0	D <sub>i</sub> /B = 1	D <sub>i</sub> /B = 5	D <sub>i</sub> /B = 0	D <sub>i</sub> /B = 1	D <sub>i</sub> /B = 5
0.10	0.70	0.75	0.80	0.80	0.85	0.90
0.15	0.60	0.65	0.70	0.70	0.80	0.85
0.20	0.50	0.60	0.65	0.65	0.70	0.75
0.25	0.40	0.50	0.55	0.55	0.65	0.70
0.30	0.35	0.40	0.50	0.50	0.60	0.65
0.35	0.30	0.35	0.40	0.40	0.55	0.60
0.40	0.25	0.30	0.35	0.35	0.50	0.55
0.45	0.20	0.25	0.30	0.30	0.45	0.50
0.50	0.15	0.20	0.25	0.25	0.35	0.45
0.55	0.10	0.15	0.20	0.20	0.30	0.40
0.60	0.05	0.10	0.15	0.15	0.25	0.35

## Bearing Capacity of Piles in Sand

Penetration resistance (N) can be used to estimate the point capacity (pile tip resistance) and the shaft resistance (skin friction) of piles and drilled shafts. The SPT method provides a preliminary guide for pile capacity and length estimates. Wave equation analyses, PDA measurements during driving, and perhaps CAPWAP analyses and pile load tests should be used to verify design assumptions.

Meyerhof (1976) developed a simple procedure for estimating pile capacities based on SPT N-values. Ultimate pile bearing capacity is the sum of the point resistance ( $Q_p$ ) and the shaft resistance ( $Q_s$ ). Both components of the ultimate capacity can be estimated using SPT N-values. The ultimate point resistance can then be calculated by:

$$Q_{p,ult} = q_p A_p$$

where

$Q_{p,ult}$  = ultimate point resistance of a pile in a cohesionless soil stratum

$q_p$  = point resistance in tsf

$A_p$  = area of pile tip in ft<sup>2</sup>

The point resistance per unit area of a pile driven into a cohesionless soil can be estimated by:

$$q_p = \frac{0.4N_1 D_b}{B} \leq q_{limit}$$

where

$N_1$  = average corrected SPT N-value near the pile tip. The original form of this equation uses an N-value corrected for overburden pressure only. It is the recommendation of this report to use  $N_{1,60}$  instead of  $N_1$ .

$N$  = measured SPT N-value

$\sigma_v'$  = effective overburden pressure at pile tip in tsf

$B$  = pile width or diameter (same length units as  $D_b$ )

$D_b$  = depth of pile driven into cohesionless soil stratum (same length units as  $B$ )

$q_{limit}$  = limiting point resistance

=  $4N_1$  for sands

=  $3N_1$  for non-plastic silts

The ultimate shaft capacity of a pile in a cohesionless soil stratum can then be calculated by:

$$Q_{s,ult} = q_s A_s$$

where

$q_s$  = skin friction in tsf

$A_s$  = surface area of pile shaft in ft<sup>2</sup>

The skin friction of a pile driven into a cohesionless soil stratum can also be estimated from SPT N-values using equations by Meyerhof (1976):

$$q_s = \frac{\bar{N}}{50} \text{ (tsf) for displacement piles}$$

$$q_s = \frac{\bar{N}}{100} \text{ (tsf) for non - displacement piles}$$

where

$q_s$  = skin friction in tsf

$\bar{N}$  = average uncorrected SPT N-value measured along the pile shaft. It is the recommendation of this report to use  $N_{60}$  instead of  $\bar{N}$ .

Figures 50 and 51 show variations of measured values of  $q_p$  and  $q_s$  with N for cohesionless soils. The plots include data for different soil types (gravel, sand, and silt) and different methods of pile installation (driven piles and drilled shafts).

The Meyerhof equations presented above apply to homogeneous conditions. Where the soil bearing layer overlies a weaker layer, the piles may punch into the weaker layer, as shown in Figure 52 (Ooi et al., 1991a). Meyerhof (1976) suggests that if the distance between the pile tip and the weak layer (H) is less than 10 pile diameters (10D), the ultimate point resistance should be calculated as:

$$q_p = q_o + \frac{(q_{limit} - q_o)}{10D} \leq q_{limit}$$

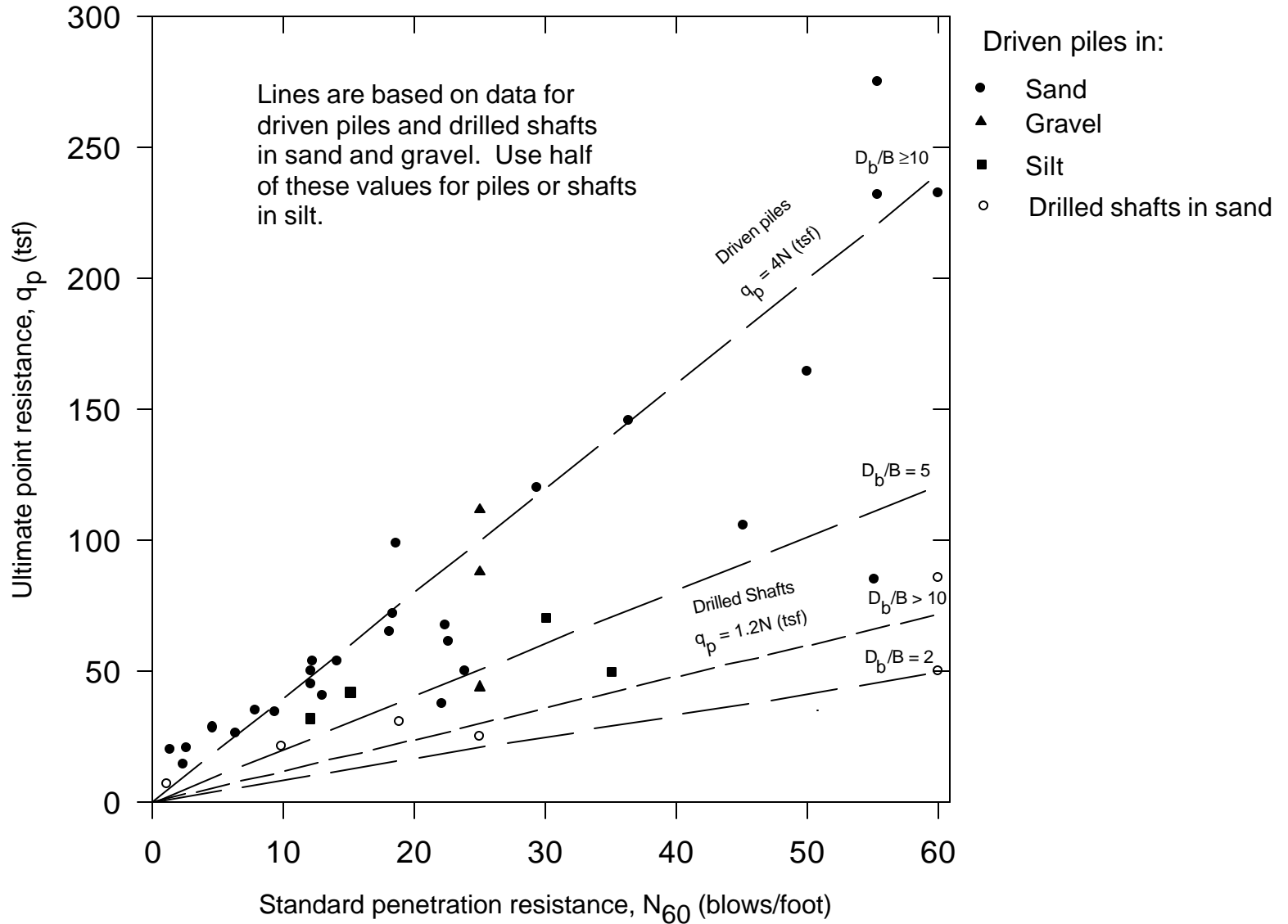


Figure 50. Empirical relation between ultimate point resistance of piles and Standard Penetration Resistance in cohesionless soil (after Meyerhof, 1976)

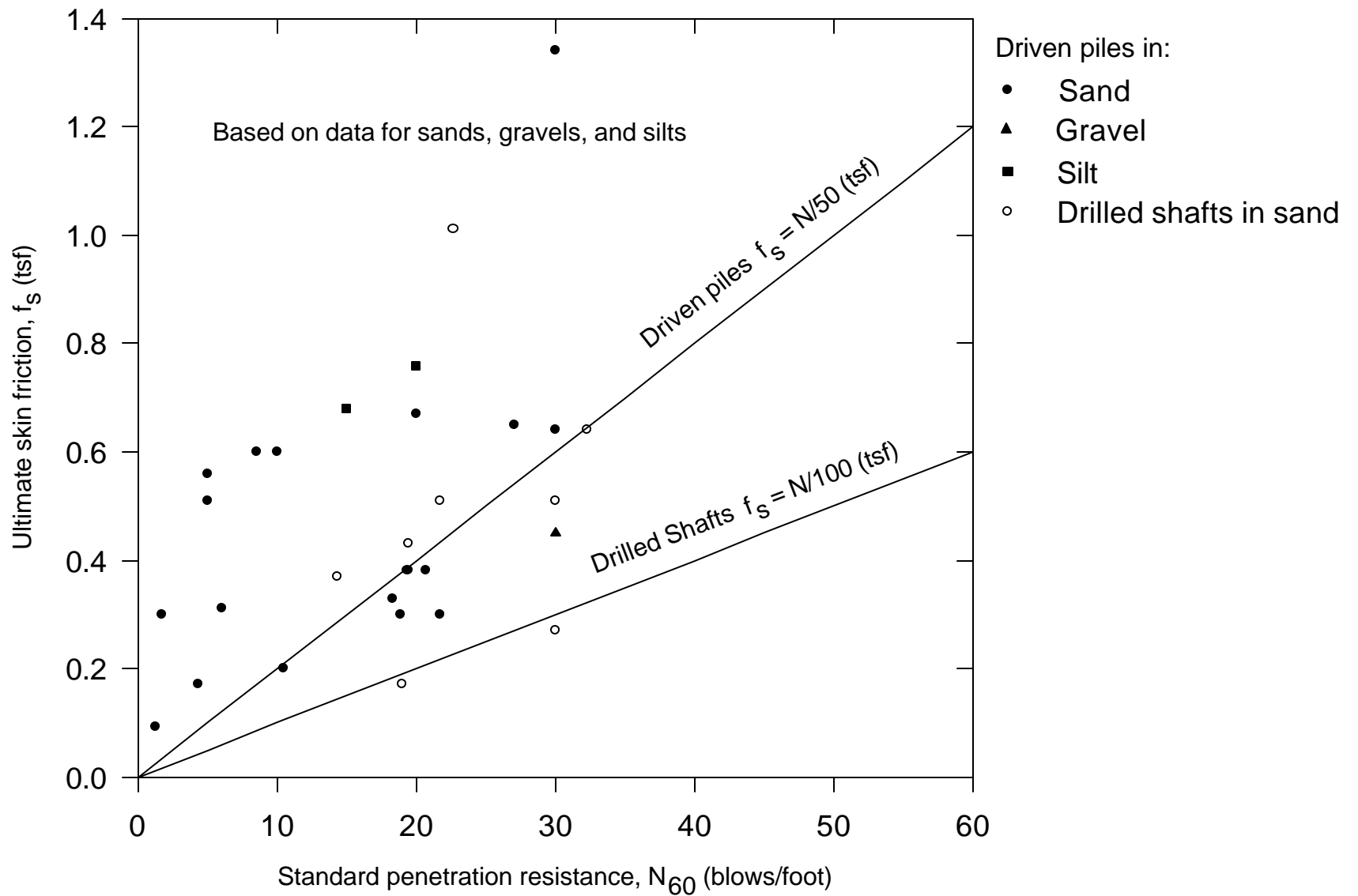


Figure 51. Empirical relationships between ultimate skin friction of piles and penetration resistance in cohesionless soil (after Meyerhof, 1976)

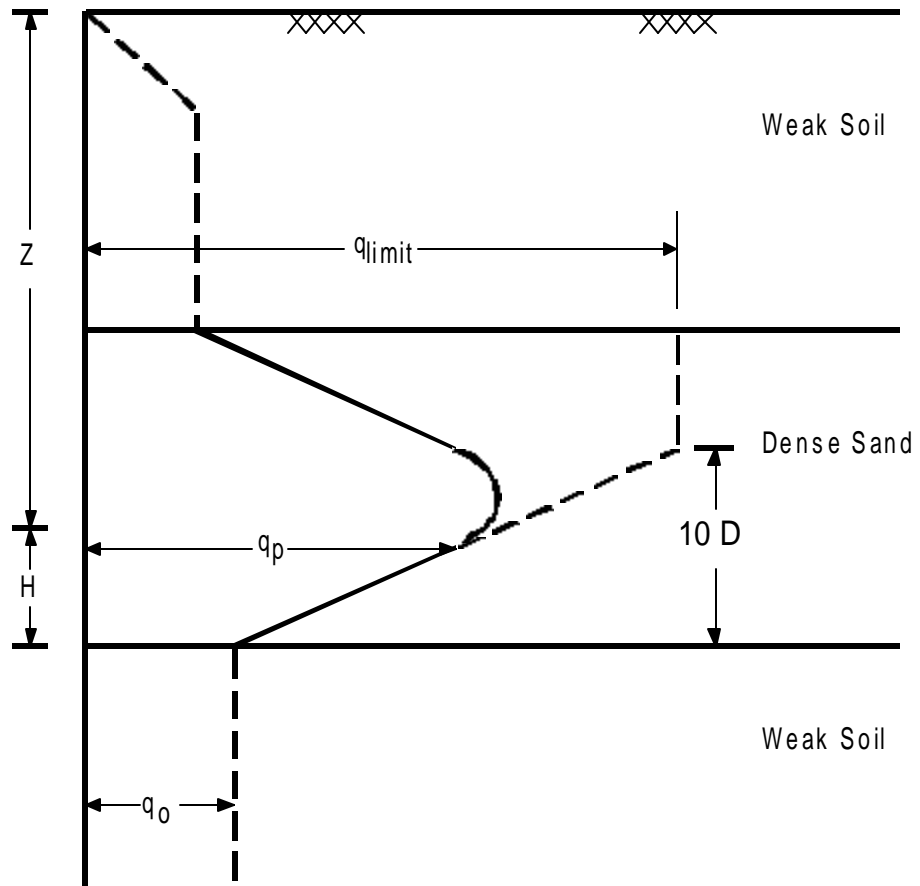


Figure 52. Relation between ultimate point resistance of pile and depth in thin sand layer overlying weak soil (after Meyerhof, 1976)

where

$q_p$  = ultimate unit tip resistance

$q_o$  = limiting unit tip resistance in the weaker stratum

$q_{limit}$  = limiting unit tip resistance in the stronger stratum

Neely (1990a) performed load tests on long and short expanded-base (Franki) piles and developed relationships between ultimate point resistance and SPT N-values for this type of pile. Expanded-base piles are illustrated in Figure 53. In his studies, Neely defined a long pile as one with a  $D/D_b$  ratio greater than 10, where  $D$  is the embedment depth of the maximum cross section of the base taken as the sum of the driven length and one-half the base diameter, and  $D_b$  is the diameter of the expanded base. A short pile is one with  $D/D_b$  less than 10. Empirical relationships between ultimate point resistance and SPT N-values are shown in Figure 54 (for long expanded-base piles) and Figure 55 (for short expanded-base piles). Note that the N-values used in these figures have been corrected to 1 tsf of overburden pressure using the Peck et al. (1974) equation:

$$N_1 = \left[ 0.77 \log \frac{20}{\sigma_v'} \right] N$$

where

$N_1$  = N-value corrected to 1 tsf of overburden pressure. It is the recommendation of this report to use  $N_{1,60}$  instead of  $N_1$  when using Figures 54 and 55.

$\sigma_v'$  = effective overburden pressure in tsf

$N$  = measured N-value

Bazaraa and Kurkur (1986) worked with different types of piles at sites with medium to stiff cohesive soils underlain by medium to coarse sand. Piles analyzed for ultimate load capacities fall into 1 of 4 categories:

- I - Prepakt piles using high pressure for mortar injection.
- II - Driven piles, Bauer piles carefully installed, Prepakt piles with low injection pressures.
- III - Bored piles carefully installed, Bauer piles with some installation defects.
- IV - Bored piles with some installation defects.



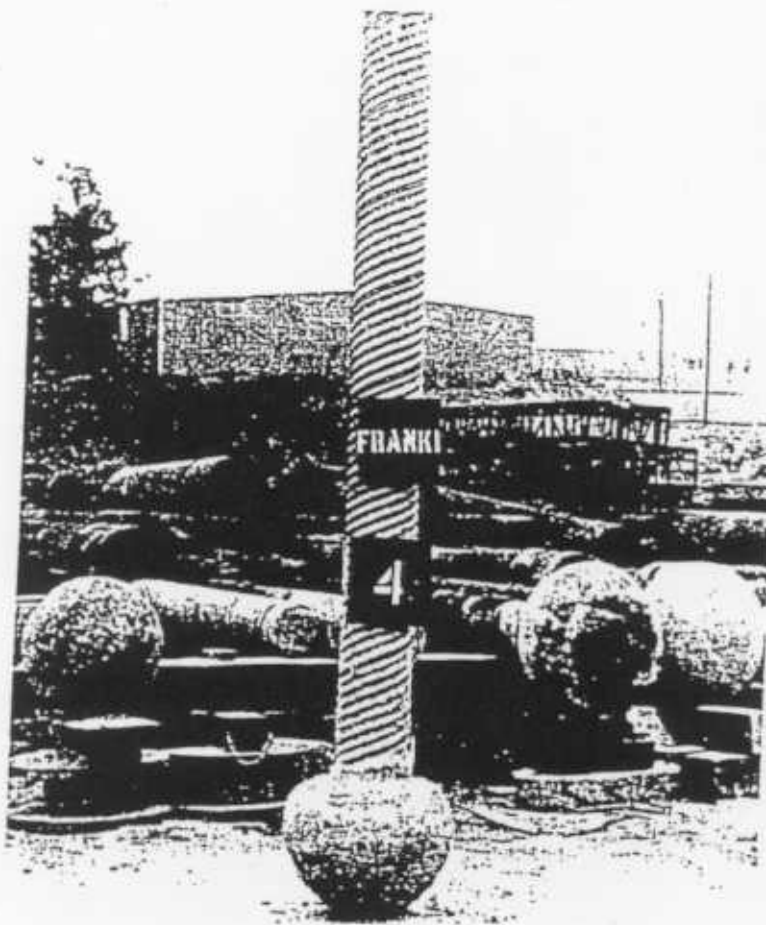


Figure 53. Photograph of exhumed Franki piles showing expanded bases (from Neely, 1990)

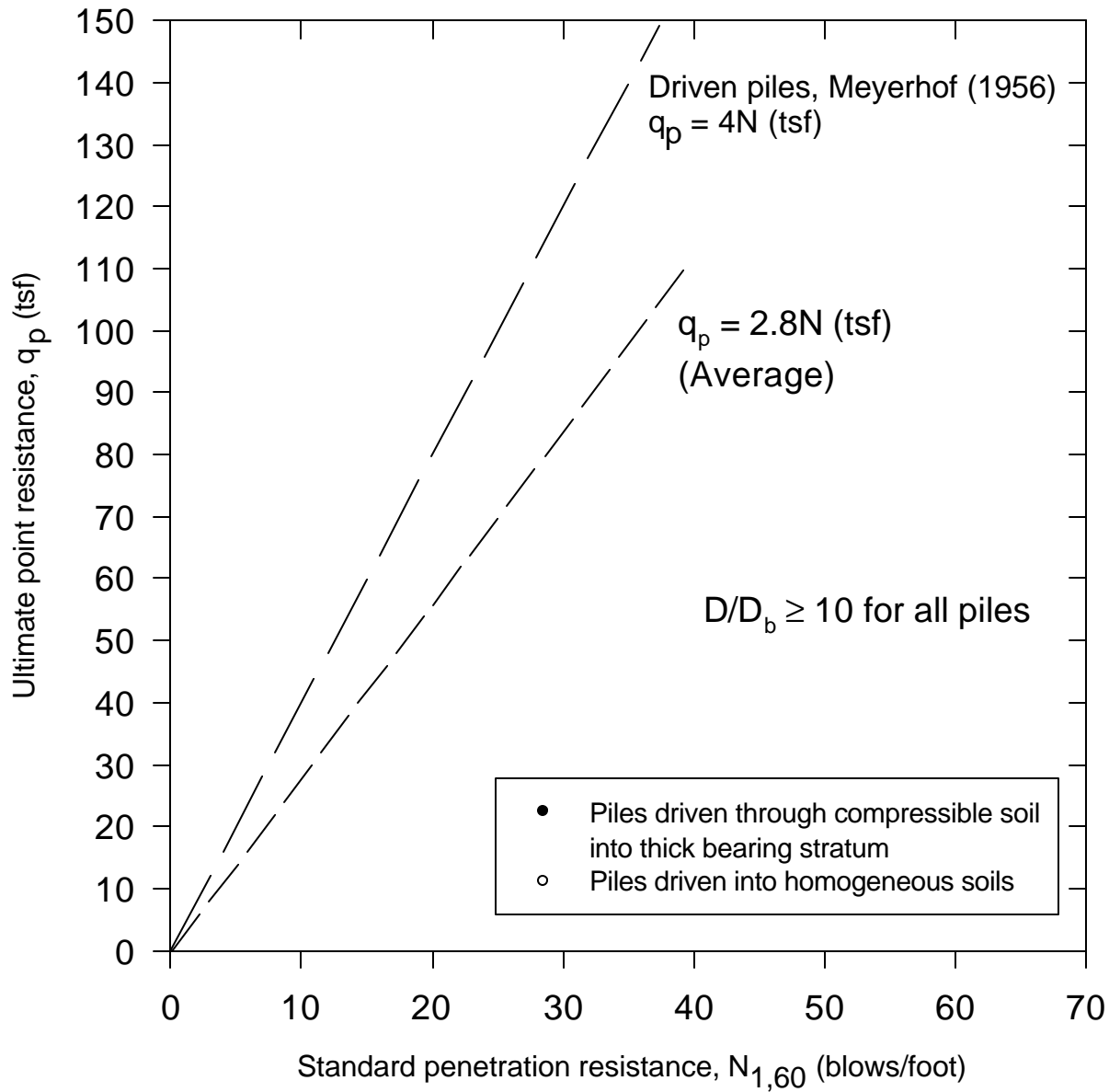


Figure 54. Empirical relation between ultimate point resistance and standard penetration resistance for long expanded-base piles (after Neely, 1990)

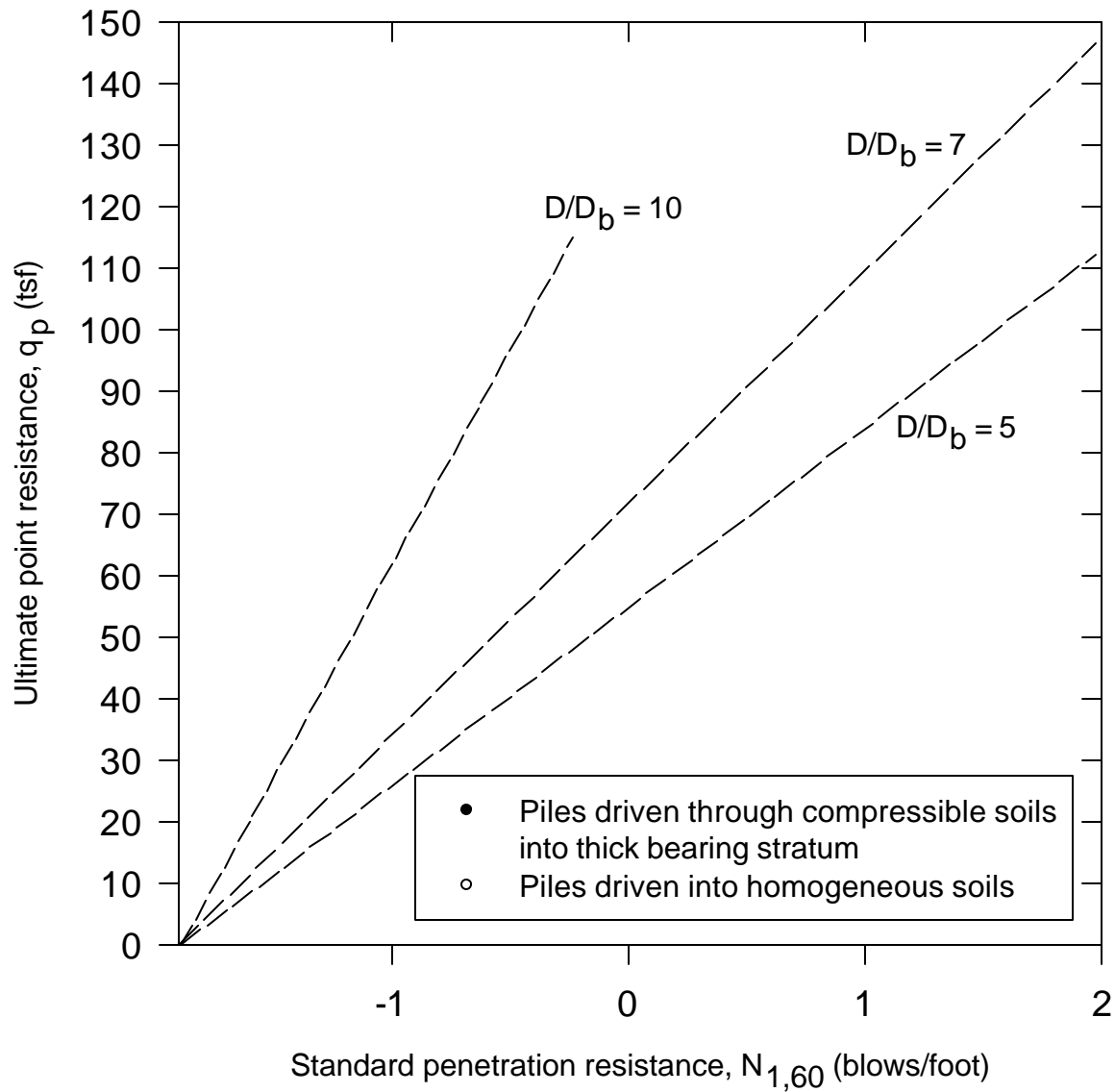


Figure 55. Empirical relation between ultimate point resistance and standard penetration resistance for short expanded-base piles (after Neely, 1990)

The authors summarized correlations of pile capacities with SPT N-values for both cohesionless and cohesive soils in Tables 32 and 33:

Table 32. Correlations of pile capacities and penetration resistance for piles in cohesionless soil (data from Bazaraa and Kurkur (1986))

Pile Type	Pile Diameter, d (cm)	Unit Shaft Resistance, $q_s$ (tonnes/m <sup>2</sup> ) (See Note)	Unit Point Resistance, $q_p$ (tonnes/m <sup>2</sup> ) (See Note)
Raymond	< 50	$4 + 0.1N_s$	--
Raymond	> 50	$(d/50)(4 + 0.1N_s)$	--
I, II	< 50	$N_s/4.5$	$20N_p$
I, II	> 50	$(d/50)(N_s/4.5)$	$(d/50)(20N_p)$
III, IV	< 50	$N_s/15$	$13.5N_p$
III, IV	> 50	$(d/50)(N_s/15)$	$(d/50)(13.5N_p)$

where

$N_s$  = average SPT N-value along pile shaft (See Note)

$N_p$  = average SPT N-value within a distance of 1d beneath the pile tip and 3.75d above it (See Note)

$\leq 50$  blows/foot

d = pile diameter or width in cm

Note: As originally proposed, this correlation used the uncorrected SPT blowcount, N. However, hammers delivering 60% of the theoretical energy have been the most commonly used hammers for SPT tests, and it seems likely that the data on which the correlation was based was obtained primarily from tests with such hammers. It therefore seems logical to use  $N_{60}$  with this correlation, and it is the recommendation of this report that this be done.

Table 33. Correlations of pile capacities and penetration resistance for piles in cohesive soil (data from Bazaraa and Kurkur (1986))

Pile Type	Unit Shaft Resistance, $q_s$ (tonnes/m <sup>2</sup> ) (See Note)	Unit Point Resistance, $q_p$ (tonnes/m <sup>2</sup> ) (See Note)
I, II	$N_s/3$	$6N_p$
III, IV	$0.2N_s$	$4N_p$

where

$N_s$  = average SPT N-value along pile shaft (See Note)

$N_p$  = average SPT N-value within a distance of 1d beneath the pile tip and 3.75d above it (See Note)

≤ 50 blows/foot

d = pile diameter or width

Note: As originally proposed, this correlation used the uncorrected SPT blowcount, N. However, hammers delivering 60% of the theoretical energy have been the most commonly used hammers for SPT tests, and it seems likely that the data on which the correlation was based was obtained primarily from tests with such hammers. It therefore seems logical to use  $N_{60}$  with this correlation, and it is the recommendation of this report that this be done.

## Bearing Capacity of Drilled Shafts

The SPT can be used to estimate shaft resistance ( $q_s$ ) and base resistance ( $q_p$ ) of drilled shafts in sands. While few field load tests have been performed on drilled shafts in sands, several methods have been developed relating N-values to drilled shaft capacity. Ooi et al. (1991b) have summarized procedures for estimating  $q_s$  and  $q_p$  for drilled shafts in sands in Tables 35 and 36.

Table 34. Summary of procedures for estimating shaft resistance ( $q_s$ ) of drilled shafts in sand (after Ooi et al., 1991b)

Reference	Description	Notes
Meyerhof (1976)	$q_s = \frac{N}{100}$ (tsf) (See Note)	Same as for non-displacement piles
Quiros and Reese (1977)	$q_s = 0.026N < 2$ tsf (See Note)	Limit of 2 tsf is the maximum value ever measured
Reese and Wright (1977)	$q_s = \frac{N}{34}$ (tsf) for $N \leq 53$ $q_s = \frac{N-53}{450} + 1.6$ (tsf) for $53 < N \leq 100$ (See Note)	

Note: As originally proposed, this correlation used the uncorrected SPT blowcount, N. However, hammers delivering 60% of the theoretical energy have been the most commonly used hammers for SPT tests, and it seems likely that the data on which the correlation was based was obtained primarily from tests with such hammers. It therefore seems logical to use  $N_{60}$  with this correlation, and it is the recommendation of this report that this be done.

Table 35. Summary of procedures for estimating base resistance ( $q_p$ ) of drilled shafts in sand (after Ooi et al., 1991b)

Reference	Description	Notes
Meyerhof (1976)	$q_p = \frac{2N_1 D_b}{15D_p} \quad (\text{tsf})$ <p>It is the recommendation of this report that <math>N_{1,60}</math> be used with this correlation</p>	<p><math>q_p &lt; 4N_1/3</math> for sands  <math>q_p &lt; N_1</math> for nonplastic silts</p> <p>Lower limiting values than for driven piles. <math>q_p</math> increases linearly with embedment up to about 10 shaft diameters and then remains approximately constant with depth.</p>
Reese and Wright (1977)	$q_p = \frac{2}{3}N \quad (\text{tsf}) \text{ for } N \leq 60$ $q_p = 40 \quad (\text{tsf}) \text{ for } N > 60$ <p>(See Note)</p>	<p><math>q_p</math> based on a downward movement equal to 5% of the base diameter (from load tests)</p>
Reese and O'Neill (1988)	<p>For shaft diameters &lt; 50 inches</p> $q_p = 0.6N \quad (\text{tsf}) \text{ for } N \leq 75$ $q_p = 45 \quad (\text{tsf}) \text{ for } N > 75$ <p>For shaft diameters &gt; 50 inches</p> $q_{pr} = \frac{50}{D_p} q_p \quad (\text{tsf}) \quad (\text{see notes})$ <p>(See Note)</p>	<p><math>q_p</math> based on a downward movement equal to 5% of the base diameter (from load tests)</p> <p><math>q_{pr}</math> = reduced base resistance for <math>D_p &gt; 50</math> inches</p> <p><math>D_p</math> = diameter of drilled shaft (pier) base in inches</p> <p><math>q_p</math> = ultimate end bearing resistance as calculated by methods in this table</p>

where

$N_1$  = SPT blowcount corrected to 1 tsf of overburden pressure (See Note)  
=  $[0.77 \log (20/\sigma_v')]N$

$\sigma_v'$  = effective overburden pressure in tsf

N = uncorrected blowcount

$D_p$  = base diameter of drilled shaft (pier) in feet (in inches for Reese and O'Neill (1988))

$D_b$  = embedment of drilled shaft in sand bearing layer

Note: As originally proposed, this correlation used the uncorrected SPT blowcount, N. However, hammers delivering 60% of the theoretical energy have been the most commonly used hammers for SPT tests, and it seems likely that the data on which the correlation was based was obtained primarily from tests with such hammers. It therefore seems logical to use  $N_{60}$  with this correlation, and it is the recommendation of this report that this be done.



## Correlations Between SPT and Liquefaction Potential of Sands

Sites containing saturated granular soils at low relative densities are susceptible to liquefaction during earthquakes. Liquefaction is defined by Youd and Idriss (1997) as "the phenomena of seismic generation of large pore-water pressures and consequent severe softening of granular soils." Liquefaction has been responsible for significant damage to structures during earthquakes.

A simplified procedure for evaluating the liquefaction resistance of soils was developed by Seed and his colleagues and has been in use for many years. The procedure was developed from evaluations of field observations (presence of sand boils, ground fissures, and lateral spreads) and field and laboratory test data. Data collected for development of the simplified procedure comes mostly from sites with level to gently sloping terrain and Holocene alluvial or fluvial sediment at depths less than 50 feet (Youd and Idriss, 1997). In December 1997, the NCEER Workshop on Evaluation of Liquefaction Resistance of Soils was held to further update liquefaction analyses.

To evaluate liquefaction resistance of soils using the simplified procedure, two variables are estimated or calculated:

1. The cyclic stress ratio (CSR). CSR is a measure of the seismic loading applied to a soil during an earthquake.
2. The cyclic resistance ratio (CRR). CRR is a measure of the capacity of the soil to resist liquefaction. Curves separating combinations of CRR and CSR that cause liquefaction from those that do not are shown in Figure 56 for soils containing different percentages of fines.

The CSR can be calculated using the equation from Seed and Idriss (1971) as presented by Youd and Idriss (1997):

$$\text{CSR} = (\tau_{av}/\sigma_{vo}') = 0.65(a_{\text{max}}/g)(\sigma_{vo}/\sigma_{vo}')r_d$$

where

$a_{\text{max}}$  = peak horizontal acceleration at the ground surface

$g$  = acceleration due to gravity

$\sigma_{vo}$  = total vertical overburden stress

$\sigma_{vo}'$  = effective overburden stress

$r_d$  = stress reduction coefficient

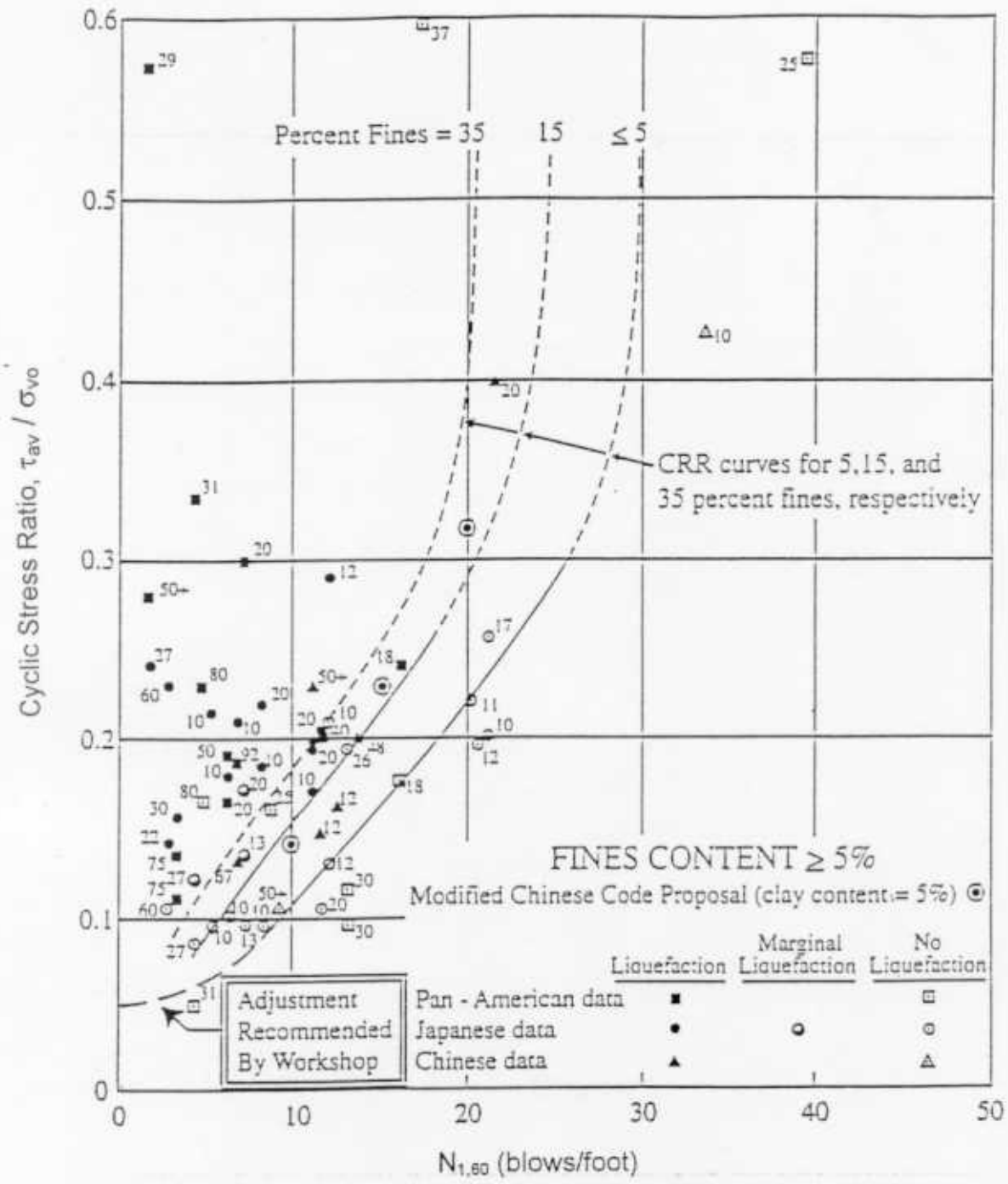


Figure 56. Simplified base curve recommended for estimating liquefaction potential from SPT data along with empirical liquefaction data (modified from Seed et al., 1985 by Youd and Idriss, 1997)

Participants at the 1997 NCEER workshop recommend the following equations for calculating  $r_d$ :

$$\begin{aligned}r_d &= 1.0 - 0.00765(z) && \text{for } z \leq 9.15 \text{ m (30 feet)} \\r_d &= 1.174 - 0.0267(z) && \text{for } 9.15 \text{ m} < z \leq 23 \text{ m (75 feet)} \\r_d &= 0.744 - 0.008(z) && \text{for } 23 < z \leq 30 \text{ m (100 feet)} \\r_d &= 0.50 && \text{for } z > 30 \text{ m}\end{aligned}$$

where

$z$  = depth below ground surface in meters

The calculated value of CSR can then be used along with  $N_{1,60}$  to determine the likelihood of liquefaction using Figure 56. It is only valid for earthquakes of magnitude 7.5. If the magnitude is different than 7.5, the CSR value must be scaled by a magnitude scaling factor (MSF) as shown below:

$$CSR_{M \neq 7.5} = MSF(CSR_{7.5})$$

where

$CSR_{7.5}$  = cyclic stress ratio based an earthquake of magnitude 7.5

$MSF = 10^{2.24/M^{2.56}}$  (Idriss 1990). This is a lower bound and is conservative to use.

$M$  = moment magnitude of the earthquake

Figure 56 can be used two different ways:

#### Method 1

- Calculate CSR as outlined above
- Use  $N_{1,60}$  without any additional corrections
- Use the percent fines curve in Figure 56 that corresponds to the fines content (the portion passing the #200 sieve) of the soil being analyzed. If the point defined by the values of CSR and  $N_{1,60}$  falls to the left of the approximate curve, liquefaction is likely. If the point falls to the right of the curve, liquefaction is unlikely.

#### Method 2

- Calculate CSR as outlined above
- Correct  $N_{1,60}$  to  $N_{1,60 - cs}$  (clean sand blow count) as shown below:

$$N_{1,60 - cs} = \alpha + \beta(N_{1,60})$$

where  $\alpha$  and  $\beta$  are shown below:

Table 36. Fines content corrections (from Youd and Idriss, 1997)

Fines content, FC (%)	$\alpha$	$\beta$
$\leq 5$	0	1.0
5 - 35	$\exp [1.76 - (190/FC^2)]$	$[0.99 + (FC^{1.5}/1000)]$
$\geq 35$	5.0	1.2

- Use Figure 56 with the clean sand curve (the  $FC \leq 5$  curve) and the corrected blow count =  $N_{1,60 - cs}$

If the point defined by the values of CSR and  $N_{1,60}$  falls to the left of the curve, liquefaction is likely. If the point falls to the right of the curve, liquefaction is unlikely.

## **Appendix A**

### **ASTM Specification D 1586**

## **Appendix B**

### **Unit Conversions and Drill Rod Sizes**

## Units Conversion Factors

### Force

Pounds	Kips	U.S. Tons	Newtons	Kilonewtons	Metric Tons
1.00	0.001	0.0005	4.45	0.00445	0.000454
1000	1.00	0.500	4450	4.45	0.454
2000	2.00	1.00	8900	8.90	0.908
0.225	0.000225	0.000112	1.00	0.001	0.000102
225	0.225	0.112	1000	1.00	0.102
2200	2.20	1.10	9800	9.80	1.00

### Length

Inches	Feet	Centimeters	Meters
1.00	0.083	2.54	0.0254
12.0	1.00	30.5	0.305
0.394	0.0328	1.00	0.01
39.4	3.28	100	1.00

### Stress

lb/ft <sup>2</sup>	lb/in <sup>2</sup>	k/ft <sup>2</sup>	t/ft <sup>2</sup> (1)	KN/m <sup>2</sup> (KPa)	t/m <sup>2</sup> (2)
1.00	0.00694	0.001	0.0005	0.0479	0.00488
144	1.00	0.144	0.0720	6.90	0.702
1000	6.94	1.00	0.500	47.9	4.88
2000	13.9	2.00	1.00	95.8	9.76
20.9	0.145	0.0209	0.0104	1.00	0.102
205	1.42	0.205	0.102	9.81	1.00

(1) U.S. Ton (2) Metric Ton

### Unit Weight of Water

= 62.4 lb/ft <sup>3</sup>	= 0.000433 k/in <sup>3</sup>	= 0.000217 t/in <sup>3</sup> (U.S. ton)
= 0.0361 lb/in <sup>3</sup>	= 9.81 KN/m <sup>3</sup>	= 1.00 t/m <sup>3</sup> (Metric ton)
= 0.0624 k/ft <sup>3</sup>	= 0.00000981 KN/cm <sup>3</sup>	= 0.00000100 t/cm <sup>3</sup> (Metric ton)

## Drill Rod Sizes

Size	O.D. (inches)	I.D. (inches)	Threads Per Inch	Weight (lbs./ft.)	(Weight kg/m)
E	1-15/16	7/8	3	2.7	4.0
EW	1-3/8	15/16	3	2.8	4.2
A	1-5/8	1-1/8	3	3.8	5.7
AW	1-3/4	1-1/4	3	4.3	6.4
B	1-7/8	1-1/4	5	3.6	5.4
BW	2-1/8	1-3/4	3	4.3	6.4
N	2-3/8	2	4	5.0	7.4
NW	2-5/8	2-1/4	3	5.5	8.2
HW	3-1/2	3-1/16	3	8.8	13.1



## References

- Al-Khafaji, A. W. and Andersland, O. B., 1992. *Geotechnical Engineering and Soil Testing*. Saunders College Publishing, Fort Worth.
- American Society for Testing and Materials (ASTM), 1997. Standard Test Method for Penetration Test and Split-Barrel Sampling of Soils (D1586-84), *Annual Book of Standards*, Vol. 4.08, pp. 137-141, Philadelphia, PA.
- Bazaraa, A. R. S. S., 1967. Use of Standard Penetration Test for estimating settlements of shallow foundations on sand. Ph. D. dissertation submitted to Dept. of Civil Engineering, University of Illinois, 380. pp.
- Bazaraa, A. R. and Kurkur, M. M., 1986. N-value used to predict settlements of piles in Egypt. Use of In Situ Tests in Geotechnical Engineering, ASCE GSP 6: 462-474.
- Bowles, J., 1968. *Foundation Analysis and Design*. McGraw-Hill, New York.
- Broms, B. B. and Flodin, N., 1988. History of soil penetration testing. Proc. 1st Int. Symposium on Penetration Testing, Rotterdam, pp. 157-220.
- Burland, J. B. and Burbridge, 1985. Settlements of foundations on sand and gravel. Proc. Inst. Civ. Engrs. Part 1, No. 78, Dec. 1325-1381.
- Caliendo, J. A., Bartholomew, M., Lai, P. W., Townsend, F. C., and McVay, M. C., 1995. Static pile capacity predictions with SPT91. Panamerican Conference on Soil Mechanics and Foundation Eng., 10(2): 1045-1057.
- Campanella, R. G. and Sy, A., 1994. Recent developments in energy calibration of penetration tests at UBC. International Conference on Soil Mechanics and Foundation Eng., 13(1): 151-156.
- Carter, M. and Bentley, S. P., 1991. *Correlations of Soil Properties*. Pentech Press Publishers, London.
- Casagrande, A., 1936. Characteristics of cohesionless soils affecting the stability of slopes and earth fills. Journal of Boston Society of Civil Engineers.
- Decourt, L., 1990. The Standard Penetration Test State-of-the-Art-Report. Norwegian Geotechnical Institute Publ. No. 179, Oslo, Norway.
- de Mello, V., 1971. The Standard Penetration Test -- A State-of-the-Art Report, Proc. of the fourth Panamerican Conference on Soil Mechanics and Foundation Engineering, Puerto Rico, pp. 1-86.

Duncan, J. M. and Buchignani, A. L., 1976. An Engineering Manual for Settlement Studies. The Charles E. Via, Jr. Department of Civil Engineering, Virginia Polytechnic Institute and State University.

Duncan, J. M., Helmers, M. J., and Mokwa, R. L., 1997. Design method for drilled shaft sound wall foundations. A Report of Research performed under sponsorship of the Virginia Transportation Research Council, June 1997.

Duncan, J. M., Horz, R. C., and Yang, T. L., 1989. Shear strength correlations for geotechnical engineering. Virginia Tech Department of Civil Engineering - Geotechnical Engineering, August, 1989.

Dunham, J. W., 1954. Pile foundations for buildings. Proc. ASCE Soil Mechanics and Foundation Division.

Farrar, J.A., Nickell, J., Allen, M.G., Goble, G., and Berger, J., 1998. Energy loss in long rod penetration testing - Terminus Dam Liquefaction Investigation. Proc. of the Geotechnical Earthquake Engineering and Soil Dynamics III Specialty Conference, ASCE GSP No. 75, pp. 554-567.

Fletcher, G. F. A., 1965. Standard penetration test: Its uses and abuses. ASCE Journal of Geotechnical Engineering, 91(4): 67-75.

Gibbs, H. J. and Holtz, W.G., 1957. Research on determining the density of sands by spoon penetration testing. International Conference on Soil Mechanics and Foundation Eng., 4(1): 35-39.

Harder, L. F., Jr., 1997. Application of the Becker Penetration Test for evaluating the liquefaction potential of gravelly soils. Proc. of the NCEER Workshop on evaluation of liquefaction resistance of soils. NCEER Report No. 97-0022, NCEER, Dec. 1997.

Harder, L. F., Jr. and Seed, H. B., 1986. Determination of penetration resistance for coarse-grained soils using the Becker hammer drill. Earthquake Engineering Research Center, University of California, Berkeley, Report UCB/EERC-86/06.

Hatanaka, M. and Uchida, A., 1996. Empirical correlation between penetration resistance and internal friction angle of sandy soils. Soils and Foundations, 36(4): 1-9.

Idriss, I. M., 1990. Response of Soft Soil Sites During Earthquakes. Proceedings of the H. Bolton Seed Memorial Symposium, Vol. 2, Bitech Publishers, Ltd., Vancouver, B.C, Canada, pp. 273.290.

Japan Road Association, 1990. Specifications for Highway Bridges, Part IV.

Kovacs, W. D., 1979. Velocity Measurement of Free-Fall SPT Hammer. ASCE Journal of Geotechnical Engineering, 105(1): 1-10.

Kovacs, W. D., 1980. What constitutes a turn? ASTM Geotechnical Testing Journal, 3(3): 127-130.

Kovacs, W. D., 1994. Effects of SPT equipment and procedures on the design of shallow foundations on sand. Vertical and Horizontal Deformations of Foundations and Embankments, ASCE GSP 40: 121-131.

Kovacs, W. D., Evans, J. C., and Griffith, A. H., 1977. Towards a More Standardized SPT. International Conference on Soil Mechanics and Foundation Engineering., 9(2): 269-276.

Kovacs, W. D. and Salomone, L. A., 1982. SPT hammer energy measurement. ASCE Journal of Geotechnical Engineering, 108(4): 599-620.

Kovacs, W. D., Salomone, L. A., and Yokel, F. Y., 1981. Energy measurement in the Standard Penetration Test. U.S. Department of Commerce and National Bureau of Standards. Washington , D.C.

Kramer, S. L., 1996. *Geotechnical Earthquake Engineering*. Prentice Hall, New Jersey.

Kulhawy, F. H. and Trautmann, C. H., 1996. Estimation of in-situ test uncertainty. Uncertainty in the Geologic Environment, ASCE GSP 58: 269-286.

Liao, S. S. and Whitman, R. V., 1986. Overburden correction factors for SPT in sand. ASCE Journal of Geotechnical Engineering, 112(3): 373-377.

Marcuson, William F., III. and Bieganousky, Wayne A., 1977. Laboratory standard penetration tests on fine sands. ASCE Journal of Geotechnical Engineering, 103(6): 565-588.

Meyerhof, G. G., 1956. Penetration tests and bearing capacity of cohesionless soils. ASCE Journal of Geotechnical Engineering, 82(1): 866/1-866/19.

Meyerhof, G. G., 1976. Bearing capacity and settlement of pile foundations. ASCE Journal of Geotechnical Engineering, 102(3): 54-85.

Mitchell, J. K. and Gardner, W. S., 1975. In-situ measurement of volume change characteristics. State-of-the-art report. Proceedings of the Conference on In-situ Measurement of Soil Properties, Specialty Conference of the Geotechnical Division, North Carolina State University, Raleigh, Vol II, pp 279-345.

Mitchell, J. K., Guzikowski, F., and Villet, W. C. B., 1978. The measurement of soil properties in-situ - present methods - their applicability and potential. LBL 6363. University of CA, Berkeley. pp 7-11.

Mobile Drilling Company, 1986. Auger and Soil Sampling brochure.

Muromachi, T., Oguro, I., and Miyashita, T., 1974. Penetration Testing in Japan. Proc. European Symposium on Penetration Testing, Stockholm, Vol. 1, pp. 193-200.

Neely, W. J., 1990. Bearing capacity of expanded-base piles in sand. ASCE Journal of Geotechnical Engineering, 116(1): 73-87.

Ooi, P. S. K., Duncan, J. M., Rojiani, K. B., and Barker, R. M., 1991a. Engineering Manual for Driven Piles. The Charles E. Via, Jr. Department of Civil Engineering, Virginia Polytechnic Institute and State University, May 1991.

Ooi, P. S. K., Rojiani, K. B., Duncan, J. M., and Barker, R. M., 1991b. Engineering Manual for Drilled Shafts. The Charles E. Via, Jr. Department of Civil Engineering, Virginia Polytechnic Institute and State University, May 1991.

Parcher, J. V. and Means, R. E., 1968. *Soil Mechanics and Foundations*. Charles E. Merrill, Columbus, Ohio.

Parry, R. H. G., 1977. Estimating bearing capacity in sand from SPT values. ASCE Journal of Geotechnical Engineering, 103(9): 1014-1019.

Peck, R. B. and Bazaraa, A. R. S., 1969. Discussion to settlement of spread footings on sand. ASCE Journal of Geotechnical Engineering, 95(3): 905-909.

Peck, R. B., Hanson, W. E., and Thornburn, T. H., 1974. *Foundation Engineering*. 2nd Edition. John Wiley and Sons, New York.

Robertson, P. K., 1986. In situ testing and its application to foundation engineering. Canadian Geotechnical Journal, 23(4): 573-594.

Sanglerat, G, and Sanglerat, T. R. A., 1982. Pitfalls of the SPT. Proc. of the Second European Symposium on Penetration Testing. Vol. 1, pp. 143-145.

Schmertmann, J. H., 1971. Discussion to de Mello (1971) Proceedings of the fourth Panamerican conference on soil mechanics and foundation engineering, Vol. 3, pp. 90-98.

Seed, R. B. and Harder, L. F. Jr., 1990. SPT-Based analysis of cyclic pore pressure generation and undrained residual strength. H. Bolton Seed Memorial Symposium Proceedings. Edited by J. M. Duncan. Vol. 2, pp. 351-376.

- Seed, H. B., Tokimatsu, K., Harder, L. F., and Chung, R. M. 1984. The Influence of SPT Procedures in Soil Liquefaction Resistance Evaluations, Report No. UCB/EERC-84/15, Earthquake Engineering Research Center, University of California, Berkeley.
- Seed, H. B., Tokimatsu, K., Harder, L. F., and Chung, R. M., 1985. Influence of SPT procedures in soil liquefaction resistance evaluations. *ASCE Journal of Geotechnical Engineering*, 111(12): 1425-1445.
- Skempton, A. W., 1986. Standard penetration test procedures and the effects in sands of overburden pressure, relative density, particle size, aging and overconsolidation. *Geotechnique*, 36(3): 425-447.
- Stroud, M. A., 1974. The standard penetration test in insensitive clays and soft rock. *Proc. European Symposium on Penetration Resistance*, Stockholm, Vol. 2:2.
- Sy, A., 1993. Energy measurements and correlations of the Standard penetration test (SPT) and the Becker penetration test (BPT). Ph. D. thesis, Dept. of Civil Engineering, University of British Columbia, Vancouver, BC.
- Sy, A., 1997. Twentieth Canadian Geotechnical Colloquium: Recent developments in the Becker penetration test: 1986-1996. *Canadian Geotechnical Journal*, 34(6): 952-973.
- Sy, A. and Campanella, R. G., 1993. Dynamic performance of the Becker hammer drill and penetration test. *Canadian Geotechnical Journal*, 30(4): 607-619.
- Sy, A. and Campanella, R. G., 1994. Becker and standard penetration tests (BPT-SPT) correlations with consideration of casing friction. *Canadian Geotechnical Journal*, 31(3): 343-356.
- Sy, A. and Lum, K. K. Y., 1997. Correlations of mud-injection Becker and standard penetration tests. *Canadian Geotechnical Journal*, 34(1): 139-144.
- Tan, C. K., Duncan, J. M., Rojiani, K. B., and Barker, R. M., 1991. *Engineering Manual for Shallow Foundations*. Prepared for NCHRP Project 24-4, Charles E. Via, Jr. Department of Civil Engineering, Virginia Polytechnic Institute and State University, May, 1991.
- Terzaghi, K. and Peck, R. B., 1976. *Soil Mechanics in Engineering Practice*. John Wiley, New York.
- Terzaghi, K., Peck, R. B., and Mesri, G., 1996. *Soil Mechanics in Engineering Practice*. John Wiley and Sons, New York.
- Thorburn, S., Schmertmann, J. H., Nixon, I. K. Decourt, L., Muromachi, T., and Zolkov, E., 1989. International Reference Test Procedure for the Standard Penetration Test (SPT).

Report of the ISSMFE Technical Committee on Penetration Testing of Soils - TC 16 with Reference Test Procedures. Swedish Geotechnical Institute, No. 7:17-19.

Tokimatsu, K., 1988. Penetration tests for dynamic problems. Proc. 1st Int. Symposium on Penetration Testing, Rotterdam, pp. 117-136.

Trofimenkov, J. G., 1974. Penetration Testing in Eastern Europe. Proc. European Symposium on Penetration Resistance, Stockholm, Vol. 2:1, National Swedish Building Research, 1975, pp. 24-28.

Tschebotarioff, G. P., 1973. *Foundations, Retaining, and Earth Structures*. 2nd. Edition, McGraw-Hill, New York.

U.S. Dept. of the Navy. 1982. Soil Mechanics. NAVFAC Design Manual DM-7.1, Alexandria, VA.

Yoshida, Y. and Ikemi, M., 1988. Empirical formulas of SPT blow-counts for gravelly soils. Proc. 1st Int. Symposium on Penetration Testing, Rotterdam, pp. 381-387.

Youd, T.L. and Idriss, I.M., 1997. Summary Report. Proc. of the NCEER workshop on evaluation of liquefaction resistance of soils. NCEER Report No. 97-0022, NCEER, Dec. 1997.